University of Southern Queensland

Faculty of Health, Engineering and Sciences

KINETIC ENERGY RECOVERY IN MOTOR VEHICLES USING COMPRESSED GAS

A dissertation submitted by

Mr. Rick William Kruger

In fulfilment of the requirements of

Bachelor of Engineering (Honours) (Mechanical)

October 2014

Abstract

It's no secret that we are depleting our natural resources at an unsustainable rate while polluting our natural environment. This is especially true when it comes to motor vehicles. As a result, manufacturers are investing billions of dollars every year to produce energy efficient vehicles that reduce fuel consumption and vehicle emissions. One method is to introduce regenerative braking. This is the process of recovering kinetic energy from a moving vehicle under braking conditions. The energy is used to increase performance and efficiency, hence addressing the issues of sustainability and the environment.

The research of this project was focused on the concept of using an internal combustion (IC) engine as a compressor to recover kinetic energy as compressed gas. This is a concept that has been considered over the last decade and a half, with the one of the first being Schechter (1999). This research project investigates the ability to use the engine as a compressor and assesses its performance and viability when compared with two other main regenerative braking technologies: hybrid electric vehicles (HEV) and flywheels.

A literature review was undertaken, and revealed the major aspects that affect the ability of an IC engine to compress gas. The major component needed for this concept was a variable valve timing (VVT) system that allows the engine to operate as a compressor, and even a pneumatic motor if needed. The system would also require modifications to the cylinder head to add a charge/discharge valve, and of course, a pressure tank for storing the compressed gas.

The research methodology considered a quasi-dimensional numerical simulation of an IC engine operating as a reciprocating two-stroke compressor. The simulation was based on a model previously prepared by Buttsworth (2002) to determine the performance of a fuel inducted engine with a heat release profile as a function of the crank angle – the method that closely followed that described by Ferguson (1986).

After testing, the model was simulated during the deceleration phases of the NEDC test cycle. The valve timing was optimised to produce the least amount of work during the simulation, while the engine speed was optimised to reduce the reliance on the friction brakes. The results showed that the energy recoverable was 574 kJ over the entire cycle with the assumption that the energy recovered was used after each deceleration event. Based on an engine efficiency of 30% and usable energy of 80%, this translates to energy savings of 1.5 MJ and fuel savings of 43 ml over the full cycle.

Overall, the concept of using compressed gas to recover kinetic energy appeared to be viable. With additional components and modifications, an engine can be used as a compressor. The advantages seem to be the mass of the system and its simplicity when compared to HEVs and flywheels. The fuel savings also appear to be competitive. However, it seems to be less suited for storing energy over longer periods of time, and has a lower regenerative efficiency as shown in the results of this research and the research of others. It is unclear whether or not it could compete with HEVs in the market. The research suggests that more effort needs to be invested in producing experimental results, and subsequently optimising the system to improve performance.

Acknowledgements

I would like extend thanks to my supervisor Dr Ray Malpress for his ongoing support and guidance during completion of this dissertation.

I would also like to thank my wife Kahla for her unwavering support throughout this endeavour and my studies, for her understanding when study commitments meant that my time was limited, for her infinite patience during the demanding times when mine was exhausted, and for keeping me focused on the light at end of the tunnel.

University of Southern Queensland

Faculty of Health, Engineering and Sciences

ENG4111/ENG4112 Research Project

Limitations of Use

The Council of the University of Southern Queensland, its Faculty of Health, Engineering & Sciences, and the staff of the University of Southern Queensland, do not accept any responsibility for the truth, accuracy or completeness of material contained within or associated with this dissertation.

Persons using all or any part of this material do so at their own risk, and not at the risk of the Council of the University of Southern Queensland, its Faculty of Health, Engineering & Sciences or the staff of the University of Southern Queensland.

This dissertation reports an educational exercise and has no purpose or validity beyond this exercise. The sole purpose of the course pair entitled "Research Project" is to contribute to the overall education within the student's chosen degree program. This document, the associated hardware, software, drawings, and other material set out in the associated appendices should not be used for any other purpose: if they are so used, it is entirely at the risk of the user.

University of Southern Queensland

Faculty of Health, Engineering and Sciences

ENG4111/ENG4112 Research Project

Certification of Dissertation

I certify that the ideas, designs and experimental work, results, analyses and conclusions set out in this dissertation are entirely my own effort, except where otherwise indicated and acknowledged.

I further certify that the work is original and has not been previously submitted for assessment in any other course or institution, except where specifically stated.

Rick William Kruger

Student Number: 0061016558

_____

Signature

_____

Date

Table of Contents

List of Figures

List of Tables

Glossary

APA:	Air Power Assist
BDC:	Bottom Dead Centre
BMEP:	Brake Mean Effective Pressure
CVT:	Continuously Variable Transmission
EUDC:	Extra-Urban Driving Cycle
FMEP:	Friction Mean Effective Pressure
HEV:	Hybrid Electric Vehicle
IC:	Internal Combustion
ICE:	Internal Combustion Engine
IMEP:	Indicated Mean Effective Pressure
KE:	Kinetic Energy
KER:	Kinetic Energy Recovery
KERS:	Kinetic Energy Recovery System
LHV:	Lower Heating Value
Mbd:	Million barrels per day
NEDC:	New European Driving Cycle
PV:	Pressure-Volume
RPM:	Revolutions per Minute
SI:	Spark Ignition
TDC:	Top Dead Centre
VVT:	Variable Valve Timing

1 Introduction

Automobile manufacturers invest billions of dollars every year on research and development. Technological developments are mainly driven by return on investment and a desire to enhance future profits. However, there are two main socio-economic concerns that appear to be governing the direction of technological development and innovations within the automobile manufacturing industry. These are:

1. Sustainability: According to data produced by U.S. Energy Information Administration (n.d.-a), oil consumption is growing year-on-year. Moreover, projections of future demand estimated by Organization of the Petroleum Exporting Countries (2013) further illustrate the need for an alternate solution. The depletion of this natural resource is a cause for concern given the heavy dependence on this energy source from the transport industry and the general population.
2. Environment: Easy access to information has resulted in an increased awareness of the effects of automobile emissions on the environment and health. This public awareness has grown exponentially in modern times. For this reason, public pressure is driving corporations to become both socially and ethically responsible. Global corporations are beginning to acknowledge this is a key component to maintaining the financial success, evidenced by the shift to integrate sustainability and the environment into company values and goals.

Both sustainability and the environment are high among current social agendas. The ability for a manufacturer to produce a product that addresses these issues would be a powerful marketing tool. The economics of supply and demand also dictate that a dwindling supply of oil will increase fuel prices - another reason for those more self-orientated to own a fuel efficient motor vehicle. Nevertheless, it is important that we do not lose sight of the significance of protecting the environment and addressing sustainability. If trends continue without new research and development, the potential impact on current and future generations could be disastrous.

One area of technological development that is currently growing is kinetic energy recovery (KER). This is the practice of harvesting the kinetic energy of a moving vehicle and redistributing this recovered energy at a later time. In motor sport, these systems are used for both fuel efficiency and also short bursts of increased performance. In domestic use, it is predominantly used to reduce fuel consumption and emissions through hybrid power systems.

This report will consider one of the less explored methods for kinetic energy recovery. It seeks to establish the viability of the technology and analyse its performance against current technologies.

1.1 Project Background

The depletion of oil supplies is major concern given it is the primary resource used to fuel internal combustion (IC) engines. The U.S. Energy Information Administration (n.d.-a) reports that in 2013, the worldwide consumption of oil was 89.4 mbd. This demand is expected to increase to 108.5 mbd by 2035 (Organization of the Petroleum Exporting Countries 2013). In comparison, supply was estimated to be more than 90.3 mbd in 2013 (U.S. Energy Information Administration n.d.-a). This means that the global supply of crude oil at current consumption rates will no longer be able to satisfy future global demand.

Supply and demand of oil is only half of the sustainability problem. The other issue refers to how much oil is actually recoverable. Oil reserves indicate the amount of oil that can be extracted at an assumed cost level. Estimation of reserves is an ongoing process and depends on the availability of new data. World reserves in 2013 were estimated to be 1,646 billion barrels (International Organization of Motor Vehicle Manufacturers n.d.-a). At the current consumption rate of 89.4 mbd, current known world oil reserves could be expected to be exhausted in the next 50 years.

A shortage in oil, both in supply and reserves, presents many significant economic problems. This is particularly critical for the transportation sector which accounted for

57% of oil consumption in 2010 (Organization of the Petroleum Exporting Countries 2013). Other industries which rely heavily upon machinery such as construction, mining and agriculture would also suffer from shortage and would see a decline in productivity. An increase in the fuel price could make many industries less viable or no longer profitable, which can produce an economic domino effect on other economic drivers such as unemployment.

1.1.1 Energy Losses in Passenger Vehicles

Producing more energy efficient vehicles is one of many solutions proposed for decreasing emissions and reducing oil consumption. Considering an estimated 1.143 billion vehicles were in use world-wide during 2012 and another 87.25 million were manufactured in 2013 alone (International Organization of Motor Vehicle Manufacturers n.d.-a), it is apparent that both demand and the consumption of oil should increase. Therefore it is important to understand how vehicle energy is being used so that areas that maximise efficiency can be targeted. Most spark ignition (SI) engines have an efficiency of only 20-30%. This means that most of the fuel burned is unusable energy. The estimated losses per category are listed in Table 1.

Energy Losses (city and highway)	**Percentage (%)**
Engine Losses (Engine friction, pumping air in and out, and wasted heat)	68-72
Parasitic Losses (Air condition, power steering, etc.)	4-6
Drivetrain Losses	5-6
Power to Wheels (Aerodynamic drag)	9-12
Power to Wheels (Rolling resistance)	5-7
Power to Wheels (Braking)	5-7
Idle Losses (Represented as engine/parasitic losses)	3*

* Idle losses will be much higher in city metropolitan driving as opposed to highway driving.

Table 1 – List of motor vehicle energy losses and the percentage of losses they represent. Sourced from U.S. Government (n.d.-a).

Upon examining Table 1, several solutions can be formulated for reducing energy losses. These include:

- Producing lower friction transmission systems, reducing friction losses;
- Produce more aerodynamically efficient vehicles, reducing drag;
- Limit the use or produce more efficient parasitic sub-systems such as air conditioning;
- Produce more efficient engines; and
- Cutting off the engine while braking and stationary, reducing idling losses.

Braking is the only energy loss that cannot be reduced through efficiency. Energy lost during braking is essentially wasted energy which is dissipated as heat. In comparison, all other losses can be reduced by improving component technology and efficiency. Using current technology, braking losses could potentially be recovered through a process known as regenerative braking. Regenerative braking involves the recovery of the kinetic energy of motion, and therefore the recovery of the energy used to propel the vehicle. The energy recovered is then usually recycled back into the drivetrain during acceleration to reduce fuel consumption or improve vehicle performance.

1.1.2 Kinetic Energy

The energy available for recovery during the braking phase can be estimated by the kinetic energy of the car before braking begins. Loss of this kinetic energy is mainly dissipated as heat in the brakes; however losses also occur due to the friction of the drivetrain, rolling resistance and drag force (to a lesser extent). The kinetic energy equation is represented by:

$$KE = \frac{mV^2}{2} \quad [\text{J}] \qquad \text{Equation [1]}$$

Where m is the mass of the vehicle [kg] and V is the velocity [m/s].

From this equation, the potential recoverable kinetic energy of moving vehicle can be estimated by applying the mass and speed of the vehicle to the equation. For a 2,000 kg vehicle travelling at 60 km/h, this equates to nearly 278 kJ of energy or approximately 8 ml of fuel with a lower heating value of 44.4 MJ/kg and a density of 0.745 kg/L. For a vehicle with efficiency of 10L/100km, this is equivalent to driving 63m if 75% of this energy can be recovered and reused. Although in practice, the kinetic energy of the vehicle will be higher due to the kinetic energy stored in the many moving parts of the vehicle.

1.1.3 Current Technologies

The following section outlines the two main technologies currently being used in regenerative braking systems.

1.1.3.1 Hybrid Electric Vehicles

Several kinetic energy recovery technologies have emerged in recent times in response the growing oil supply and demand problems along with the shift to more environmentally friendly technologies. Currently, the most predominant technology used converts kinetic energy to electric energy, commonly known as hybrid electric vehicles (HEV). This technology also now extends itself to popular motor racing formats such as Formula 1 and Le Mans. However, the technology is mostly used in hybrid passenger vehicles such as the Toyota Prius.

The technology works by combining a gasoline engine with an electric motor, as shown in Figure 1. Current vehicles using HEV technology usually operate in parallel with the gasoline powertrain. Therefore the gasoline engine and electric motor can provide power independently, meaning that the gasoline engine can be shut-off to reduce fuel consumption. During deceleration and braking an electric motor is used as a generator to recover the kinetic energy. The electricity produced is stored in a battery for later use. When the vehicle starts to accelerate again, an electric motor uses the stored energy to accelerate or assist in accelerating the vehicle to reduce reliance on the gasoline engine and hence fuel consumption. Toyota Motor Corporation Australia Ltd

(n.d.) claim that their Prius model can achieve better fuel economies of up to 50% compared to conventional petrol vehicles of similar size.

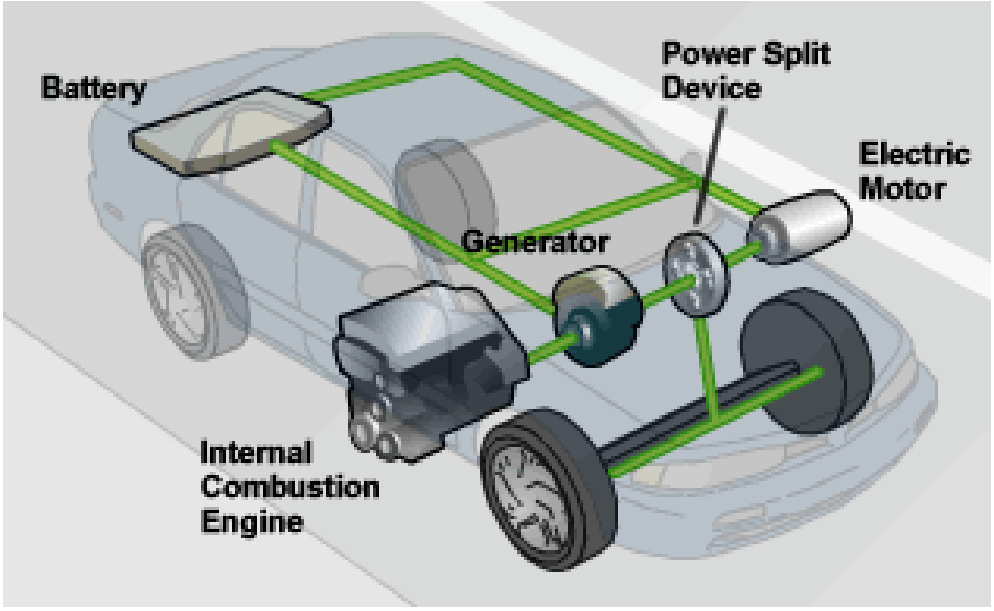

Figure 1 – Illustration of the setup of a Hybrid Electric Vehicle (U.S. Government n.d.-b).

The lead acid battery has been widely used for decades in automobile applications. It is perhaps one of the oldest and cheapest batteries currently on the market. While they are relatively inexpensive, they have a shorter lifecycle of around 1,000 cycles (approximately 3 years' service) with a charge/discharge efficiency of up to 92% (Fuhs 2009). However, according to Fuhs (2009) the life of the battery can be extended to 5 years with controlled charging and discharging. Compared to other battery types (shown in Table 2), they have a lower specific energy of approximately 30-40 Wh/kg and specific power of 180 W/kg. Therefore, higher storage capacity requirements will result in greater battery mass which will reduce the overall efficiency of the system.

Other battery technologies seem to address some of the shortcomings of the lead acid battery. Nickel metal hydride (NiMH), the battery type used in Toyota's Prius model for example, has higher specific energy of around 70 Wh/kg and specific power of 200 W/kg (per Table 2) and the ability to operate within a larger temperature range

(Fuhs 2009). However, the advantages of NiMH batteries come at a higher initial cost, while battery life is also lower at approximately 600 cycles (2 years' service) (Fuhs 2009). Furthermore, cooling also assists with faster recharge times (Fuhs 2009), which is another design requirement.

The most promising technology for future rechargeable batteries is lithium-ion (Li-ion). Capable of specific energy of 180 Wh/kg and energy density of 350 Wh/L (Fuhs 2009), it requires less space and has less weight. Charge/discharge efficiency can also be as high as 99% and the expected life of Li-ion is 4 years (Fuhs 2009). While it costs up to 50% more than NiMH, the expected lifecycle cost is lower according to Fuhs (2009). It also has a lower self-discharge rate of around 5-10%/month compared to 3-20%/month for lead acid and 30%/month for NiMH (per Table 2).

Whilst considered promising, Li-ion doesn't come without its disadvantages. Li-ion battery life suffers from calendar age, not just the number of cycles (Fuhs 2009), meaning that capacity loss can occur due to aging. Battery durability is also affected by operating and storage temperatures. Safety is another concern and careful control of charging and discharging to avoid the potential of cells catching fire. In the event of such instances, CO_2 or dry chemical extinguishers are recommended over water extinguishers.

	Lead Acid	NiMH	Li-ion
Specific Energy (Wh/kg)	30-40	30-80	150-200
Specific Power (W/kg)	180	250-1000	300-1500
Energy Density (Wh/L)	60-75	140-300	250-350
Self-Discharge (%/month)	3-20	30	5-10
Consumer Price (Wh/$)	-	1.37	2.80
C/D Efficiency (%)	70-92	66	99

Table 2 – Summary of battery performance properties for three battery types. Sourced from Fuhs (2009).

The performance characteristics of the three battery types are summarised in Table 2. The word ‘specific’ has been used to mean per unit mass and ‘density’ to mean per unit volume. This is in alignment with the terminology used by Fuhs (2009). It has been noted that while the values in the Table 2 have been reproduced from tables in Fuhs (2009), he does occasionally refer to values that may differ deviate slightly from those recorded in the tables.

An alternative to using batteries is to use a capacitor. A capacitor is a device that stores electrostatic energy using an electric field. It has many advantages over batteries, the first being that capacitors have higher efficiency, in the range of 90-98% (per Table 3). This means that less energy is wasted because most of the energy stored can be discharged. They also have higher storage and discharge speeds due to higher specific power levels of up to 4kW/kg (Fuhs 2009). This provides an advantage in scenarios requiring short bursts of high peak power (faster acceleration) and quick energy storage (shorter braking distances).

Further, capacitors require less maintenance when compared with batteries and do not deteriorate with use. They have an expected life in excess of 10 years and over 1 million discharge cycles (per Table 3), compared to batteries that have a life of up to 5 years and 10,000 discharge cycles. This means that replacement is less frequent and generally costs less over time. However, the cost of capacitors compared to conventional lead acid batteries is generally high, and won’t be considered competitive until their cost drops below $5/Wh (Fuhs 2009). Another major problem with capacitors is their low specific energy in the order of 1 to 10 Wh/kg (per Table 3). Their low specific energy makes them unsuitable for long discharge times.

	Batteries	UCs
Lifetime w/o maintenance	1-5 years	10+years
No. in lifetime of high rate discharge/charge cycles	1-000 – 10,000[a]	1,000,000[b]
C/D efficiency	40-80%	90%-98%
Charge time	1-5h	0.3-30s
Discharge time	0.3-3h	0.3-30s
Specific Energy (Wh/kg)	10-100	1-10
Specific Power (kW/kg)	~1	<10
Adequate energy to meet peak power duration	Yes	Yes
Limitation on SOC	Low SOC limits life	No effect SOC on life
Cost $/kWh	Lead acid least; other than types three to ten times more	Slightly more lead acid[c]
Working temperatures	-20 to +65	-40 to +65

[a] Depends on the application and BMS.

[b] Less dependent on application and monitoring.

[c] Significantly cheaper than all batteries except lead acid

Table 3 – Comparison of performance characteristics between batteries and ultra-capacitors (Fuhs 2009).

1.1.3.2 Flywheels

Another method for recovering energy in regenerative braking is the use of flywheels. Flywheels are mechanical devices used to store rotational energy. Figure 2 shows a flywheel module in a containment housing. They work much to the same principles of HEV. During braking, energy is recovered stored in the flywheel, while helping to reduce vehicle velocity. As the vehicle slows down, the speed of the flywheel will increase. When kinetic energy stored by the flywheel is transferred back into the system, it helps to accelerate the vehicle while reducing the speed of the flywheel. This puts less strain on the IC engine and therefore requires less power and reduces fuel consumption.

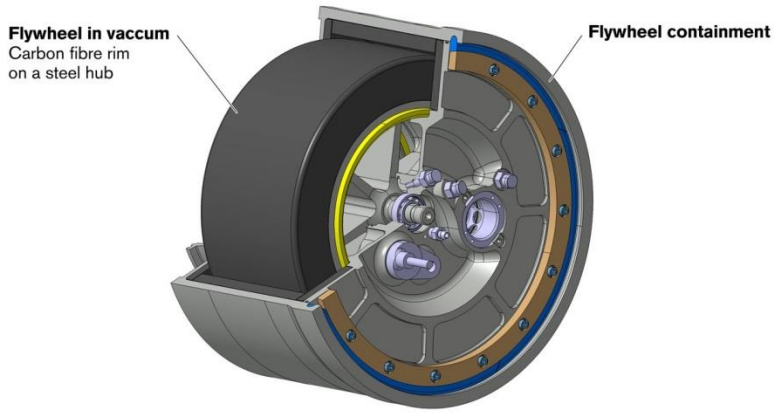

Figure 2 – Diagram of a flywheel KERS module (Motor Trend Magazine 2014a).

The kinetic energy is transferred using a continuously variable transmission (CVT) unit as shown in Figure 3. The CVT allows for a seamless transfer of energy to and from the flywheel through an infinite number gearing ratios. A clutch is used to disengage the flywheel when not in use.

The potential energy storage can be expressed by the equation:

$$E = \frac{1}{2} J \omega^2 \quad [\text{J}] \qquad \text{Equation [2]}$$

Where ω is the angular velocity [rad/s] and J is the mass moment of inertia [kg.m^2].

From Equation 2 it can be understood that increasing the angular velocity will deliver better results than simply improving the moment of inertia. This can be achieved using the CVT unit.

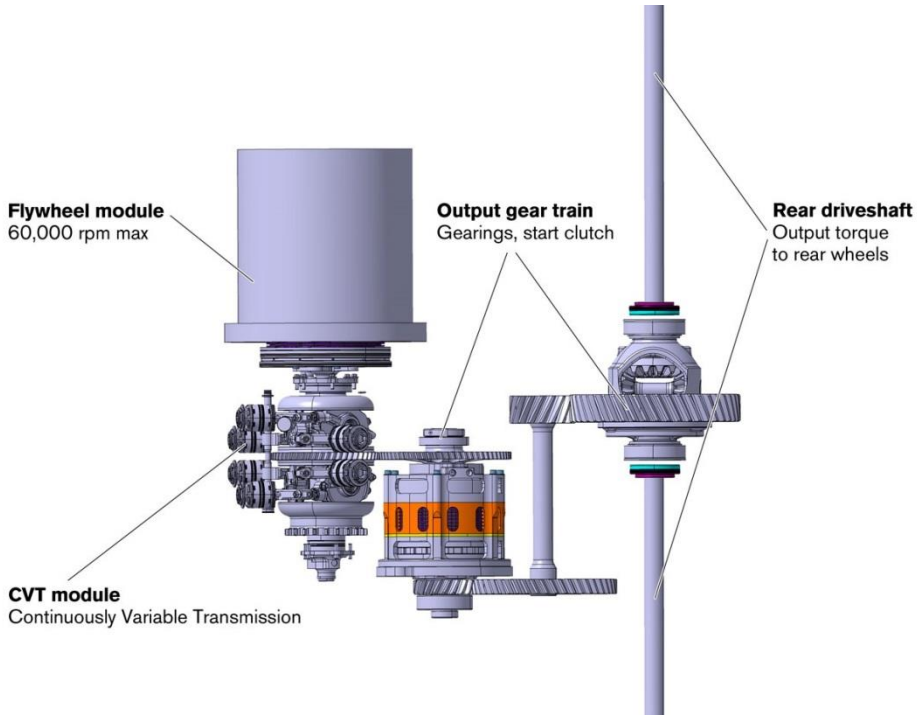

Figure 3 – Flywheel KERS system layout (Motor Trend Magazine 2014b).

Flybrid Automotive Limited (2014) states that fuel consumption savings have been demonstrated to be more than 18% over the New European Driving Cycle (NEDC) and more than 22% in real world conditions. These statistics are supported by similar claims by Volvo Car Group, who conducted joint tests with Flybrid Automotive. They claim that the technology adds 80hp performance while reducing fuel consumption by up to 25% (Volvo Car Group 2014).

Furthermore, the simplicity of the technology allows for long life spans with proper maintenance. The life of some flywheels is designed to be more than 250,000 km with no performance degradation (Flybrid Automotive Limited 2014). Flywheels can be reliable with repeatable characteristics. The amount of energy stored at any given time can be reliably measured by monitoring rotational speed.

Efficiency is another key characteristic. Physics dictates that transforming energy from one source to another will inevitably incur losses. As flywheels store mechanical energy using mechanical energy, conversion losses can be reduced. They can also generate and absorb energy quickly. A mechanically driven flywheel can have an

overall charge/discharge efficiency of more than 70% during a full regenerative cycle in stop start traffic (Body & Brockbank 2009 cited in Boretti 2010). However, due to the relatively higher friction losses, flywheels tend to discharge at quicker rates making the technology inefficient for storing energy for longer periods of time.

Flywheel systems also require safety design considerations. Increasing angular velocity results in higher centrifugal stresses on the flywheel. If the speed of the flywheel exceeds the design tensile strength of the material used, the flywheel will predictably fail, releasing all of the stored energy instantaneously. Therefore, the flywheel housing needs to be manufactured using materials that can safely withstand the energy during failure and prevent flywheel material from breaching the housing; increasing the overall mass of the system.

Increasing the weight of the flywheel results in greater moments of inertia, which generally results in higher energy densities. However, more weight will result in greater friction forces meaning energy losses and self-discharging. Furthermore, windage losses caused by friction with the atmosphere contribute to the overall losses of the system. In order to reduce these losses, manufacturers are now designing low friction bearings using magnets and vacuum sealed housings; these can add to the overall cost of the system.

1.1.4 Conclusion

In order to overcome the disadvantages of the technologies listed above, over the past decade and a half, another technology has been gaining momentum in the literature. Research and studies have been conducted into recovering kinetic energy using compressed gas stored as potential energy. This can be achieved by either using the IC engine as a compressor, or using a dedicated compressor much like the generator is used in HEVs. The technology seeks to address the following problems:

1. Efficiency: One of the biggest problems associated with the recovery of kinetic energy in HEVs is the efficiency of transforming one form of energy to another.

During energy recover, efficiency is reduced by the transformation from kinetic energy into electrical energy using a motor or generator, which is then transformed into chemical energy in a battery. These losses are also true for discharging the energy back into the system. The other problem affecting efficiency is the additional mass of KER system components. Additional mass essentially reduces the global efficiency of the vehicle system due to energy losses caused by friction.

2. Design Constraints: The available volumetric space within the engine compartment causes design challenges. For flywheels, it limits the overall size of the device and the mounting points available. In HEVs it demands efficient use of the space due to the addition of several components. The position of the mass of the additional components must also be considered. It can cause a change in vehicle dynamics such as braking and cornering.

3. Safety: Working with electricity introduces new safety requirements within automobiles. High voltages used in regenerative braking systems are a major health and safety concern, particularly if the vehicle is involved in an accident. Furthermore, although generally considered safe, batteries are produced using hazardous materials. The risks are relevant for both the handling and disposing of damaged batteries. For example, lead is a toxic material that can cause serious health issues in high levels. Cadmium is also considered more toxic than lead and can cause health problems if a person is exposed to the metal for a prolonged time.

1.2 Concept

The concept of this research is to use a conventional IC engine to recover kinetic energy of a motor vehicle during braking. It proposes that the kinetic energy recovered would be converted to potential energy, stored as compressed gas using a high pressure vessel. During acceleration, the stored energy would be used to reduce with the goal of reducing fuel consumption.

Depending on how the recovered energy is used, the IC engine may have one or two additional operational modes. The first would be a pneumatic pump mode. During the braking phase, the IC engine would be used as a reciprocating compressor powered by the kinetic energy of the vehicle due to its motion. Air would be pumped by the engine to a pressure vessel and stored until required. This should reduce the need for any major additional components.

If the compressed air is used to supercharge the engine, it may not require a second operation mode. However, the air could be used to power a pneumatic motor. Alternatively, a second additional operation mode may be used - pneumatic engine mode. Given sufficient air pressure, this mode uses the potential energy to accelerate the vehicle or provide more torque during acceleration. Using the recovered kinetic energy could potentially reduce the fuel needed to accelerate the vehicle under conventional operating conditions.

1.3 Aims and Objectives

The aim of this project is to evaluate the plausibility of recovering the kinetic energy of a motor vehicle by using the internal combustion engine to compress gas. Specifically, the aim of the project can be divided into several significant objectives characterised as follows:

- Understand current kinetic energy recovery technologies including their respective benefits and weaknesses to establish a suitable benchmark for comparison;
- Determine the ability to use an internal combustion engine to produce compressed gas. Critically analyse the similarities and divergences with positive displacement compressors and identify any significant design deviations that may need to be addressed;
- Determine the practical and feasible uses for the compressed gas within motor vehicles and analyse the effects on performance;
- Measure the energy recoverable using compressed gas using a numerical model, with appropriate assumptions, created to simulate an IC engine operating as a compressor; and

- Analyse the results, comparing key performance parameters with current technologies and conclude on the viability of compressed air as an alternative.

1.4 Scope

The research undertaken in this project focuses specifically on passenger automobiles powered by naturally aspirated internal combustion engines. The internal combustion engine considered will be a SI four-stroke piston engine. As a result, this specifically excludes automobiles powered by Wankel engines (rotary), diesel engines employing Homogenous Charge Compression Ignition (HCCI) and other stroke configurations including two-stroke engines.

The energy recovery analysis within this report is limited to the operating conditions of automobiles and the potential energy recoverable that is directly related to systems under these conditions. The project will not undertake an energy cost analysis, therefore the energy expended to manufacturing additional components needed to recover kinetic energy versus the energy recoverable.

2 Literature Review

2.1 Internal Combustion Engine as a Compressor

2.1.1 Introduction

The purpose of a compressor is to increase the pressure of a gas and store this gas as confined kinetic energy. Understanding how compressors work is pertinent to establishing the feasibility of using an IC engine as a compressor. For this reason the following section will focus on comparing the characteristics of modern compressor technology with that of an IC engine. While many types of compressors exist in the market place, this analysis will concentrate on comparisons with a reciprocating compressor (a positive displacement compressor) due to their similar functionality. It will compare and contrast their operating cycles, componentry and discuss any potential performance limitations.

2.1.2 Ideal Operating Cycles

The following section will compare and contrast the ideal operating cycles of a reciprocating compressor and a four-stroke IC engine.

2.1.2.1 Ideal Positive Displacement Compressor Cycle

The simplest way to estimate performance is to use a thermodynamic cycle. The analysis uses the ideal gas laws and a set of assumptions to simplify the actual process. Under the ideal compression cycle, the process is assumed to be isentropic. This implies that the process is adiabatic and that no heat will transfer from the control volume to the outside, meaning no losses due to heat transfer and friction.

The ideal compression cycle is illustrated in Figure 4a and Figure 4b. The figures display the pressure compared to the volume of the cylinder (P-V diagram), at each crank angle.

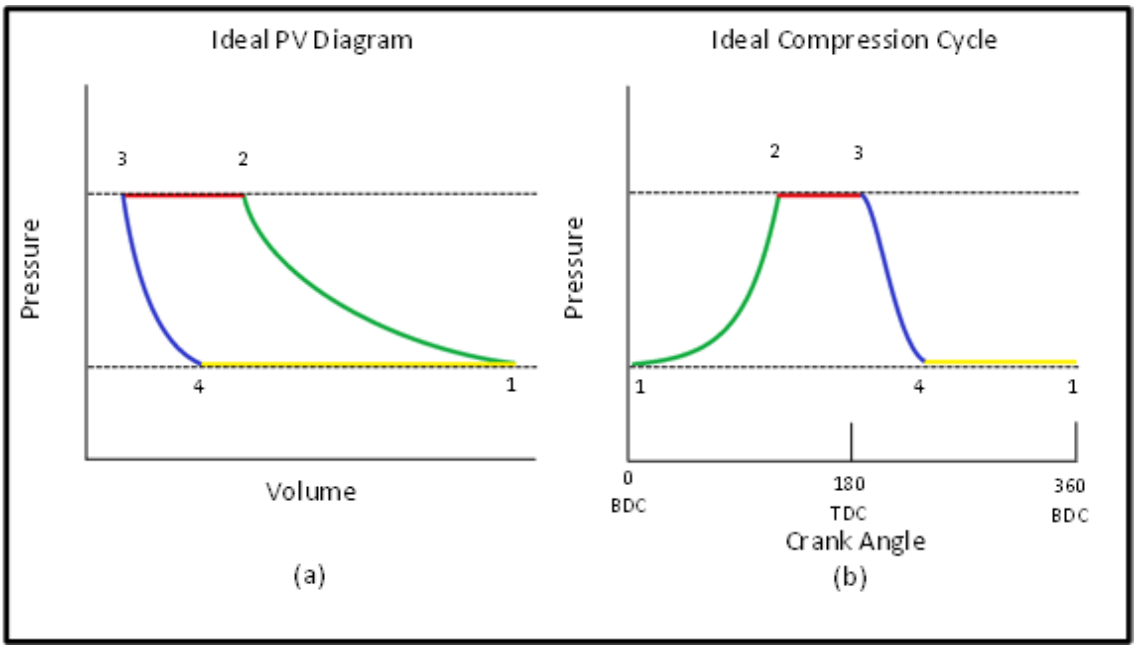

Figure 4 – Ideal compression cycle and pressure-volume diagram of a reciprocating compressor showing the four processes. Sourced from (Hanlon 2001).

At point 1, the piston starts at bottom dead centre (BDC) and maximum cylinder volume. At BDC the gas in the cylinder is at suction pressure. As the crank turns, the piston starts to move upwards decreasing the volume of the cylinder and compressing the gas. This decrease in volume causes the gas to increase in both temperature and pressure (process 1-2) at an exponential rate. This process can be considered as adiabatic and reversible.

The process continues until the pressure in the cylinder equals the discharge pressure at point 2, causing the discharge valve to open. After point 2, the pressure in the cylinder remains constant while the piston continues to displace the gas into the discharge line. This process is considered isobaric and isothermal.

This continues until the crank angle reaches top dead centre (TDC) at point 3 and the valve closes. At this point, the residual gas left in the clearance volume begins to expand back to suction pressure – decreasing in pressure (process 3-4) and in temperature. The expansion process is considered adiabatic and reversible.

At point 4 the pressure in the cylinder equals the suction pressure, which is usually close to the atmospheric pressure surrounding the compressor. The suction valve opens and the volume of the gas in the cylinder increases until the crank angle reaches BDC. The intake process 4-1 is isobaric and isothermal at intake pressure and temperature.

2.1.2.2 Otto Cycle

The ideal cycle for reciprocating engines follows a very similar method to the ideal compressor cycle. However, the majority of IC engines operate under a four-stroke configuration (with two complete revolutions per cycle) which accommodates the compression and power strokes. Figure 5 shows the ideal air-standard Otto cycle using a PV diagram.

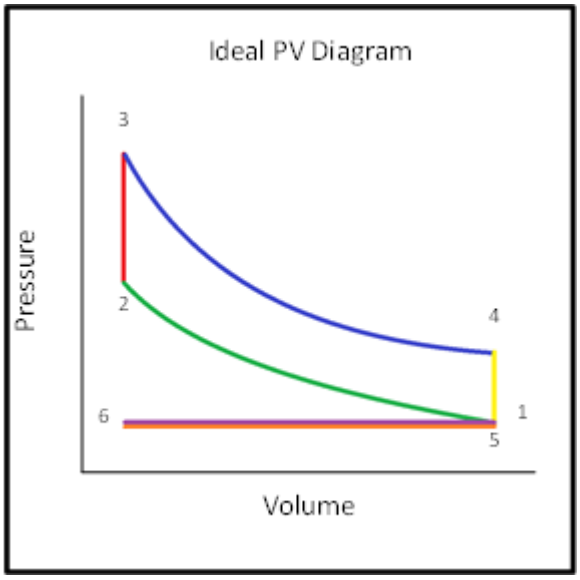

Figure 5 – Pressure-volume diagram of the Otto cycle showing the six processes.

Starting at TDC, the intake stroke begins by drawing in a fresh mixture of air and fuel into the cylinder. This occurs at constant pressure per process 6-1 of Figure 5. Usually, the inlet valve opens just before the stroke starts to maximise the mass of the air inducted. The inlet valve then remains open until shortly after the stroke ends when the cylinder is at BDC.

The compression stroke begins when both valves are closed at point 1. In the Otto cycle the compression is regarded as isentropic as an approximation to the real IC engine. The gas inside the cylinder undergoes compression (process 1-2) until combustion is initiated by an electric discharge across the spark plug at point 2.

The combustion process is considered to be a constant-volume heat input process shown as points 2-3. The gases in the cylinder increase rapidly in both temperature and in pressure. This occurs between 10 and 20 crank angle degrees before TDC (Heywood 1988).

Next, the expansion (power) stroke begins when the cylinder reaches TDC and peak pressure at point 3. The high pressure and enthalpy values of the gas thrust the cylinder down forcing the crank to rotate. The Otto cycle assumes this process is isentropic. Pressure then decreases and the volume increases (process 3-4) until the stroke ends when the cylinder reaches BDC. Just before this point, the exhaust valve opens to begin the exhaust stroke.

When the exhaust valve opens, blowdown is experienced and the pressure in the cylinder drops until the pressure equalises with the exhaust pressure. The process is approximated assuming a closed system, constant-volume pressure reduction from points 4-5.

As the piston travels back up the cylinder, the remaining exhaust gases exit the cylinder. The Otto cycle assumes a constant pressure at atmospheric pressure (process 5-6). As the piston approaches TDC, the inlet valve begins to open once more to start the cycle again while the exhaust valve closes just after TDC.

2.1.2.3 Operating Analysis

The previous section illustrates the similarities and differences between the ideal compression cycle and the Otto cycle. The key comparisons are the intake, compression and expansion processes. However, due to the difference in stroke

configuration (two-stroke for the compressor and four-stroke for the engine), these processes do not follow the same operational sequences.

The removal of certain processes will be necessary for operating the IC engine as a compressor. While the combustion process in the Otto cycle is fundamental during conventional operation of the engine, it is not required in the compression cycle, as this process adds no value. Removing this process will not only reduce fuel consumption, but also reduce the losses that occur during the blowdown process. As an example of switching off the combustion process, simulations performed by Dönitz et al. (2009a) demonstrated that fuel savings of 6% could be achieved by adding a stop/start capability to an engine for the NEDC test cycle. Furthermore, the exhaust process needs to be replaced with the charging process. Therefore, instead of discharging the gases to the atmosphere, the gas would be discharged to a storage tank.

Equally important is removing the second revolution, allowing the engine to operate in a two-stroke configuration. Otherwise, the gas would unnecessarily undergo a second compression and an expansion process. While these processes would not add any work under the ideal cycle, it also would not be the most efficient way of recovering kinetic energy as compressed gas would only be accumulated every second revolution.

Accordingly, an appropriate solution would be required to allow the engine to operate as a compressor. The solution must address the stroke configuration, the removal of the combustion (and hence the blowdown) and exhaust processes, and the addition of a charging process. Henceforth, the discussion on potential losses during compression is based on the assumption that a suitable solution exists.

2.1.3 Real Losses

The isentropic process assumed by the ideal compression cycle infers that no losses occur within the system. Although this outcome would be ideal, the laws of physics dictate that this is unachievable. The main losses associated with all compressors are

caused by heat transfer, flow losses and leakage. These losses are also apparent in IC engines.

Furthermore, with the assumption that the combustion process is removed during braking, we can exclude losses due to finite combustion timing, exhaust blowdown and incomplete combustion due to their irrelevance during operation as a compressor.

Figures 6a and 6b show the pressure-volume diagrams of a reciprocating compressor with suction and discharge losses. The shaded areas in the figures indicate, during the charging and intake processes, where some of the losses can occur.

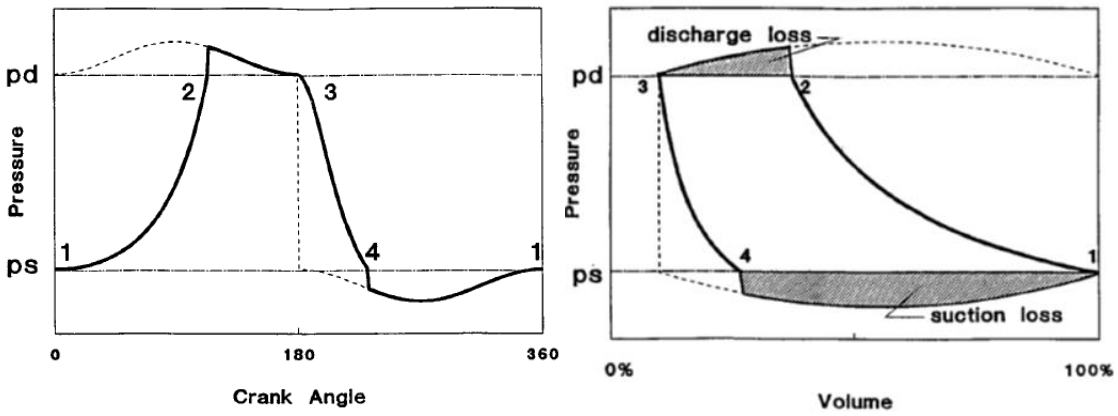

(a) (b)

Figure 6 – Pressure-volume diagram of a compressor with approximate suction and discharge losses (Hanlon 2001).

2.1.3.1 Heat Transfer in Compressors

Heat transfer is inevitable in the compression cycle and will affect compressor performance. The cylinder walls and the piston will operate at a temperature somewhere between the suction temperature and the discharge temperature (Hanlon 2001). This temperature can be considered steady even with the fluctuating temperatures of the gas during the cycle (Hanlon 2001). However, the temperature of the cylinder wall will not be uniform, particularly around the intake and discharge

valves, which makes calculating the effects of heat transfer imprecise and problematic. Furthermore, the temperature of the intake port and discharge lines will also have an effect on the overall performance of the system due to flow restrictions (Hanlon 2001).

In compressors, the most influential effect of heat transfer occurs during the intake (or suction) process (Hanlon 2001). During this process, heat is added to the gas as it flows through the suction passage and through the valve, reducing the density of the gas. Without any change in pressure, this will result in a decrease in the mass flow compressed and hence reduce the efficiency of the system.

Dynamic heat transfer also occurs during the compression stroke (Hanlon 2001). During the initial phase of the stroke, the cylinder wall is at a higher temperature than the gas – meaning heat is transferred to the gas which results in increased pressure and temperature. During the second phase of compression, the heat of the gas elevates to temperatures above the cylinder wall – meaning heat is transferred to the cylinder wall and the gas loses temperature and pressure. Hanlon (2001) suggests that the net effect of the heat exchange during the compression stroke is a slight reduction in capacity. This is due to the cylinder wall being closer to suction temperature, as the gas in the cylinder spends more time at or near suction temperature.

2.1.3.2 Heat Transfer in IC Engines

Perhaps one of the greatest differences compared to compressors is the operating temperatures of an engine. According to Pulkrabek (1997) the hot intake manifold increases the temperature of the air by approximately 25-35°C. Without an increase in pressure, this lowers the density of the incoming air which reduces volumetric efficiency. Pulkrabek (1997) states that at lower engine speeds, this effect is magnified as the air remains in the intake manifold for longer periods of time due to lower mass flow rates.

For compressor operations, the convective heating caused by the intake manifold is not ideal. However, the intake manifold is sometimes purposely heated by design.

Increasing the air temperature can enhance fuel evaporation resulting in a more homogenous mixture (Pulkrabek 1997). This is important when the IC engine is operating under normal conditions and not as a compressor. Henceforth, any solution to reduce these heating effects must also consider the underlying intake manifold design during normal operating conditions.

The other important form of heat transfer occurs in the cylinder. The cylinder temperatures of an IC engine are much higher than those in a reciprocating compressor due to the combustion process. Figure 7 illustrates the typical temperature distribution within an SI engine operating at steady state. The highest temperatures occur around the spark plug, piston face and exhaust components. However, the component with the greatest area in the cylinder is the cylinder walls. Pulkrabek (1997) states that the temperature of the wall should not exceed 180°-200°C.

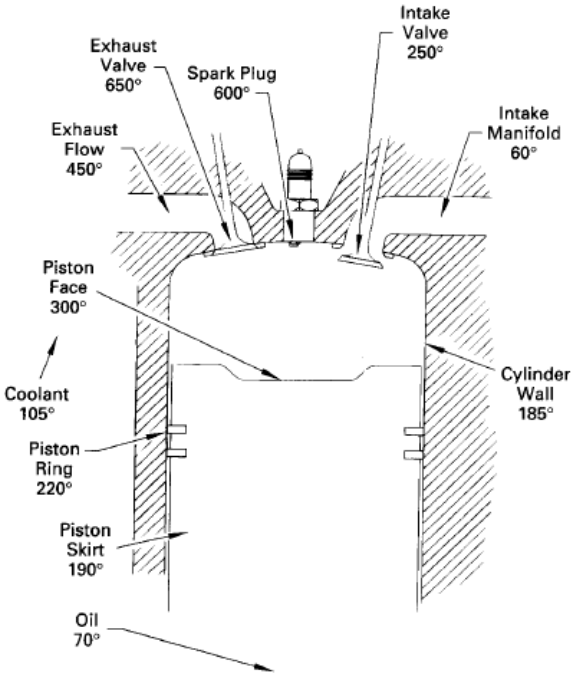

Figure 7 – Typical temperature values found in an SI engine operating at normal steady state conditions. Temperatures are in degrees C (Pulkrabek 1997).

When the air enters the cylinder, convective heat transfer occurs from the cylinder to the gas. According to Pulkrabek (1997) and Heywood (1988), the convection heat transfer

coefficient will vary greatly due to factors such as turbulence, swirl and velocity. However, perhaps the most popular correlation for determining the overall heat transfer coefficient is that produced by Woschni (1967). This is shown in Equation 3.

$$h_c = 3.26B^{-0.2}p^{0.8}T^{-0.55}w^{0.8} \qquad [\text{W/(m}^2\cdot\text{K)}] \qquad \text{Equation [3]}$$

Where B is the diameter [m] of the piston, p is the average gas pressure [kPa], T is the temperature [K] and w is the average gas velocity [m/s].

The average gas velocity can be related to the mean piston speed by the equation:

$$w = \left[C_1\bar{S}_P + C_2\frac{V_dT_g}{p_gV_g}(p - p_m)\right] \qquad [\text{m/s}] \qquad \text{Equation [4]}$$

This equation can be further simplified where $C_1 = 2.28$ and $C_2 = 0$ for the intake, compression and exhaust processes.

$$w = [C_1\bar{S}_P] \quad [\text{m/s}] \qquad \text{Equation [5]}$$

Woschni (1967) also attempted to account for the gas velocities induced by combustion during the combustion and expansion processes. However, as combustion won't take place during compression mode, the expansion process could be estimated by the same heat transfer coefficients.

Heat transfer from the cylinder to the gas is important for keeping the cylinder walls cool and within design temperatures. Under closed boundary conditions, the addition of heat to the gas increases the energy of the system. While it is not expected that a significant amount of heat will be transferred given the time the air spends in the cylinder, it would serve to increase the overall efficiency by recovering this heat that would otherwise be dissipated into the ambient environment.

2.1.3.3 Compressor Valve Timing

Valves are one of the most critical components in reciprocating compressors (Hanlon 2001). A key reason for this is the effect on the reliability of a compressor. Valves are required to function under harsh operating conditions. They are also required to operate in a highly corrosive environment with dirty gases and residues that can build up at the inlet and discharge valves. This is critical given that opening and closing times are measured in milliseconds and are required to have a life of more than a billion cycles (Hanlon 2001).

Valve performance is also affected by timing. Reciprocating compressors generally use check valves to restrict the flow to a single direction (Hanlon 2001). Due to inertia, these valves do not open and close instantaneously as assumed by an ideal valve. Therefore, valves do not stay at full lift for the entire duration of the charging and intake processes.

The spring of the valve affects the capacity of the compressor. If the spring of the valve is too heavy, the valve will close too early. This means that the average valve flow area during the intake and charging processes will be reduced. If the valve spring is too light, it can result in the valve not closing at dead centre, which is the optimal timing according to Hanlon (2001) – TDC for the discharge valve and BDC for the suction valve.

2.1.3.4 IC Engine Valve Timing

Compared to compressor valves, the intake and exhaust valves are commonly operated mechanically using a cam shaft and spring loaded poppet valves.

Valve timing

Valves are opened and closed at a rate sufficient enough to avoid noise and excessive cam wear (Pulkrabek 1997). Comparable to compressors, valves are not at full lift for the entire process. For this reason engine valve timing ensures that the valves are fully open at peak piston velocity (Pulkrabek 1997). Unfortunately, a consequence of this

can be the overlapping of valves. Valve overlap occurs when the intake and exhaust valves are open at an instant in time. It arises when the intake valve is opening and exhaust valve is closing. While it is an issue in combustion engines, it should not be a concern while operating in compression mode.

Opening intake valve before TDC

The opening of the intake valve is designed to be fully open at TDC when the intake stroke begins in order to maximise air intake (Pulkrabek 1997). For this to happen, the valve must start to open at 10 to 25° before TDC (Pulkrabek 1997) due to the finite opening speeds. During compression mode, the intake valve will open much later after the expansion process has finished. In compressors, this is controlled by the pressure differential (between the pressure in the cylinder the intake pressure) and the heaviness of the spring (Hanlon 2001). It is currently unclear whether or not the intake valve should open before pressure in the cylinder reaches intake pressure to maximise air intake. The consequence of opening too early is that air in the cylinder could escape back into the intake manifold due to the cylinder pressure being higher than intake pressure.

Closing intake valve after BDC

The closure timing of the intake valve affects the amount of air accumulated in the cylinder (Pulkrabek 1997). In an engine, the intake valve is not fully closed until after BDC. According to Heywood (1988) the intake valve can remain open until 50 to 70° after BDC to allow the air to continue to flow into the cylinder. This is in contradiction to the closing timing of the intake valve for compressors as specified by Hanlon (2001). It is assumed that this is due to the difference in the type of valves used. Unlike check valves, poppet valves do not rely upon pressure differentials and therefore provide more timing flexibility.

During intake, a pressure differential exists even when the piston reaches BDC and air still flows into the cylinder. The air continues to enter until it is compressed to equalise with the intake pressure. This is the optimal time for the intake valve to close according to Hanlon (2001), who states that volumetric efficiency will be reduced if the valve

closes too early. However, if the valve closes too late, air will be forced back through the intake manifold with the same effect on volumetric efficiency (Hanlon 2001).

Pulkrabek (1997) states that the optimal valve closing point is highly dependent on engine speed. Higher speeds require later closing times due to the greater pressure drop across the intake valve caused by higher mass flow rates of air, while earlier closing positions are more ideal for lower speeds with smaller pressure differentials.

Closing exhaust valve after TDC

Similar to the intake valve, the exhaust valve remains fully open until TDC to ensure the maximum amount of exhaust is displaced out of the cylinder chamber. Furthermore, it also reduces the back pressure on the cylinder head which can reduce the total efficiency of the engine. Closing therefore begins very close to TDC which means total closure doesn't occur until 8 to 50° after TDC (Pulkrabek 1997).

The closure timing of the exhaust valve could be compared with the valve closure timing required for the tank charging process when operating in compression mode. Again, the optimal closure timing stated by Hanlon (2001) conflicts with the timing of the exhaust valve for an IC engine. Adding to the complexity of this however is the difference in exhaust pressure and the pressure of the air storage tank. Therefore, at higher tank pressures, it could be expected that TDC is the optimal closure timing. However, at lower tank pressures, it may depend on engine speed.

2.1.3.5 Compressor Flow Losses

When dealing with the flow of gases through pipes, the gas will always experience losses to some extent. A loss of flow rate due to fluid friction is one source of losses, along with choked flow which can occur in high speed flows. Furthermore, due to the intermittent flow nature of reciprocating compressors, a pulsating flow can occur which leads to pressure losses.

The unsteady nature of the gas inflow and outflows from the compression cylinder causes pulsations in the suction and discharge piping. Should the amplitude of the pulsation levels be sufficient, this can affect the valve open and close timing (Hanlon 2001). This can cause the average inlet and discharge pressures to deviate from design pressures and result in power and capacity values differing from performance standards, either favourably or adversely.

Additionally, gas flowing through a restriction will experience a pressure drop due to the increase in velocity caused by the restriction. This is evident in Benoulli's equation for incompressible flows. This can be exacerbated by valve restriction, commonly caused by the build-up of solids, improper springing of valves, pulsation of gasses and design inefficiencies.

2.1.3.6 IC Engine Flow Losses

Fluid Friction Losses

When air flows through passages it undergoes a pressure drop due to a viscous flow friction (Pritchard 2011). The pressure entering the cylinder will therefore be less than the surrounding atmospheric air pressure resulting in a reduction of volumetric efficiency. The pressure drop effect is worsened by flow restrictions that can be found in the engine intake system of a motor vehicle. These restrictions include the air filter, throttle plate, intake manifold and intake valve. The viscous drag caused by these components increases with the square flow velocity, as shown by Heywood (1988) in Equation 6, where the total quasi-steady pressure loss due to friction can be related to the mean piston speed. Heywood (1988) states that the intake pressure can be 10 to 20 % lower than atmospheric when the piston is moving at close to its maximum speed.

$$p_{atm} - p_c = \rho \bar{S}_p^2 \sum \xi_j \left(\frac{A_p}{A_j}\right)^2 \qquad \text{[Pa]} \qquad \text{Equation [6]}$$

Where, p_{atm} is the atmospheric pressure [Pa], p_c is the cylinder pressure [Pa], $\bar{S}$ is the mean piston speed [m/s], ξ_j is the resistance coefficient for the component, and A_p and

A_j represent the piston area [m^2] and the component minimum flow area [m^2] respectively.

Besides designing the intake to reduce restrictions, one method to reduce these effects is to increase the diameter of the intake manifold. Flow velocity will be decreased and pressure losses can be reduced. However, Pulkrabek (1997) notes that a decrease in velocity will also result in poorer mixing of the air and fuel along with less accurate cylinder-to-cylinder distribution.

An alternate solution proposed is to use a variable intake system. These have been used to optimise SI engine performance including improvements in fuel efficiency (Ceviz & Akin 2010) by varying the intake plenum length/volume. Usually this is achieved with the use of two separate intake ports governed by valves to two different manifolds with different lengths. Alternatively a single path runner system with variable lengths using mechanical methods could also be used. The shorter manifold used at higher engine speeds to deliver maximum power would help reduce pressure losses associated with fluid friction and improve volumetric efficiency for compressing air.

Valve Flow Losses

The losses across the valves in an engine will be different to those experienced by reciprocating compressors. This is due to the difference in geometry between poppet valves and reed valves. The mass flow rate across a poppet valve can be estimated by Equation 7 (Heywood 1988). This equation shows that the mass flow rate $\dot{m}$ [kg/s] is related to a change in pressure across the valve.

$$\dot{m} = \frac{C_D A_R p_0}{(RT_0)^2}\left(\frac{p_T}{p_0}\right)^{1/\gamma}\left\{\frac{2\gamma}{\gamma-1}\left[1-\left(\frac{p_T}{p_0}\right)^{(\gamma-1)/\gamma}\right]\right\}^{1/2} \qquad \text{Equation [7]}$$

Where γ is the specific heat ratio. The flow rate is related to the upstream stagnation pressure p_0 [Pa] and the stagnation temperature T_0 [K], which is the intake system gas state for flow through the intake valve, and the cylinder gas state for flow through the exhaust valve; the downstream pressure p_T [Pa] which is the cylinder pressure for flow through the intake valve, and the exhaust pressure for flows through the exhaust valve;

and the reference area A_R [m2] which is a characteristic of the valve design. The discharge coefficient C_D allows for the real gas flow effects and is usually determined experimentally.

Due to finite valve opening and closing speeds, flow losses will be higher due to reduced flow areas. Figure 8, illustrates the change in flow area caused by valve lift as a function of crank angle. Figure 8a shows the valve lift in centimetres compared to the camshaft angle on the x-axis. Figures 8b and 8c show the flow area in cm^2 with respect to the income and exhaust valves respectively. Therefore it would be expected that valves with quicker lift times will increase the time at maximum flow area and reduce flow losses.

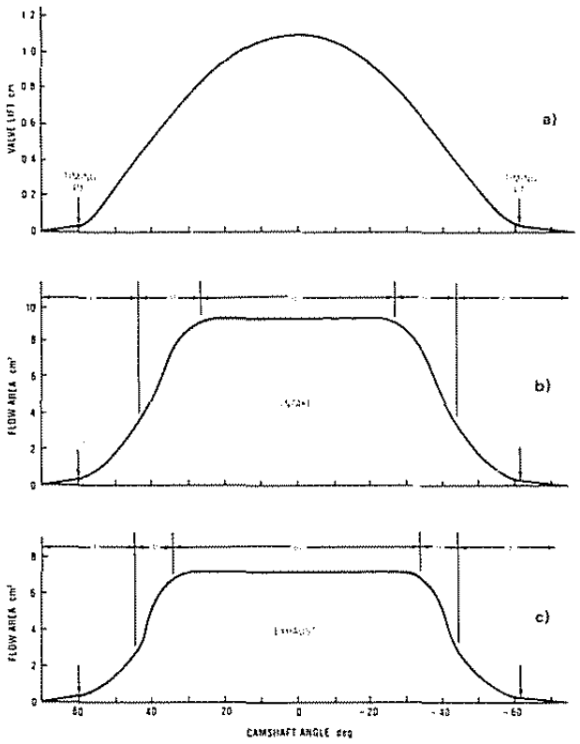

Figure 8 – Valve-lift curve showing the minimum intake and exhaust flow area as a function of crank angle (Asmus 1982).

Choked flow

Choked flow occurs in IC engine systems when a maximum flow rate is achieved and cannot be increased even with a change in downstream conditions. High air flow

velocities eventually reach sonic velocity at some point in the intake system, usually the most restricted passage such as the intake valve. The effect of this limiting condition is a decrease in efficiency at higher speeds.

Flow pulses

Unlike compressors, the pulsed gas flow in engines will not have an effect on valve timing. This is due to the valves being controlled mechanically. Instead, the pressure waves created can affect volumetric efficiency (Pulkrabek 1997). Pulkrabek (1997) explains that the wavelength is dependent on pulse frequency and flow rate or velocity. When waves reach the end of the manifold or an obstruction, they create a reflected pressure wave. This reflected pressure wave travels in the opposite direction and interacts with the primary wave. In phase pressure waves that reinforce at the intake valve will result in pressure pushing the air into the cylinder, increasing volumetric efficiency (Pulkrabek 1997). Out of phase pressure pulses result in reduced pressure pushing air into the cylinder and lower volumetric efficiency.

The solution proposed by Pulkrabek (1997) is to use active intake systems which adapt to different engine speeds. For example, a single path manifold with variable length or a dual path system with or without secondary throttle plates. This solution is supported by experimental research undertaken by Ceviz (2007), who showed that a variation in the plenum volume caused an improvement on both engine performance and pollutant emissions at different speeds.

2.1.3.7 Leakage

Leakage is common in all compressors in some form. While the magnitude of these leakages varies to some extent, it will always have a negative impact on efficiency. Hanlon (2001) states that the general leakage paths in reciprocating compressors occur around the piston rings and the valves which do not form a perfect seal to prevent reverse flow.

Hanlon (2001) explains that leakage through the suction valve has two effects. First, it causes hot gas to enter the inlet passage. This is essentially equivalent to heat transfer,

therefore reducing gas density and reducing efficiency. Secondly, it directly results in a loss of the compressed gas. This is also the effect of discharge valve leakage. Gas previously compressed is wasted as it escapes back into the cylinder. This will decrease the mass flow compressed without any decrease in the power into the system.

As the designs of SI four-stroke piston engines are similar to reciprocating compressors, they will also experience small losses due to leakage. Increased cylinder pressure can result in unwanted gas flow into crevices such as between the piston and piston wall and also through the piston rings. Pulkrabek (1997) states that leakage in a properly designed and well maintained engine is small and usually only accounts for less than one percent of the cylinder volume. However, with the addition of an air storage tank the losses may slightly increase if the valve to the charging line is not sealed sufficiently.

2.1.3.8 Mechanical Frictional Losses

Friction in engines reduce the amount of power delivered to the wheels and is dissipated as heat. The work produced per cycle is marginally consumed to overcome the friction which is the result of adjacent components rubbing against each other. In comparison, during compression the friction reduces the amount of power available to compress the air which reduces efficiency of the system. Sources of friction can include friction due to the engine, transmission and drivetrain.

The friction mean effective pressure (FMEP) can be calculated using Equation 8. The equation is a correlation based on the data collected by Barnes-Moss (1975) (cited in Heywood 1988) for the total motoring friction for four-stroke SI engines with a displacement between 845 and 2000 cm^3 at wide open throttle. The correlation has been adjusted for a two-stroke cycle with the output in [Pa] as opposed to bar.

$$FMEP = \left[0.97 + 0.15\left(\frac{N}{1000}\right) + 0.05\left(\frac{N}{1000}\right)^2\right] \cdot \frac{10^5}{2} \qquad \text{Equation [8]}$$

Where N is the engine speed in revolutions per minute.

2.2 Applications of Compressed Gas

2.2.1 Introduction

The literature reveals that there are two main areas for which compressed gases has useful application in automobiles. These are:

- Supercharging; and
- Pneumatic Engines.

While each of these has different operations, fundamentally they both serve the purpose to improve vehicle performance through efficiency and a reduction in emissions. These will now be individually discussed in greater detail.

2.2.2 Supercharging

Supercharging is not a new concept. Two types of supercharging technologies are used in many of the motor vehicles on our roads today: superchargers and turbochargers. Both are used to increase the intake pressure supplied to the IC engine. The increased intake pressure results in more air and fuel (for a given air/fuel ratio) into the combustion chamber each cycle. The additional air and fuel results in an increase in the net power output (or work done) and has also been shown to increase volumetric efficiency. In addition, it means that smaller engines can be used which can result in decreased fuel consumption.

The turbocharger essentially works like a centrifugal compressor. Mounted in the exhaust flow of the engine, the exhaust gases are used to spin the turbine (usually a radial inflow turbine) which in turn drives the centrifugal compressor. As the pressure in the exhaust system is only slightly higher than atmospheric pressure, only a very small pressure drop can occur. For this reason, it is necessary to operate the turbine at high speeds which requires design consideration to ensure safety and reliability.

The major advantage of turbochargers is that the compressor is driven only by waste energy in the exhaust. Therefore, very little of the useful energy produced by the engine is used to power the compressor. However, the disadvantage of using the exhaust to drive the compressor is the occurrence of turbo-lag. This refers to the slow response to torque demand at low engine speeds. It consequently requires several engine cycles before the change in exhaust flow is at a rate sufficient to accelerate the turbine to produce the desired inlet pressure.

A solution to the issues associated with turbocharging is highlighted by Dönitz et al. (2009a). Using a hybridized IC engine to compress air (therefore the ability to alternate between normal operation and a compressor mode), the stored air can be used in a manner that allows the design of turbochargers to be focused entirely on engine efficiency. The research conducted by Dönitz et al. (2009a) focused on fuel consumption using a dynamic programming technique. The results of their research showed that engine hybridization combined with downsizing a turbocharged engine and cylinder deactivation can save as much as 34% fuel. They concluded that engine downsizing was the most important contributing factor in overall fuel consumption.

Superchargers on the other hand, compress air using a positive displacement system, the two most common being a screw type compressor or a lobe pump. The compressor is mechanically driven by either a belt, chain or gears directly off the engine crankshaft. Ultimately, the mechanical drive of the supercharger is both its biggest advantage and greatest downfall. The major advantage is the very quick response times to throttle changes. Supercharged engines do not suffer the lag experienced by turbochargers as the change in engine speed is immediately transferred from the crankshaft to the compressor. However, the power to drive the compressor is essentially a parasitic load much like air conditioning.

Alternatively, the compressed air accumulated in a high pressure tank could be used as a direct alternative to superchargers and turbochargers. This would overcome the parasitic effect of the supercharger, the lag associated with turbochargers, along with the additional weight associated with each system. One method for achieving this is

explained by Higelin, Charlet and Chamaillard (2002) and illustrated in Figure 9. During the compression process (1-2 in Figure 9), the charge valve can be opened to add an additional compression step to the process as illustrated in process 10-11 in Figure 9. Higelin, Charlet and Chamaillard (2002) explain three main differences this strategy offers:

1. Using the conventional intake stroke, the life of the high pressure tank air charge can be enhanced (2 to 4 times) as the amount of air displaced only needs to be in excess of the cylinder charge at atmospheric pressure.
2. A higher high-pressure cycle IMEP due to the dual stage compression stroke. It can be further maximised by opening the charge valve as late as possible while closing when the cylinder pressure reaches tank pressure.
3. Adversely, the higher exhaust pressure compared to the intake pressure means that the low-pressure cycle IMEP is negative.

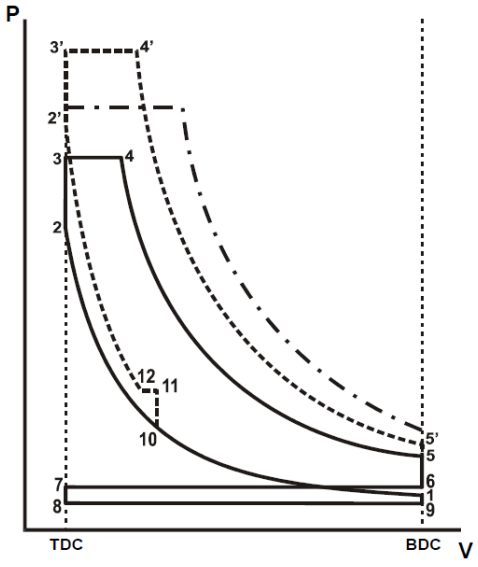

Figure 9 – Idealised pressure-volume diagram of an engine with the option of charging an air tank during the compression process (Higelin, Charlet & Chamaillard 2002).

The main problem associated with the increase in the intake air pressure is the increase in air temperature caused by the compressive heating. Higher intake temperatures result in higher gas temperatures during the whole cycle, particularly during the compression

stroke. This is undesirable in SI engines as it can cause self-ignition and knocking problems. In order to avoid this, cooling mechanisms such as intercoolers can be used to lower the temperature of the newly compressed air. However, the introduction of these systems can add to design issues due to space constraints and losses caused by the additional weight.

2.2.3 Pneumatic Engines

Two different types of systems have been theorized and tested: a pneumatic engine operation mode using the IC engine, and a hybrid pneumatic power system.

2.2.3.1 Pneumatic Engine Operation (Hybridized IC Engine)

Under this concept, an additional operating mode of the IC engine is considered. It assumes that the engine can operate as either a conventional IC engine or a pneumatic motor powered by compressed air. The pneumatic motor operation cycle is illustrated in Figure 10. It follows a two-stroke configuration that can lead to higher torque outputs as well as lower friction losses (Higelin, Charlet & Chamaillard 2002).

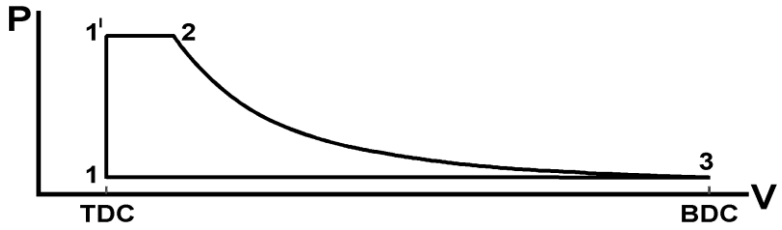

Figure 10 – Ideal pressure-volume diagram of an engine operating as a pneumatic motor (Schechter 1999).

The first step is cylinder charging (process 1-1' of Figure 10). The charging valve opens at point 1 allowing the compressed air to discharge into the cylinder until the cylinder pressure reaches the tank pressure at point 1'. This process occurs at constant volume and is assumed to be adiabatic. Discharge continues from process 1' to 2 at constant pressure under the assumption that the process is isobaric.

The second step is cylinder expansion (process 2-3). The charging valve is closed from points 2 to 3 and the air charge expands in the cylinder. The process produces work and forces the piston down. This process is considered adiabatic and reversible. It is important to note that the closure timing of the charging valve should be selected to ensure that full expansion takes place until pressure reaches atmospheric pressure. If the timing is not controlled, losses could occur, much like the blowdown process when the exhaust valve opens after expansion in a four-stroke engine.

The final step is the exhaust stroke (process 3-1). The exhaust valve opens at point 4 allowing the cylinder to discharge into the exhaust system until it reaches atmospheric pressure (or exhaust pressure). Alternatively, Schechter (1999) says that the air could be expelled through the intake valve to avoid excessive cooling of the catalyst. The potential energy of the air at point 4, but can be managed by optimising the closure timing of the charging valve. The remaining air is expelled during process 4 to 1 which is considered isobaric.

Using the IC engine to compress air while braking and in a pneumatic motor mode during acceleration, several researchers concluded that efficiencies could be achieved. Simulations performed by Higelin, Charlet and Chamaillard (2002) showed a reduction of around 15% of the global fuel consumption without system optimisation. Furthermore, Trajkovic et al. (2007) reported regenerative efficiencies of up to 33%, where regenerative efficiencies is defined as the ratio between the positive IMEP and the negative IMEP of the pneumatic motor and compression modes respectively. It has been noted however that the simulations performed by Higelin, Charlet and Chamaillard (2002) were based on real world simulations while Trajkovic et al. (2007) focused on controlled simulations with some optimisation. The results are therefore difficult to compare.

Another similar method that has been considered was introduced by Schechter (1999), called the Air-Power-Assist (APA) cycle. This cycle can operate in both a two-stroke and a four-stroke operation, however for the purposes of this analysis we will only consider the four-stroke operation as illustrated in Figure 11. Under this cycle the

engine continues to operate as an IC engine. The main difference is that the high pressure tank delivers a charge of compressed air during the intake stroke at point 1 in Figure 11. The air expands and performs work on the cylinder head causing displacement. The charging valve then closes at point 3. This air charge is then used in the combustion process. This part of the cycle is comparable to that in Figure 10.

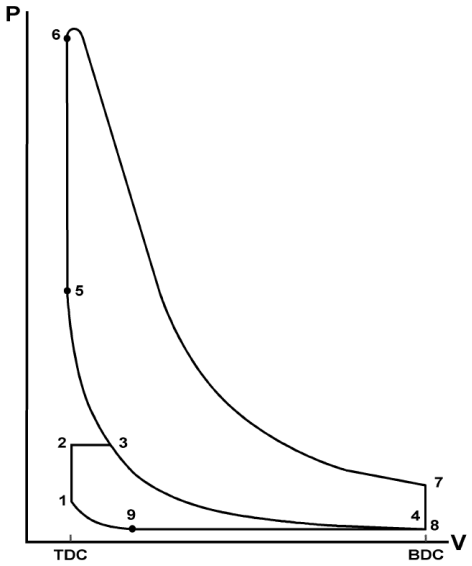

Figure 11 – Pressure-volume diagram of the Air-Power-Assisted cycle for a four-stroke cycle (Schechter 1999).

The advantage of the APA cycle is the work performed by the compressed air supplements the work performed by combustion in the other cylinders while reducing pumping losses. Thus reducing work needed to be performed by the combustion process, which means that the fuel consumption could potentially be reduced. Furthermore the APA cycle allows for higher engine torque during acceleration.

The mathematic model used by Schechter (1999) to demonstrate the performance of the cycle resulted in a reduction in fuel consumption by more than 50% when compared to a conventional engine. Further work conducted by Tai et al. (2003) used the APA cycle to model and calculate savings under typical city and highway driving conditions. The air hybrid model reported a 38% reduction in fuel consumption (Tai et al. 2003). The APA cycle was taken one step further by Kang et al. (2008) who demonstrated that the

APA cycle could be implemented into an engine system for use in heavy duty applications.

2.2.3.2 Pneumatic Hybrids

A hybrid pneumatic power system (HPPS) comprises a similar setup to many modern HEVs. A dedicated air compressor is used in place of a generator, which applies a steady load on the engine to charge a high pressure vessel. The high pressure vessel is used much the same way as a battery to store energy while the flow of compressed air replaces the flow of electrical energy. A pneumatic motor is then used to put work back into the drive train like an electric motor would in a HEV.

Huang and Tzeng (2005) used this model in addition to recycling the exhaust energy by merging it with the compressed air. Thus, the pressure of the compressed air was enhanced resulting in higher flow rates and increasing the overall thermal efficiency of the IC engine. The results of their study showed an efficiency increase of 18% of the modelled vehicles overall efficiency under controlled operating conditions. Further analysis was undertaken using a regulated running-vehicle test mode in Huang et al. (2005). Using experimental verification and analysis they showed that the HPPS system could meet the requirements of a standard operational mode.

2.2.4 Other Applications

While this literature review has focused mainly on supercharging and pneumatic motor applications, the compressed gas may have additional uses. For example, it could be used for pneumatic valve actuation. Alternatively, it could be used to restart an engine and reduce the need for an electric starter – also freeing up space and decreasing vehicle mass at the same time. This allows the engine to be shut down and eliminate fuel consumption losses while idling or coasting.

2.3 Other Design Factors

2.3.1 Air Storage Tank

The air tank is a pressure vessel used as the storage medium for the recovered energy. Fundamental to the system will be the volume and the temperature control of the vessel. Both of these affect the rate of which pressure will increase, compression braking characteristics, and also the safety of the vessel.

2.3.1.1 Volume

The optimal tank volume should be determined by the amount of energy recoverable under typical braking (deceleration) conditions. However, it is usually a compromise between fuel savings, cost and design constraints. The optimal tank volume should not be designed based on the sole objective of being capable of recovering energy for the maximum possible change in speed. This requires larger tanks which are more expensive and space restrictive. To overcome this, once the air tank reaches capacity, the brakes can be used if the compression braking effect is not sufficient to stop the vehicle.

The amount of kinetic energy recovered will be dependent upon the kinetic energy (i.e. mass and change in speed) of the vehicle, less the work lost due to friction of the engine and drivetrain, aerodynamic drag and rolling resistance. The volume of the tank can therefore be expressed as a function of the vehicle mass, friction losses and change in vehicle speed.

2.3.1.2 Pressure and Temperature

Eliminating heat losses from the air tank would minimise the energy losses within the KER system. One method to achieve this is to ensure the tank is sufficiently insulated. Alternatively, temperature could be controlled by using the heat of the engine or the heat of the exhaust gases. Schechter (1999) illustrates that temperature can be

controlled using a double-wall heating jacket. Exhaust gases flow through the jacket which is controlled by an actuator depending on the amount of heat required. It can result in greater regenerative efficiencies of the KER system.

Another method is the hot tank solution. Heat may be added to the tank so that it can increase the temperature of the stored air, resulting in an increase in the pressure of the tank and the internal energy. This allows the pressure to exceed the pressures achievable from pumping alone. This strategy would therefore supplement the pneumatic motor application for the compressed gas. Consequently, the additional heat may render the compressed gas less desirable for supercharging due to the phenomena known as engine knock.

A hot tank strategy of course would require strict monitoring to ensure that the heat of the tank or the pressure in the tank is within design specifications. It may also require the tank to be manufactured from a more costly material with better heat resistivity and strength properties.

The alternative cold tank strategy noted by Dönitz et al. (2009b) is mainly focused on the supercharging application for the compressed gas. The tank is no longer used to store enthalpy, rather its primary function is to store air mass. The lower temperature of the air stored reduces probability of knock, and promotes engine downsizing. However, the heat losses reduce the overall regenerative efficiency of the KER system. Therefore, the maximum pressure attainable for this strategy is defined by the compression ratio ε of the engine, and therefore the maximum cylinder pressure.

$$p_{tank,max} = p_{in} \times \varepsilon^{n} \qquad \text{[Pa]} \qquad \text{Equation [9]}$$

Where p_{in} [Pa] is the pressure in the cylinder at BDC, ε is the compression ratio and n is the polytropic coefficient for compression. Hence, it may be inferred that engines with higher compression ratios will be able to recover more energy than engines with lower compression ratios.

2.3.1.3 Safety

Safety in pressure vessels is very important due to the state of the gases that could be substantially different to the ambient conditions. Should the pressure vessel fail, it could cause serious injury or could be potentially fatal.

Therefore several safety measures would be required to be undertaken.

- Operation of the pressure vessel should be monitored to ensure that the tank pressure and temperature do not exceed design specifications. Pressure switches may be used for disengaging tank charging if and when the pressure in the storage vessel reaches pre-set design pressure. A safety valve may also be employed which can open if the pressure exceeds pre-set design pressure.
- Inspections should be carried out regularly to assess key components. This may include monitoring metal thickness and maintaining pressure relief (or safety) valves.

2.3.2 Cylinder Modifications

In order to achieve the compression operating mode, modifications may be required for the intake system, exhaust system or a combination of both. As a result, the literature reveals that the best way to achieve the change in operation with minimal system modifications is to use a dedicated valve for charging and discharging compressed gas to and from the storage tank. This valve would only operate when the engine is functioning as a compressor. If the timing of this valve can be controlled, it could be optimised for volumetric efficiency at different engine speeds. It also reduces the need to use a reed valve to limit the flow to a singular direction. Hence, only one additional valve would be needed.

However, the introduction of an additional valve will present as a design issue. The issue stems from the limited available space in an already overcrowded cylinder head. This includes multiple components such as intake and exhaust valves, spark plugs and direct injection devices. As a consequence, a compromise must be made that allows the

compressor operation mode performance to be maximised, without restricting engine performance during conventional operation mode.

2.3.3 Variable Valve Timing

Fully variable valve timing (VVT) is a necessity to the proposed concept. It provides a flexible timing system using electromagnetic or pneumatic actuators as opposed to the mechanical actuation using a camshaft. It allows for an infinite number of opening and closing times. Furthermore, the system would provide many advantages:

1. The engine can easily change between operation modes. It allows for complete control over valve actuation and timing.
2. It could be used to optimise valve timing during conventional operation mode at different engine speeds. Studies performed by Fontana and Galloni (2009) showed that VVT could be used to optimise valve timing to improve engine efficiency at part loads. Furthermore, simulations performed by Dönitz et al. (2009a) concluded that a fuel savings of 12.5% was possible when all valves have variable actuation.
3. Faster opening and closing times can also be achieved compared to those operated by camshafts (Pulkrabek 1997). This was demonstrated by Elkady et al. (2013) who concluded that a proposed electromagnetic VVT system could increase the average valve lift, therefore reducing flow resistance and increasing volumetric efficiency.

However, certain design requirements would need attention.

1. Firstly, should the opening and closing speeds be increased, the valves must avoid a collision with the piston at all times. All engine designs will already consider this for intake and exhaust valves. However, it must also be taken into account for the charge valve. This is pertinent for engines with high compression ratios with less cylinder head volume.

2. The air flow discharging from the air tank to the cylinder must be adjustable, while providing precision and reproducibility. This is imperative to supercharging due to the air and fuel mass ratios.
3. The system should require minimal energy consumption. Particularly for holding the charging valve shut to reduce leakage.

2.3.4 Compression Braking

Calculating the braking force required will help to determine the braking mean effective pressure (BMEP) and whether the compression braking is a sufficient substitute for friction brakes. Braking force is calculated in Equation 10 as the force of the car due to inertia less the rolling friction and the aerodynamic drag.

$$F_b = F_i - F_{rf} - F_D \quad [\text{N}] \qquad \text{Equation [10]}$$

Where the force due to inertia, rolling friction and aerodynamic drag are calculated as:

$$F_i = M_v a \quad [\text{N}] \qquad \text{Equation [11]}$$

$$F_{rf} = M_v g f \quad [\text{N}] \qquad \text{Equation [12]}$$

$$F_D = C_D \frac{1}{2} \rho \bar{V}^2 A \quad [\text{N}] \qquad \text{Equation [13]}$$

Where,

M_v is the vehicle mass [kg];

a is the deceleration in [m/s^2];

g is gravity [m/s^2];

f is the coefficient of rolling friction;

C_D is the drag coefficient;

ρ is air density [kg/m^3];

$\bar{V}$ is the average velocity of the vehicle [m/s]; and

A is the total surface area in contact with the air [m^2].

The required BMEP is:

$$BMEP = F_b 2\pi r_t \eta_t / (r_g V_d) \quad [\text{Pa}] \qquad \text{Equation [14]}$$

Where, r_t is the tire radius [m], η_t is the mechanical efficiency of the transmission and driveline, r_g is the gear ratio between the engine and wheels and V_d is the engine displacement [m^3].

Finally, the required BMEP can be related to indicated mean effective pressure (IMEP) of the compression braking as calculated using Equation 15. IMEP is the net work of the pistons per cycle per unit volume displaced.

$$IMEP = BMEP - FMEP \quad [\text{Pa}] \qquad \text{Equation [15]}$$

The IMEP produced by the cylinders is calculated by taking the work of the piston W_P [W] and dividing it by the volume displaced V_D [m^3] as shown in Equation 16.

$$IMEP = \frac{W_P}{V_D} \quad [\text{Pa}] \qquad \text{Equation [16]}$$

Should the IMEP of the engine in compressor mode not be sufficient to produce enough BMEP, the friction brakes would need to be engaged. However, Schechter (1999) proposes that an alternate solution is to change the opening timing of the charge valve. The charge valve could be opened early as shown in Figure 12. The pressure in the cylinder quickly rises to the pressure in the air tank at point 3', therefore producing higher levels of work and a higher IMEP and BMEP. This backflow effect was shown in the experimental results of Kang et al. (2008). Alternatively, the charging valve could be opened later as shown in Figure 13. When the valve opens at point 3, the cylinder pressure drops to the pressure level in the air tank at point 3'.

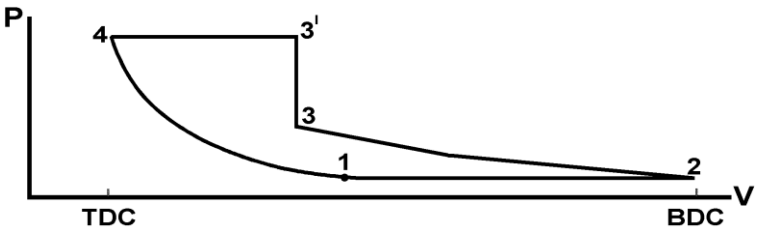

Figure 12 – Pressure-volume diagram of Type 2 compression braking with early charge valve opening showing a higher IMEP (Schechter 1999).

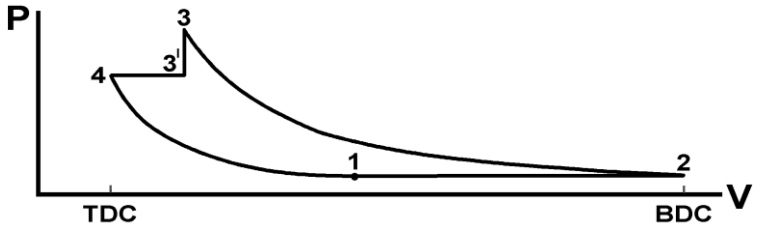

Figure 13 – Pressure-volume diagram of Type 2 compression braking with late charge valve opening showing a higher IMEP (Schechter 1999).

2.4 Conclusion

The preceding section highlights the parallels and differences between IC engines and reciprocating compressors. With the addition of a VVT system and design modifications to the cylinder head for an additional valve, it is more than plausible that an IC engine can operate as a compressor and even a pneumatic motor. This is demonstrated by researchers such as Kang et al. (2008) who are starting to perform experimental analysis based on early studies completed by Schechter (1999).

Some of the key areas that will affect the performance of an IC engine as a compressor include heat transfer, flow losses, leakage and mechanical friction. However, these are also present in compressor technologies. It is important to note that they may have different magnitudes of effect due to IC engines having higher temperatures in the

intake system and cylinder, different valves types used, and different valve control systems.

The applications for the compressed gas are promising. With the use of VVT the engine could be used as a pneumatic motor. Alternatively, the compressed gas could be used to power a dedicated pneumatic motor in conjunction with exhaust gases. Supercharging provides an alternate solution, with the advantage that it won't suffer parasitic losses or turbo-lag. However, the heat of the compressed gas could increase the likelihood of engine knock.

3 Methodology of the Numerical Simulation

3.1 Introduction

This research methodology considers a quasi-dimensional numerical simulation of an IC engine operating as a reciprocating two-stroke compressor. The objective of the simulation is to determine the amount of kinetic energy that is recoverable during the deceleration of a motor vehicle.

The numerical simulation of the engine was modelled using MATLAB. The simulation is based on a model previously prepared by Buttsworth (2002) to determine the performance of a fuel inducted engine with a heat release profile as a function of the crank angle. The method used for that simulation is aligned closely with the IC engine calculations presented by Ferguson (1986). Taking this model, it has been adjusted to simulate the compression and accumulation of gas in a storage tank.

The methodology was dissected into four main sections:

1. Model parameters – this section describes the key assumptions that have been made during the modelling process and the input parameters used for the simulation. It also details how the compressor losses have been accounted for.
2. Compressor simulation – this section details how the simulation functions and the procedures developed to simulate each process in the compression cycle, including valve timing and any further assumptions made specific to each process.
3. Model validation – initial results were calculated and tested for appropriateness. This was done to ensure that the model works as intended and demonstrates the validity to the results.
4. Drive cycle – the model was simulated using a drive cycle. This section describes the test cycle used to produce the results.

3.2 Model Parameters

This section specifies the parameters used in the model including the operating assumptions, modelling assumptions and the input parameters.

3.2.1 Operating Assumptions

A number of other key assumptions have been made about the operation of the IC engine and the simulation as a compressor.

1. Two-stroke compressor mode: During braking, it is assumed that the engine no longer operates conventionally and will operate as a two-stroke compressor. The combustion process is therefore removed, and the exhaust process is replaced with a charging process.
2. Variable valve timing: A variable valve system is fundamental to allow switching between engine operation modes. It allows for the independent control of valve lift timing and duration for each individual valve. It is assumed that valve actuation is pneumatically controlled
3. Valve configuration: For simplicity, one extra valve is used to charge and discharge air to and from the air tank.
4. Continuously variable transmission: In order to simplify the simulation, it is assumed that the engine speed is held constant using a fully variable transmission. The engine will consequently only operate at one speed during deceleration.

3.2.2 Modelling Assumptions

The following assumptions relate specifically to the parameters of the model.

1. System boundaries: For the purposes of the simulation, the system boundaries considered include the engine cylinders and the air tank only. Due to the nature of the model, it does not extend to the intake manifold and the heating effects have been accounted for in the gas intake parameters.

2. Air tank: the air tank is assumed to be sufficiently insulated and is modelled adiabatically. Therefore, no heat exchange will take place between the gas and the air tank walls. This assumption has also been applied to the pipes connecting the cylinders and the air tank.
3. Gas properties: For the charging and intake processes, it is assumed that the properties of the air behave like an ideal gas, and can be determined using the ideal-gas equation of state. For the compression and expansion processes, the thermodynamic properties of the air are specified in the MATLAB file airdata.m as listed in Appendix C1. The data for the air scheme used in the model was taken from Gordon and McBride (1971). The function airdata.m returns the polynomial coefficients for 10 different species over a range of temperatures.
4. Farg.m: The function Farg.m in the code is used to the state of mixtures of fuel, air and residual gases for the compression and expansion processes. As the equivalence ratio has been set to zero and the residual fraction is set to zero (therefore no residual combustion products), the properties returned by the Farg.m function should reflect the state of air inside the cylinder at any interval of time during the compression and expansion processes.
5. Valve timing: The valve timing has been optimised (within the limitations of the model) to minimise the amount of work required to compress the gas. The timing is therefore based on the gas pressure in the cylinder.
    a. Charge valve opening time: Opens when the gas pressure in the cylinder is equal to the tank pressure.
    b. Charge valve closing time: Closes at TDC.
    c. Intake valve opening time: When the gas pressure in the cylinder is equal to the intake pressure.
    d. Charge valve closing time: Closes at BDC.

3.2.3 Inputs Parameters

The parameters used in the model are highlighted in this section. The inputs have been selected based on a small motor vehicle with four cylinders and an engine capacity of 2,000 cm^3. The geometry for this engine is specified in Table 4.

Engine geometry:	**Value**
Engine bore (m)	0.088
Engine stroke (m)	0.082
Half stroke to rod ratio	0.25
Compression ratio	10
Volume at TDC (m^3)	0.554×10^{-3}
Volume at BDC (m^3)	5.542×10^{-3}
No. of cylinders	4
Engine displacement (m^3)	2.0×10^{-3}

Table 4 – Engine geometry parameters used in the numerical simulation model.

The engine thermofluids are contained in Table 5. The piston blowby constant is the one used by Buttsworth (2002). The residual fraction is set to nil as the engine is operating in a compressor mode, and no residual gases should be present.

Engine Thermofluids:	**Value**
Piston blowby constant (s^{-1})	0.8
Residual gas fraction (combustion products)	0.0

Table 5 – Engine thermofluid values used in the numerical simulation model.

The parameters of the motor vehicle are specified in Table 6. The rolling friction coefficient has been selected based on the typical rolling coefficient of a road tyre, while the coefficient of drag and the drag surface area are modelled off of a small automobile.

Vehicle Parameters	Value
Mass (kg)	1360
Rolling friction coefficient	0.015
Mechanical Efficiency	0.9
Coefficient of drag	0.3
Drag Surface Area (m^2)	2.3
Tire radius (m)	0.3

Table 6 – Vehicle parameters used in the numerical simulation model.

The parameters of the air tank are specified in Table 7. The initial pressure and temperature are assumed to be at atmospheric pressure and temperature.

Air Tank Parameters	Value
Volume (m^3)	0.05
Initial pressure (kPa)	101
Initial temperature (K)	300

Table 7 – Air tank parameters used in the numerical simulation model.

3.2.4 Model Losses

The following section outlines how the heat transfer, flow losses and leakage have been accounted for in the model.

3.2.4.1 Heat Transfer

The heat exchanged between the cylinder walls and piston, and the gas has been accounted for using the correlation presented by Woschni (1967). The heat transfer is therefore a function of the gas pressure, gas temperature and engine speed per Equations 3 and 5 (refer to section 2.1.3.2). Although combustion does not take place during the

compression cycle, the change in temperature of the cylinder walls over time is not considered as it is beyond the scope of this project.

3.2.4.2 Flow Losses

Losses associated with the flow through the intake manifold have been considered by using a lower intake pressure of 90 kPa and a higher intake temperature of 330 K. All other flow losses such as the pipe acoustics have not been considered due to the limitations of the model.

3.2.4.3 Leakage

It is assumed that no leakage occurs from the air tank or the system connecting the air tank to the engine cylinders. Piston blowby has been considered for the compression and expansion processes, with the constant detailed in Table 5.

3.3 Engine Compressor Simulation

The model will simulate each revolution by splitting the compression cycle into 5 main functions as shown in Figure 14.

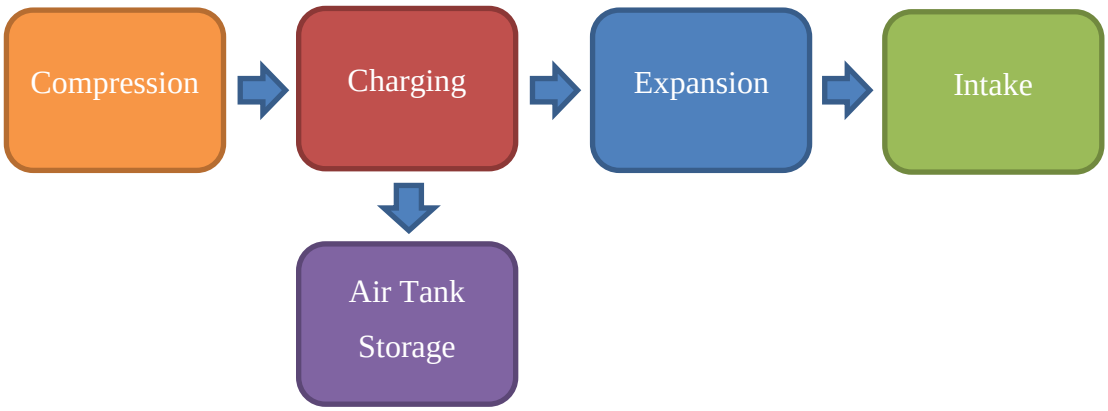

Figure 14 – Diagram of the processes numerically modelled in MATLAB.

3.3.1 Compression

At the commencement of the first stroke, the compression process begins. The model assumes that this process starts at BDC, when all valves are closed and the piston starts to move upwards into the cylinder and ends when the charge valve opens. The initial gas conditions for the first iteration have been calculated based on the intake pressure and temperature and the valve losses. For all subsequent iterations, the state of the gas is based on the new intake of gas and the expanded residual gas from the previous cycle.

The compression process is controlled by the function ratescomp.m (Appendix C6). The function returns the derivatives of pressure, temperature, work, heat transfer and heat leakage, with respect to crank angle. It takes into consideration the heat transfer and blowby for each change in crank angle, thereby affecting the pressure and temperature of the gas in the cylinder.

For simplicity purposes, the ratescomp.m function is run for crank angles of $-\pi$ to 0. Using the in-built MATLAB function ode45.m, the differential equations returned by ratescomp.m are integrated to produce the pressure, temperature and work of the gas in the cylinder for each change in crank angle. The pressure output was then used to calculate the crank angle at which the charge valve should open.

3.3.2 Charging

The charging process begins when the charging valve opens and finishes at TDC. For the purposes of this model, it is assumed that this process takes place at constant pressure (isobaric) and is isothermal.

The model operates on the basis that for every half engine revolution, mass is charged to the air tank. That is, two cylinders will pump gas into the tank every half revolution (for a 4 cylinder engine). In order to determine the change in air mass contained within the air tank (for each revolution), the change of the mass in the cylinder, before and after the charging take place, was calculated. The steps used for this calculation are:

1. Calculate the mass of the gas in the cylinder just before the charge valve opens using the ideal gas equation. The state of the gas (pressure and temperature) is given by the compression data output and the volume of the cylinders calculated at the determined crank angle.
2. Calculate the mass of the gas in the cylinder at TDC (when the charge valve closes) using the ideal gas equation. The volume at TDC was used, and the pressure and temperature of the gas when the charge valve opens (as the process is considered isobaric and adiabatic).
3. The change in mass was calculated by subtracting the mass calculated in step 3 from the mass calculated in step 2. This is the mass of the charge.

3.3.3 Air Tank Storage

The air tank is modelled on the assumption that the tank is adiabatic. The internal energy of the tank was calculated using the internal energy equation for an ideal gas.

$$dU = m_t \cdot c_v \cdot dT + T_c \cdot c_v \cdot dm \quad [\text{J}] \qquad \text{Equation [17]}$$

Where,

m_t is the initial mass in the tank [kg];

c_v is the specific heat at constant volume;

dT is the change in temperature of the gas in the tank [K];

T_c is the temperature of the charge [K]; and

dm is the mass of the charge [kg].

This has been simplified further in Equation 18.

$$dU = dm \cdot c_v \cdot dT \quad [\text{J}] \qquad \text{Equation [18]}$$

Where dT [K] is in respect of a temperature reference point, which has been set at the initial tank temperature.

Once the mass of the charge has been calculated, the new state of the gas within the air tank can be calculated. The process used to calculate the new state of the gas in the air tank is:

1. Calculate the initial internal energy of the air tank using Equation 18 and a temperature reference point of 30 K.
2. Calculate the internal energy of the charge using Equation 18 and a temperature reference point of 300 K.
3. Calculate the new internal energy of the tank by adding the energies calculated in step 1 and 2.
4. Calculate the new state of the gas in the air tank.
    - The new temperature is calculated by dividing the total energy in step 3, by the specific energy multiplied by the combined mass of the charge and the mass of the tank before charging. The reference temperature was then added back.

$$T_t = \frac{U_t + U_c}{c_v \cdot (m_t + m_c)} + T_{ref} \qquad \text{[K]} \qquad \text{Equation [19]}$$

    - The new pressure of the tank can be calculated using the ideal gas equation, with the new mass (step 3), the new temperature (step 4) and the volume of the tank.

This process is contained in the MATLAB file compressor_mode.m in Appendix C2.

3.3.4 Expansion

The expansion process begins at the start of the second stroke, when the charge valve closes (at TDC) and the piston begins to move back down. The initial conditions of pressure and temperature are taken from the pressure and temperature of the gas calculated at the end of the charging process.

The expansion process is governed by the function ratesexp.m (Appendix C7). The function is very similar to the ratescomp.m function, and returns the same derivatives (pressure, temperature, work, heat transfer and heat leakage) with respect to crank angle. It takes into consideration the effects of heat transfer and blowby.

The ratesexp.m function is run for crank angles between 0 and π, although the outputs used are only considered from 0 to the crank angle calculated when the intake valve opens. Using the function ode45.m once more, the differential equations returned by ratesexp.m are integrated to produce values of pressure, temperature and work for each change in crank angle. The pressure output was then used to calculate the crank angle at which the intake valve should open.

3.3.5 Intake

The intake process occurs when the intake valve opens and draws in fresh air. It is assumed that the process occurs when the cylinder pressure reaches intake pressure during the expansion process. The process is modelled assuming the process is isobaric and isothermal. The output from the process is used to calculate the new initial conditions before the compression process starts again.

The steps for calculating the new initial conditions are:

1. Determine the gas mass in the cylinder just before the intake valve opens. This was calculated using the ideal gas equation, with the state of the gas (given by the expansion data) at the crank angle when the charge valve opens.
2. Determine the air mass in the cylinder resulting from fresh intake. Using the ideal gas equation, this is calculated using the change in volume between BDC and at the crank angle when the intake valve opens, and the intake pressure and temperature for the fresh gas.
3. Find new initial conditions:
    a. Calculate new pressure using partial pressures with respect to the mass fraction of the fresh intake and the residual gas.

b. Calculate the new temperature using ideal gas law and the pressure calculated in step 3a, volume at BDC and the combined mass in steps 1 and 2.

3.4 Model Validation

A number of tests were carried out to ensure that the model was working correctly.

1. Compression and Expansion Processes: The model started as a combustion engine, simulating the compression, combustion and expansion strokes. Consequently, the model had to be changed to remove the combustion process. This involved setting both the equivalence ratio and the residual exhaust fraction to nil. For the purposes of this test, the piston blowby constant and the heat transfer were removed to simulate the processes as ideal. The results are shown in Figures 15, 16 and 17. The figures show that the gas pressure and temperature return to their initial states at the end of the processes, while no net work is performed on the gas. The figures therefore illustrate that the processes are adiabatic and reversible as expected.

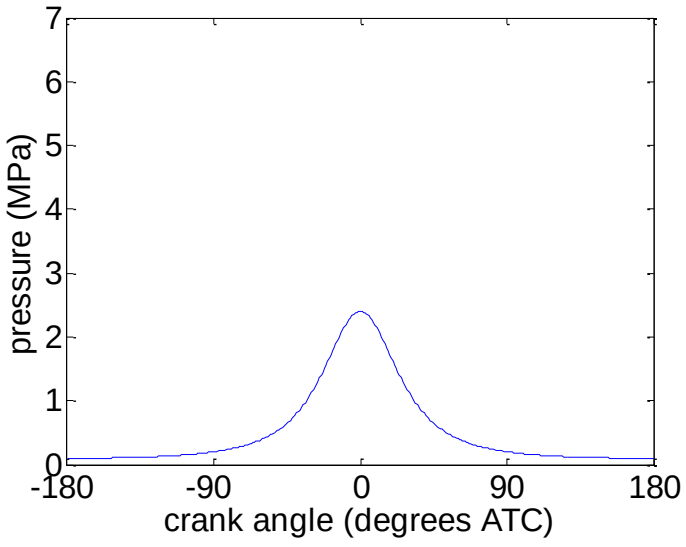

Figure 15 – Pressure vs crank angle of the gas in the cylinder for the ideal compression and expansion processes during testing of the model's validity.

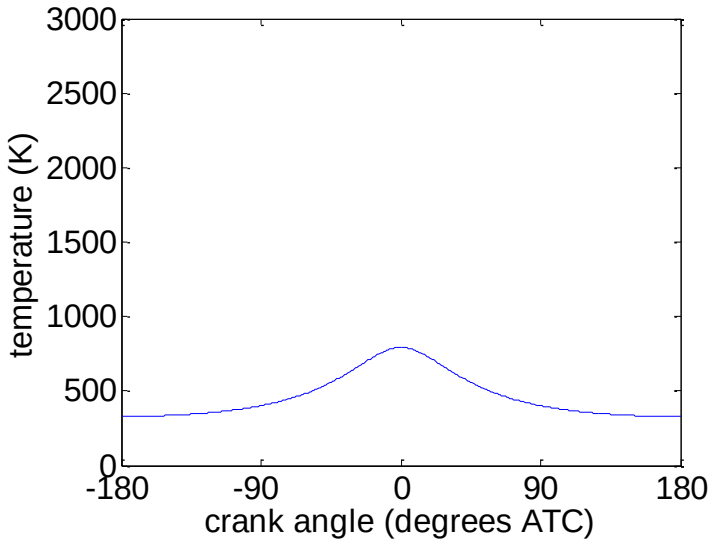

Figure 16 – Temperature vs crank angle of the gas in the cylinder for the ideal compression and expansion processes during testing of the model's validity.

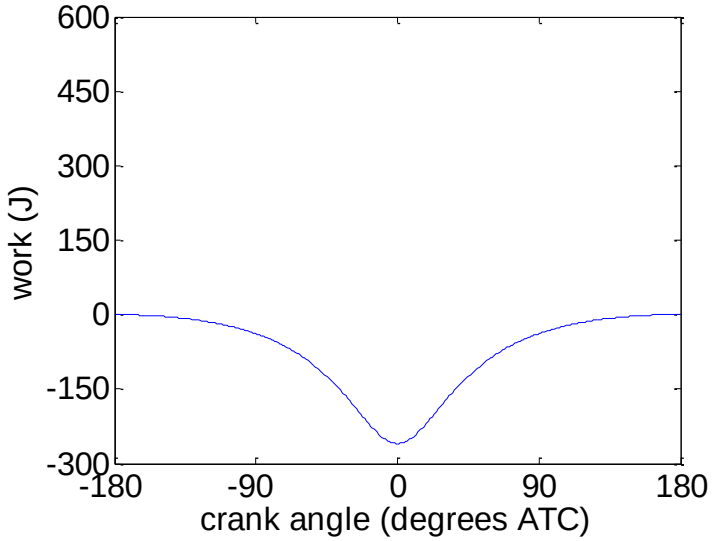

Figure 17 – Work performed (for two of the four cylinders) vs crank angle on the gas in the cylinder for the ideal compression and expansion processes during testing of the model's validity.

2. Charging and Intake Processes: The charging and intake processes were added to the model and the outputs repeated. Again, the heat transfer and piston blowby have been removed for this test. Figures 18 and 19 demonstrate that the charging and intake processes are isobaric and isothermal as expected. Furthermore, Figures 18

and 21 can be compared with ideal compressor Figures 4b and Figures 4a respectively for their similar shapes. Finally, the net work per cycle is shown in Figure 20 which illustrates that pumping work has occurred due to the difference in tank pressure and intake pressure. The results are shown after a 5 second period at 2,000 RPM.

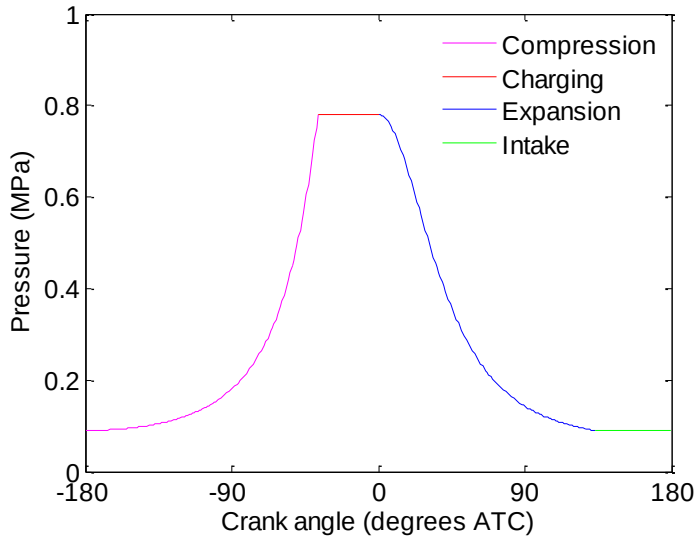

Figure 18 – Pressure of the gas in the cylinder of the ideal compression cycle during testing of the model validity.

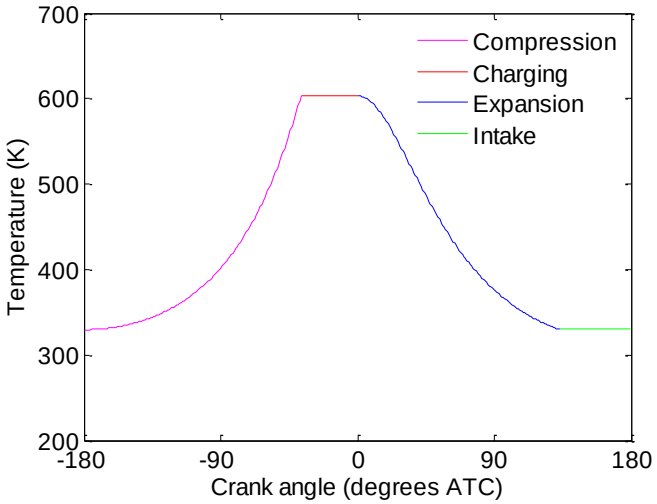

Figure 19 – Temperature of the gas in the cylinder of the ideal compression cycle during testing of the model validity.

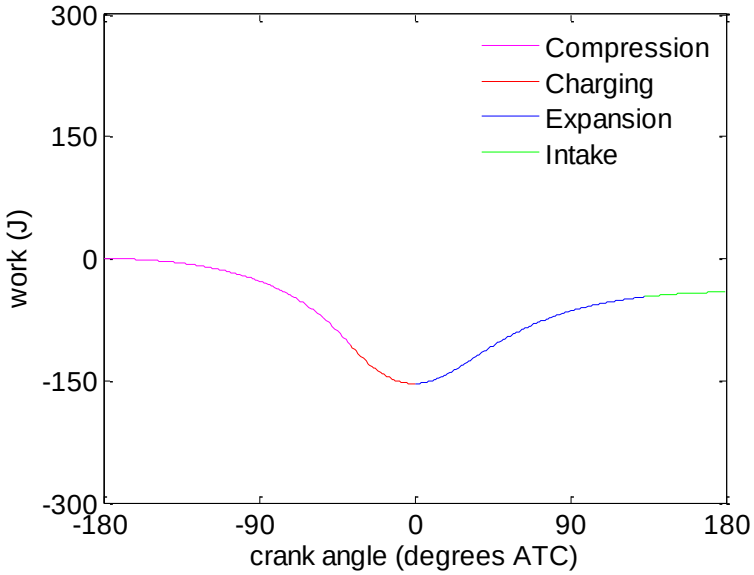

Figure 20 – Work performed on the gas in the cylinder of the ideal compression cycle during testing of the model validity.

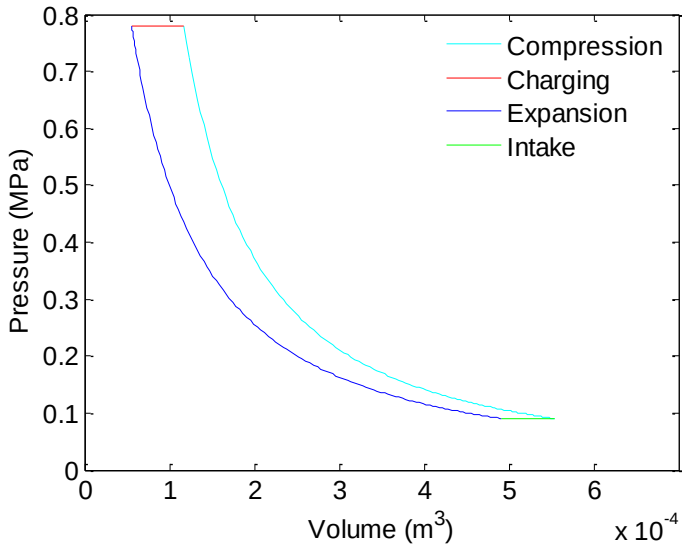

Figure 21 – PV diagram of the ideal compression cycle during testing of the model validity.

3. Tank pressure: The pressure in the tank was tested to ensure that the pressure does not go over the maximum cylinder pressure. Figure 22 shows that the pressure increasing over time does not exceed the maximum theoretic pressure indicated by Equation 9.

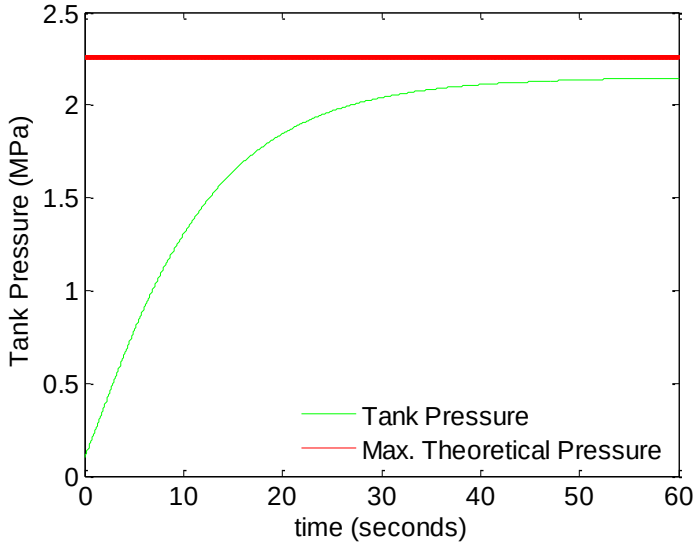

Figure 22 – Air tank pressure per engine revolutions compared to the theoretical maximum pressure for testing the model for validity.

4. Valve opening times: Now that it has been established that the processes are working correctly, the opening of the charging and intake valves was tested for appropriateness over a period of 20 seconds. Figure 23 illustrates several key effects that would be expected:
    a. As the air tank pressure increases, the crank angle at which the valves open also increases.
    b. The valve timing approaches TDC for the charging valve and BDC for the intake valve.
    c. Due to diminishing returns, the difference in valve opening times start higher, and reduce over time as the pressure in the tank approaches maximum pressure.

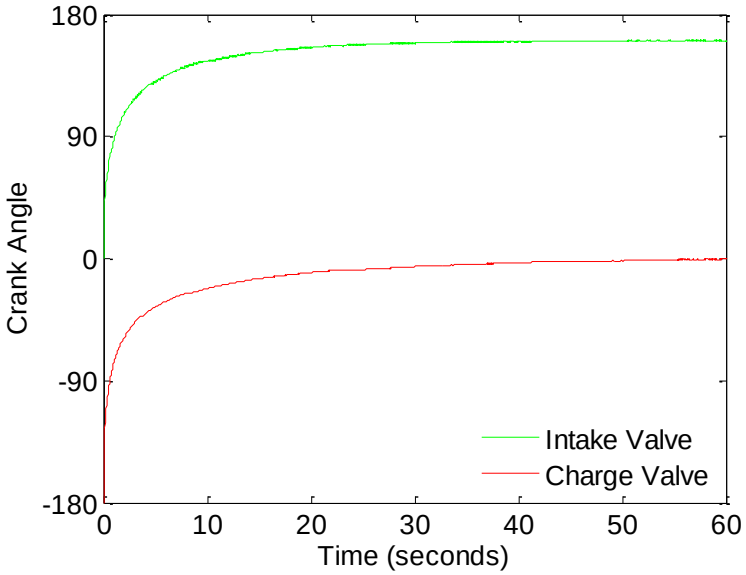

Figure 23 – Charging valve and intake valve opening timing as a function of crank angle over time during testing of the model validity.

3.5 Drive Cycle

For the purposes producing more meaningful results, the performance of the simulation will take into account a certain number of variable parameters with respect to a drive cycle. The drive cycle used in this project is the NEDC. The significant considerations taken from the model include the speed of the vehicle and the rate of deceleration. The engine speed will be optimised based on these vehicle performance requirements.

The NEDC is a test cycle designed to assess the emission levels for certification purposes of light duty vehicles in Europe. The NEDC is performed on a chassis dynamometer under controlled conditions.

The test is made up of two identifiable components. The first is the Urban Driving Cycle ECE-15 (Figure 24) which is repeated four times. It represents European city driving and is characterised by low engine load, low engine speed and low exhaust gas temperature.

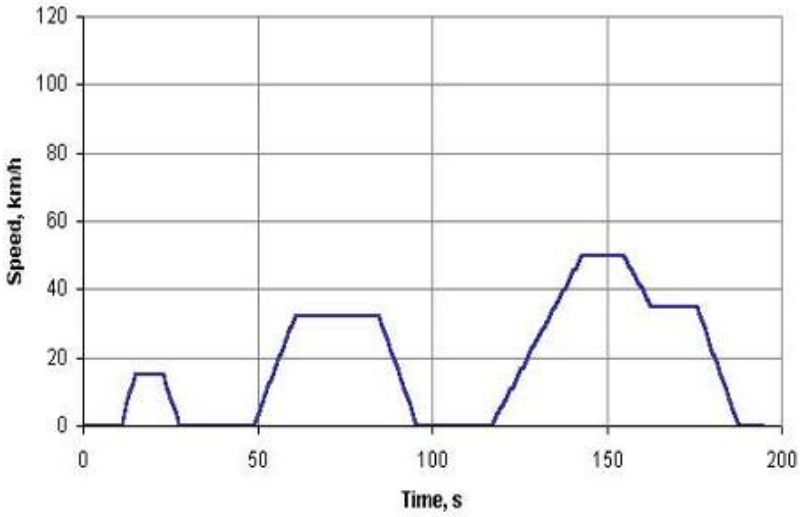

Figure 24 – Graph of speed over time for the Urban Driving Cycle ECE-15 (DieselNet 2013).

Table 8 shows the breakdown of the speed and timing of the driving cycle. It is assumed that all acceleration and deceleration is uniform. The total cycle (after repetition) lasts 780 seconds with a theoretical distance of 3,976 meters and average speed of 18.35 km/h (DieselNet 2013).

Time (seconds)	**Speed (km/h)**
0-11	0 (idle)
11-15	Acceleration
15-23	15
23-28	Deceleration
28-49	0
49-61	Acceleration
61-85	32
85-96	Deceleration
96-117	0
117-143	Acceleration
143-155	50
155-163	Deceleration
163-176	32

Time (seconds)	Speed (km/h)
176-188	Deceleration
188-195	0

Table 8 – Summary of speed, timing and duration for the Urban Driving Cycle ECE-15.

The second component is the Extra-Urban Driving Cycle (EUDC) which is completed once after the completion of the ECE-15 repetitions (Figure 25). It represents a more aggressive and higher speed driving condition with a maximum speed of 120 km/h.

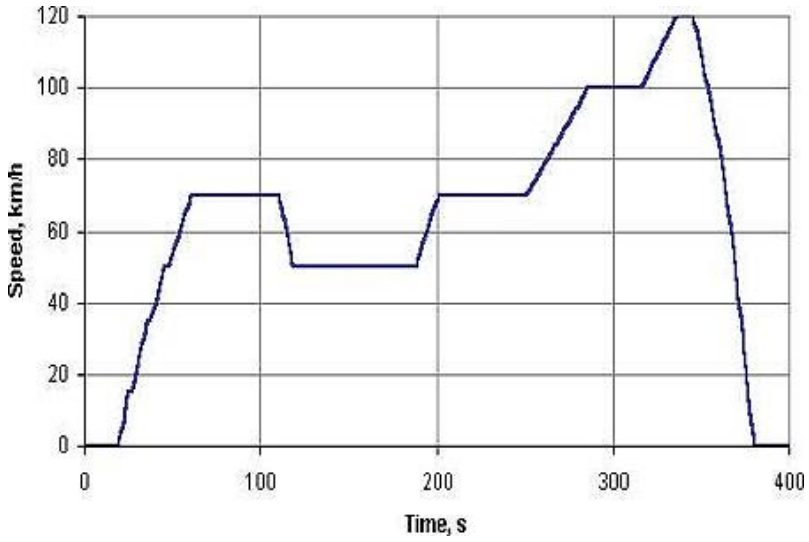

Figure 25 – Graph of speed and time for the Extra-Urban Driving Cycle (DieselNet 2013).

Table 9 (overpage) illustrates the timing and speed of the EUDC. Total duration of the cycle is 400 seconds with a theoretical distance of 6,955 meters and an average speed of 62.6 km/h (DieselNet 2013).

Time (seconds)	Speed (km/h)
0-20	0 (idle)
20-61	Acceleration
61-111	70
111-119	Deceleration
119-188	50
188-201	Acceleration
201-251	70
251-286	Acceleration
286-316	100
316-336	Acceleration
336-346	120
346-380	Deceleration
380-400	0

Table 9 – Summary of speed, timing and duration of the Extra-Urban Driving Cycle (EUDC).

The important performance characteristics that affect this model are the change in speed, the time during the speed change, and therefore deceleration. These parameters have been summarised in the Table 10 with their frequency over the drive cycle.

Deceleration Event	Initial Speed (km/h)	Final Speed (km/h)	$\bar{V}$ (m/s)	Time (s)	Deceleration (m/s^2)	Frequency
1	15	0	2.08	5	0.833	4
2	32	0	4.44	11	0.808	4
3	50	32	11.39	8	0.625	4
4	32	0	4.44	12	0.741	4
5	70	50	16.67	8	0.694	1
6	120	0	16.67	34	0.617	1

Table 10 – Summary of deceleration events during the NEDC and the frequency of their occurrence.

4 Results and Discussion

4.1 Introduction

The numerical model produced during this research was applied to the NEDC to calculate the amount of energy that can be recovered over a driving cycle. Using the six deceleration events identified in the previous section, the engine speed was optimised to produce an average BMEP that maximised the effect of compression braking, while minimising the reliance on the friction brakes.

The energy recoverable over these six events was calculated and recorded. Using this data, inferences have been made about the possible energy savings that compressed gas KER can achieve. The results were further analysed, drawing conclusions about the usefulness of the energy and the efficiency of recovering the energy. Finally, the effect of heating and flow losses were explored with respect to energy recovery, and the limitations of the model have also been highlighted.

4.2 Engine Speed Optimisation

Optimising the engine speed for each deceleration event was important for two reasons. Firstly, it was used to ensure that the braking effect due to compression braking was not in excess of the braking requirements of the driving cycle. Secondly, it was used to reduce the reliance on the friction brakes and maximise the amount of energy recovered. Therefore, the optimisation has been completed on the premise of producing a BMEP that is equivalent to, or slightly under the average BMEP required.

In order to find the average BMEP required, the braking force necessary during each deceleration event was calculated and the results compiled. This was achieved using Equations 10 to 13 of the literature review (refer to section 2.3.4), and the values shown in Tables 6 and 10 of the methodology. The results are shown in Table 11.

Event	F_i	F_d	F_{rf}	F_b
1	1,133.3	1.8	200.1	931.4
2	1,099.0	8.1	200.1	890.8
3	850.0	53.3	200.1	596.6
4	1,007.4	8.1	200.1	799.2
5	944.4	114.0	200.1	630.3
6	1,333.3	114.0	200.1	1,019.2

Table 11 – Braking force calculated for each deceleration event of the NEDC test cycle.

The average BMEP was then calculated using Equation 14 and the vehicle parameters given in Table 6. The average gear ratio used in this equation was calculated using Equation 20 below.

$$r_g = N / \left(\frac{s}{2\pi r_t}\right) \qquad \text{Equation [20]}$$

Where, N is the number of engine revolutions during deceleration, s is the distance [m] travelled during deceleration, and r_t is the operating tire radius [m].

From this equation, it can be seen that the average BMEP required is a function of the engine speed. As the average BMEP produced is also a function of engine speed, trial and error was used to find the engine speed to the nearest integer that maximised energy recovery and reduced the reliance on the friction brakes. The results are shown in Table 12 overpage.

Deceleration Event	Braking force required (N)	Average BMEP required (kPa)	Optimised Engine Speed (RPM)	Average BMEP produced (kPa)
1	931.43	101.79	509	99.68
2	890.76	130.11	820	129.44
3	596.62	137.77	1331	137.68
4	799.17	129.05	742	128.43
5	630.28	147.52	1922	147.50
6	1,019.17	129.30	3554	129.26

Table 12 – Engine speed optimised to meet the braking requirements for the NEDC deceleration events.

The results indicate that the engine braking effect is sufficient to slow the vehicle down to a stop. This is consistent with the simulation results by Higelin, Charlet and Chamaillard (2002) who only used the friction brakes during the final slowdown of the EUDC.

The results also show that the events with the highest initial speeds require a higher RPM to slow the vehicle down. However, this does not necessarily correlate to higher average BMEP required. Deceleration Event 6 appears to be the outlier in this situation. While the RPM of Event 6 exceeds all other events, the average BMEP required is actually lower than some of the other events due to the rate of deceleration, and the braking characteristics of the event.

Figures 26 and 27 show the braking characteristics for Event 1. These figures illustrate that the BMEP produced is not uniform during deceleration. Events 1 to 4 follow a similar pattern, in starting at a lower BMEP and finishing with a higher BMEP compared to the average required BMEP. This suggests that deceleration increases over time.

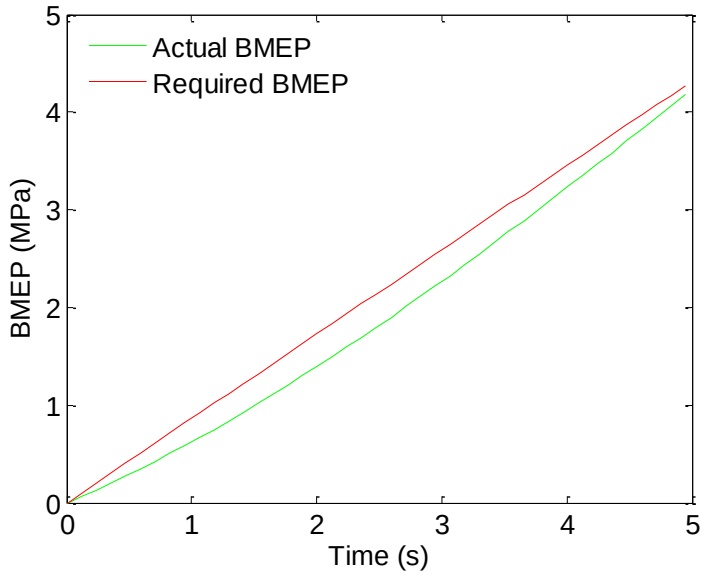

Figure 26 – Cumulative BMEP produced over time during deceleration Event 1 compared to the average BMEP required.

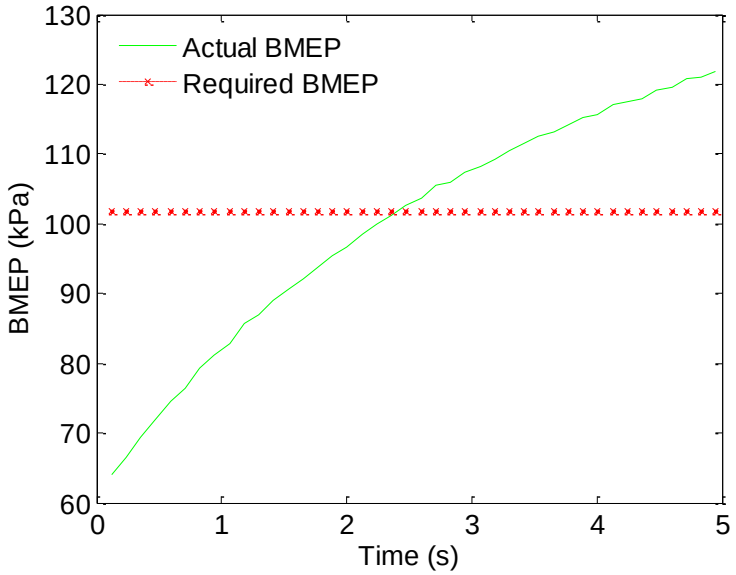

Figure 27 – BMEP produced during deceleration Event 1 compared to the average BMEP required.

The exception to this characteristic is in Events 5 and 6. The BMEP produced drops below the average required BMEP towards the end. This characteristic is especially pronounced for Event 6 in Figures 28 and 29. The figures illustrate that a peak period of deceleration occurs in the middle of the deceleration event. On further analysis, the

turning point appears to occur between 110 to 120 revolutions for all events. This appears to occur because the work recovered by the expansion process begins to increase relative to the work done during compression and the pumping losses.

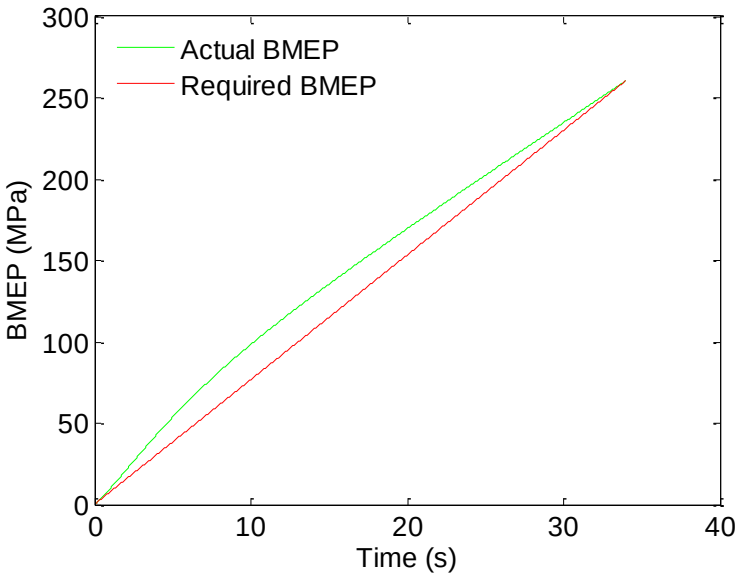

Figure 28 – Cumulative BMEP produced over time during deceleration Event 6 compared to the average BMEP required.

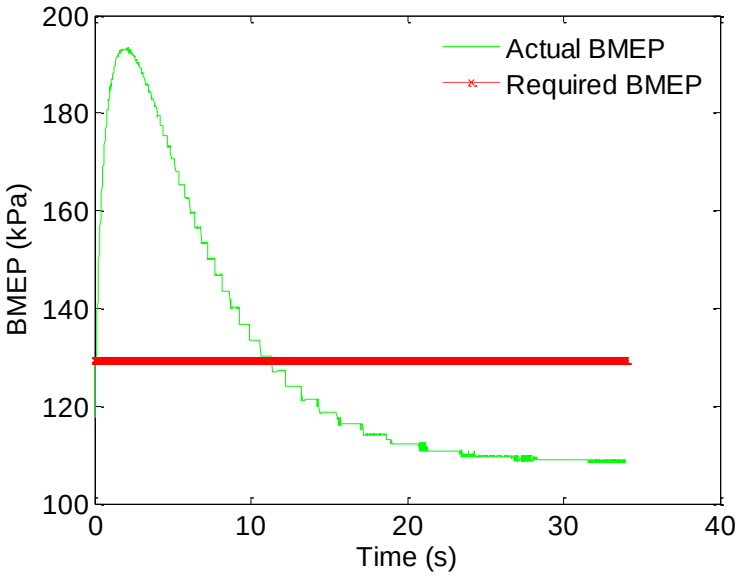

Figure 29 – BMEP produced during deceleration Event 6 compared to the required average BMEP required.

The full results of the BMEP produced for Events 1 to 6 are displayed in Figures 35 to 46 in Appendix B2.

4.3 Energy Recoverable

The simulation was run with the engine speed optimised for each braking event. Each event was run separately, with the tank pressure and temperature at initial conditions. Therefore, this assumes that the energy is put back into the system after each braking event. Table 13 shows the energy recovered for each event, multiplied by the frequency at which the event occurs during the NEDC and the total energy recoverable during the cycle.

Deceleration Event	Energy Recovered* (kJ)	Frequency	Total Energy Recovered (kJ)
1	5.069	4	20.276
2	28.699	4	114.796
3	35.457	4	141.828
4	28.165	4	112.662
5	53.439	1	53.439
6	131.019	1	131.019
TOTAL			574.020

*Calculated using the change in the internal energy of the air storage tank

Table 13 – Energy recovered with optimised engine speed for the NEDC cycle deceleration events.

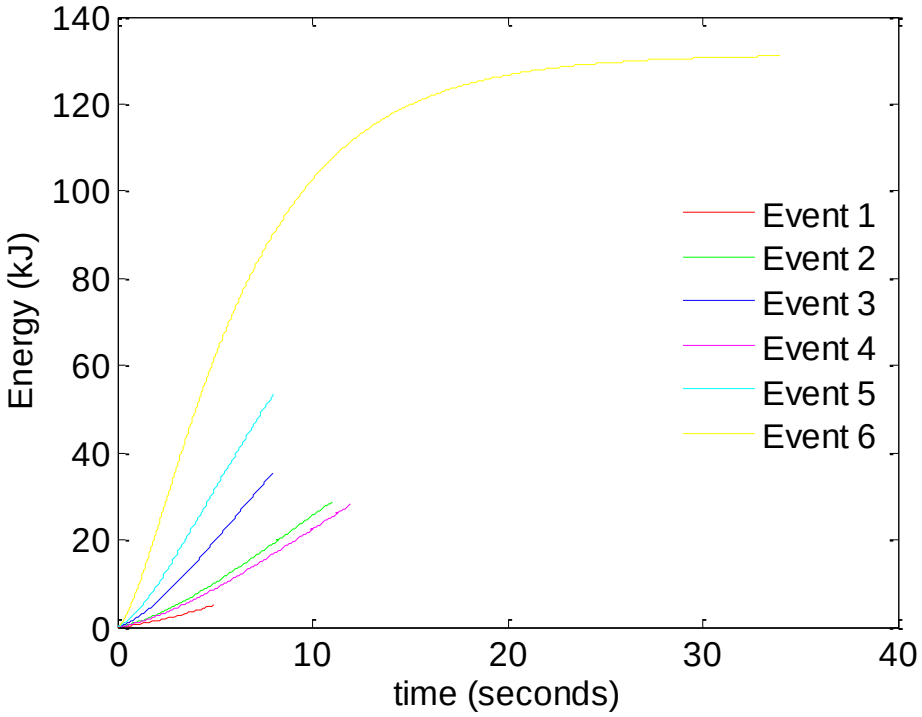

Figure 30 – Energy change of the tank during the 6 deceleration events of the NEDC.

Figure 30 shows the change in tank energy over time for the six events. It demonstrates that the rate of which energy is recovered is based on the speed of the engine. The total energy recoverable is then a function of time.

4.4 Energy Savings

Using the energy recoverable during the NEDC, inferences can be made about the potential energy savings. The energy could be used by either using the engine as a pneumatic motor, using a dedicated pneumatic motor, for supercharging or a combination like the APA cycle suggested by (Schechter 1999).

To calculate the energy savings, several assumptions have been made.

- Energy usable is 80%.
- Efficiency of the engine is 30%.
- LHV of fuel is 44.4 MJ/kg.

- Density of fuel is 0.745 kg/L.

Therefore, energy savings are estimated using Equation 21:

$$E_{savings} = E_{recovered} \cdot \frac{\eta_{usuable}}{\eta_{engine}} \quad [\text{J}] \qquad \text{Equation [21]}$$

$$= 574020 \cdot 0.80/0.30$$

$$= 1530720 \ \text{J}$$

Furthermore, these savings can be presented in terms of fuel savings per Equation 22:

$$F_{savings} = E_{savings} \cdot \frac{1}{LHV_{fuel} \times \rho_{fuel}} \quad [\text{L}] \qquad \text{Equation [22]}$$

$$= 1530720 \cdot \frac{1}{44.4 \cdot 10^6 \times 0.745}$$

$$= 0.046 \ \text{L}$$

As a result, the potential energy savings are 1.5 MJ or 46 x 10^{-3} L of fuel. At an estimated 1.143 billion cars in use globally in 2012 (International Organization of Motor Vehicle Manufacturers n.d.-b), driving on average three times a week for 48 weeks of the year, this translates to a fuel saving of 7.62 GL of fuel savings a year. At a ratio of 71.92 litres of fuel produced for every barrel of crude oil (U.S. Energy Information Administration n.d.-b), this represents a saving of 105.9 million barrels of oil per year, or 0.3% of the estimated 2013 annual consumption.

The effects of shutting down the engine during deceleration and when the vehicle is in idle have not been considered in this project. The reason for this is that any vehicle can be adapted to shut down during deceleration. Many vehicles already shut down the engine when the vehicle would otherwise be idling. However, other researchers such as Dönitz et al. (2009a) concluded that adding a start/stop capability could increase fuel savings up to 6%, but has a smaller effect for camless engines.

4.5 Effect of Losses

The simulation over the drive cycle performed several more times with an adjustment to the model parameters to test the effect that losses have on the recovery of energy. The changes to the model are defined as:

1. Scenario 1: Simulation without heat transfer.
2. Scenario 2: Simulation without blowby.
3. Scenario 3: Simulation with intake at atmospheric conditions optimised for braking.

The first two scenarios were run without any adjustments to the optimisation of the engine for a better comparison.

The energy recoverable over the cycle for each scenario is presented in Tables 18 to 21 in Appendix B3. These results have been summarised in Table 14.

	Original	**Scenario 1**	**Scenario 2**	**Scenario 3**
Total Energy Recoverable (kJ)	574.020	573.116	590.286	519.690
% Energy Change	0%	-0.15%	2.8%	-9.5%

Table 14 – Summary of energy recoverable using the engine as a compressor with adjustments to view the changes due to losses.

When no changes are made to the engine speed, the results indicate that the amount of energy recoverable slightly decreased with no heat exchange, while no leakage increased the amount of energy recoverable. Therefore, heat exchange increases the amount energy recoverable while leakage causes losses.

When the engine speed has been optimised for the change of the intake conditions, the results are not as expected. The amount of energy recoverable would be expected to increase due greater mass flow rates. However, in this case the energy recoverable has actually decreased. The reason for this is because the intake conditions at atmospheric

pressure and temperature provide a higher BMEP and hence the optimum engine speed needs to be decreased. As concluded earlier, engine speed affects the rate of energy recovery. This is shown when comparing Table 15 below with the initial engine speed optimisation results in Table 12. Consequently, the higher intake temperature with a lower intake pressure actually produces better results over the NEDC test cycle.

Deceleration Event	Braking force required (N)	Average BMEP required (kPa)	Optimised Engine Speed (RPM)	Average BMEP produced (kPa)
1	931.43	101.79	509	100.18
2	890.76	136.43	782	135.50
3	596.62	144.26	1,271	144.22
4	799.17	135.41	707	134.36
5	630.28	154.75	1,827	154.74
6	1,019.17	131.19	3,503	131.19

Table 15 – Optimised engine speed for intake conditions at atmospheric pressure and temperature.

4.6 Other observations

The following section will discuss the other observations made with respect to efficiency, tank pressure and tank temperature.

4.6.1 Efficiency of Recovery

The energy recovered for each cycle was compared with the negative IMEP during compression mode. The results are shown in Figures 31 and 32. Figure 31 shows the efficiency of each event over time. Based on the slope of the curves, the engine speed affects the efficiency of recovering the energy. The events with the lower engine speed have a smaller gradient, peak later and can achieve higher efficiencies. The highest efficiency observed was 82.74% for Event 4.

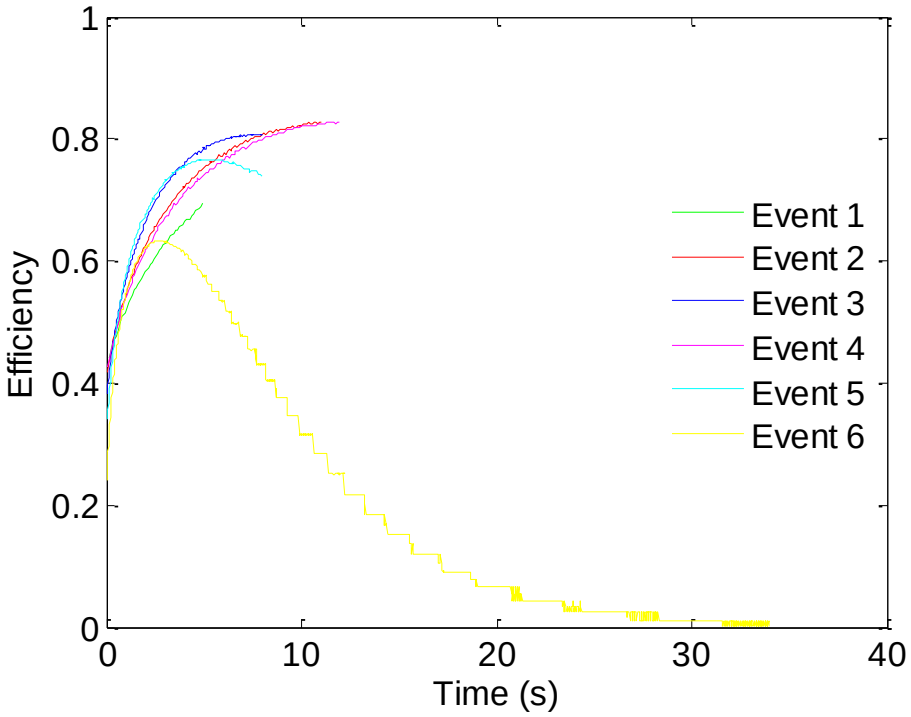

Figure 31 – Efficiency of recovering energy vs engine revolution for each deceleration event of the NEDC.

Figure 32 shows the mean efficiency of recovering the energy for each event over time. Event 6 shows that over time, the efficiency of recovery decreases. Hence, even though the most energy is recovered during this event, it is less efficient over time.

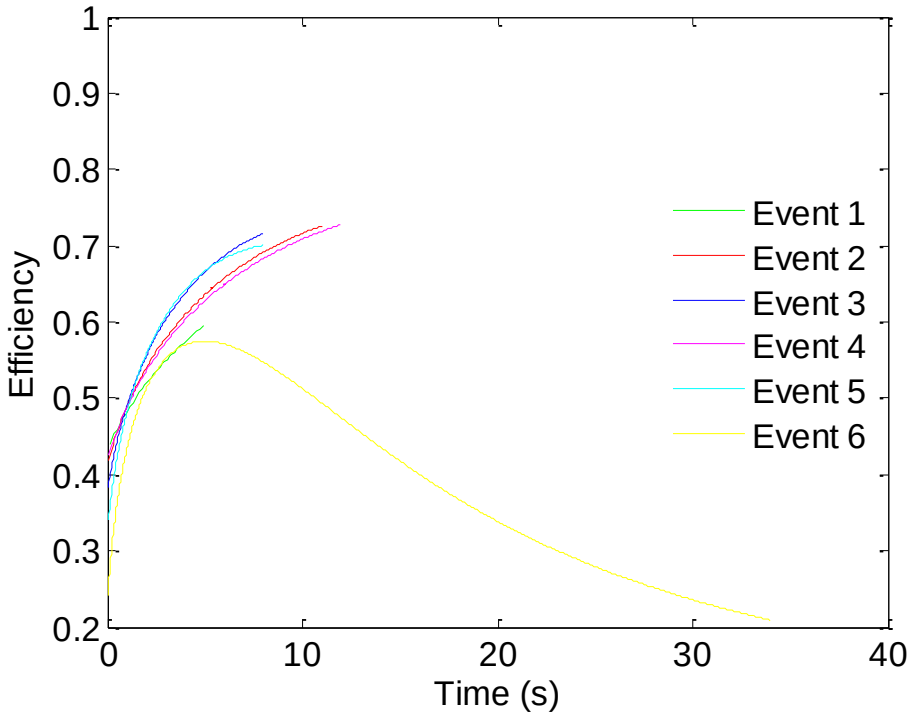

Figure 32 – Mean efficiency of recovering energy vs time for each deceleration event of the NEDC.

4.6.2 Pressure and Temperature of the Air Tank Over Time

Figures 33 and 34 indicate the pressure and temperature of the air tank over a period of time for each event. It illustrates that the rate at which the pressure and temperature increases is related to the speed of the engine. This is to be expected as it is in alignment with the increase in energy recovered over time shown in Figure 30.

The highest tank pressure recorded was around 2.16 MPa. This is lower than the theoretical maximum tank pressure of 2.26 MPa. It represents around 96% of the theoretical maximum pressure. The lowest recorded final pressure was Event 1 with only 265 kPa or around 12% of the theoretical maximum pressure.

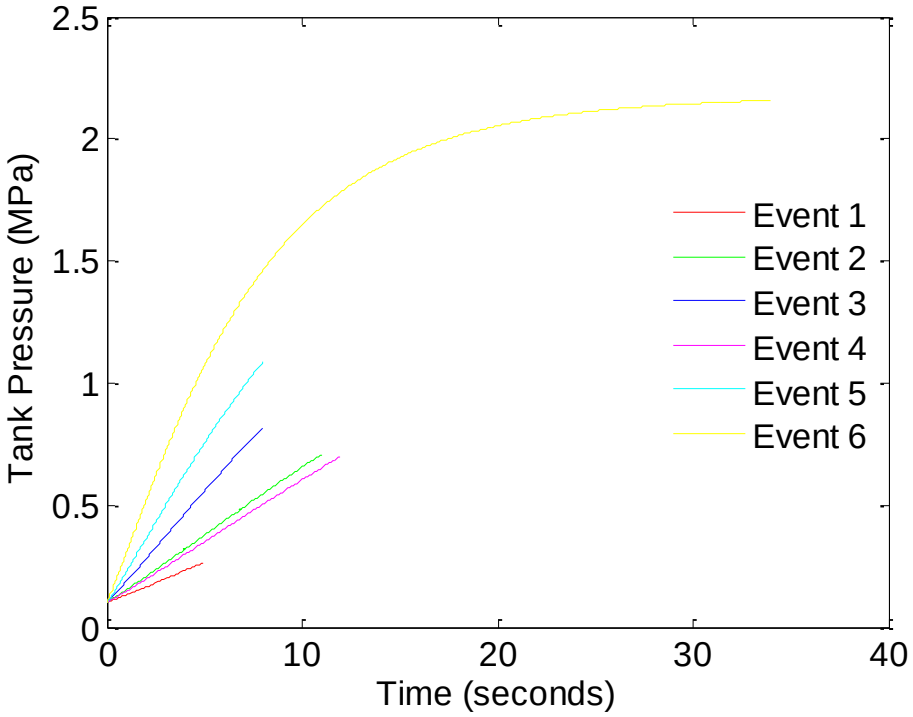

Figure 33 – Pressure of the tank during the 6 deceleration events of the NEDC.

The highest tank temperature recorded was approximately 306°C for Event 6 and the lowest final temperature was around 81°C for Event 1.

Additional research is encouraged to completely ascertain the impact these results will have on the application of the compressed gas. If used for supercharging, the higher pressure and temperature of the gas in Event 6 may cause auto-ignition or detonation which is associated with knock, making it better suited for pneumatic motor applications. However, the effects on the gas properties should be analysed closely with respect to discharging the gas back to the cylinder. Valve losses, mass flow rates and even the storage tank strategy should all be considered when advancing this study.

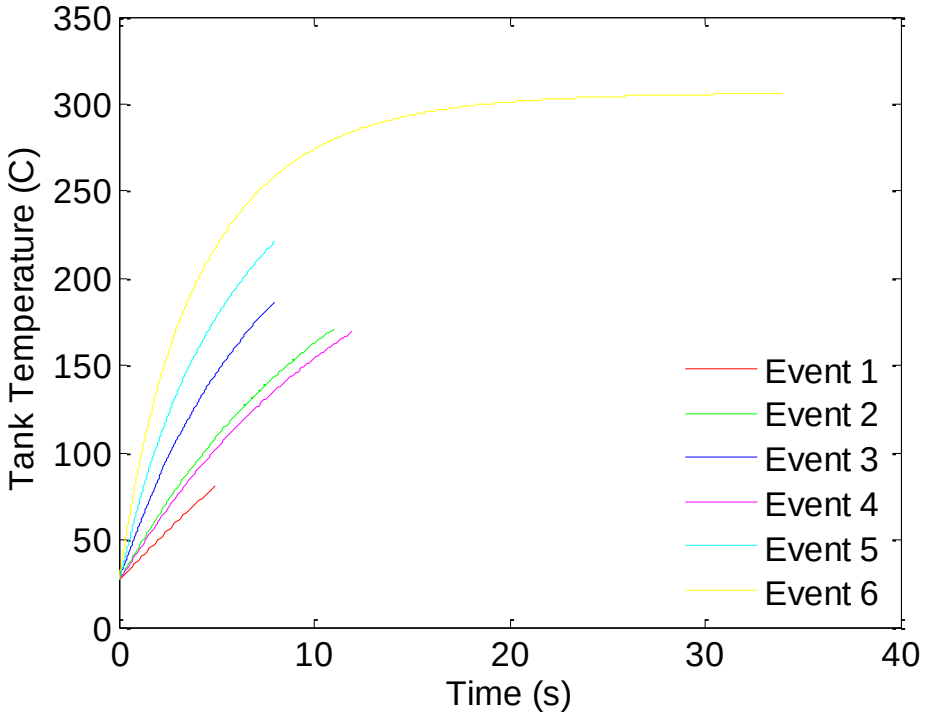

Figure 34 – Temperature of the tank during the 6 deceleration events of the NEDC.

4.7 Limitations

Of course the model is not without its limitations. Several assumptions have been made to simplify the model and the simulation of the compression cycle, while there are also some inherent limitations in the modelling. These are explored in more detail below.

4.7.1 Due to Model Limitations

The opening timing of the charge and intake valves is a limitation in the model. The step size for the integration parameters used during the compression and expansion processes was limited to $\pi/180$. Consequently, the crank angle at which the valves opened was calculated at the nearest value of pressure specified for the opening event to occur. This has two effects. Firstly, it affects the state of the residual gas mixed with the fresh intake. This is important because the initial pressure, before the compression process begins, dictates the largest pressure achievable in the tank (as shown in Equation 9 in section 2.3.1.2) and hence the amount of energy that can be recovered.

The greatest difference observed between the intake pressure and the pressure at BDC was 337 Pa greater than and 340 Pa less than intake pressure. However, the average intake pressure for all events was within 0.1% of the intake pressure.

The second effect occurs during the charging process. The crank angle at which the charge valve opens is used to calculate the change in the mass of the gas that is discharged to the air tank. If the charge valve opens too late, then less energy will be transferred to the tank for that cycle. Hence this will also reduce the efficiency of the system. In real life however, it would just be a change in work done on the gas which also affects efficiency.

Similarly, the engine speed optimisation is not exact, and will therefore reduce the energy recovered due to the assumption that the friction brakes have been used to some extent.

4.7.2 Due to Assumptions

A restriction relating to the assumptions was that the valve lift was ideal. This assumption reduces the flow losses that would otherwise occur due to the decrease in flow area. An increase in pressure drop across the valve was therefore not considered along with the reduction in mass flow rate. The result is that more energy is recovered for each cycle in the simulation than what would be expected experimentally.

Another limitation of the model was that the charging and intake processes were treated as ideal. Therefore, the effects of heat transfer were not considered. However, the heat transfer during the compression and expansion processes were shown to be negligible, if not beneficial to some extent. Furthermore, the heat transfer in the air tank was also neglected. It would be expected that the heat, and therefore energy, would be lost over time. Therefore, the tank would discharge over time much like batteries in HEVs.

4.8 Conclusion

This Results and Discussion section has analysed and discussed the various results produced from the numerical simulation of an engine operating as a compressor. The engine was optimised for braking requirements over the NEDC. The energy recoverable was calculated to be 574 kJ of energy during the braking events over the entire cycle. Energy savings based on the energy recovered were estimated as 1.5 MJ of energy for an engine with 30% efficiency and 80% usage of the energy recovered. This translates to 46 mL of fuel over the cycle.

The effect of the losses was also analysed. These showed that heat transfer actually recovered a small amount of energy (0.15%), blowby was responsible for a 2.8% energy loss, and changes in intake conditions which resulted in a decrease of 9.5%. Therefore, the lower density of the gas assumed initially actually recovered more energy due to the different BMEP produced and optimised engine speeds.

Other important observations were made about the data. The maximum observed efficiency was around 83% for energy recovered for a single cycle and 72.76% for the overall efficiency during a deceleration event. Hence, a regenerative efficiency of 58.2 % is calculated with the assumption of 80% usage of the recovered energy. The maximum tank pressure and temperature recorded was 2.16 MPa and 306°C respectively.

Finally, the limitations of the model were discussed with respect to the possible effects these limitations have had on the results.

5 Conclusions

5.1 Introduction

Fuel consumption and sustainability are major drivers influencing regenerative braking technologies. This is illustrated by the number of manufacturers now exploring and implementing technologies to recover energy. Other manufactures such as Tesla Motors are also focusing on a purely electric vehicle alternative. This project undertaken has considered one of these technologies still in its infancy; the concept of using the engine as a compressor to recover energy during braking conditions.

This project has discussed the two current kinetic energy recovery technologies: HEV and Flywheels. The advantages and disadvantages of each technology have been highlighted for comparison with the concept in the Project Background. The ability to implement the concept and use an IC engine as a compressor was shown as promising during the literature review, with several uses for the compressed gas established.

A numerical simulation was undertaken of an engine operating as a compressor during the deceleration phases of the NEDC. The energy calculated as recoverable during the modelling and simulation process could potentially have an impact on reducing fuel consumption and improving the overall efficiency of a vehicle. Although the energy savings were relatively small, improvements in the technology could make it a more viable solution.

5.2 Viability of the Concept

This section concludes on the viability of the concept, considering the two main technologies used for regenerative braking, the ability to use an IC engine as a compressor, and the possible applications for the compressed gas.

5.2.1 Comparison with Current Technologies

The Project Background introduced HEV and Flywheel regenerative braking. The literature revealed several advantages and disadvantages associated with each technology.

HEVs appear to have the advantage as a storage medium. Both batteries and capacitors can store energy for longer periods of time. Flywheels tend to self-discharge at much quicker rates due to friction, while compressed gas will lose energy through heat. Although, compressed gas with lower heats are more suitable for supercharging to avoid the effects of engine knock.

When it comes to efficiency, the literature suggests that Flywheels may have the advantage. HEVs need to convert energy from kinetic energy, to electric energy, and finally chemical energy, and then back again to use the energy. Body & Brockbank (2009) (cited in Boretti 2010) claims an overall charge, discharge efficiency of more than 70% during a full regenerative cycle in stop start traffic. In comparison to the results of the simulation conducted in this project, the regenerative efficiency is 58.2% after the assumption that 80% of the energy recovered could be used. This compares with a maximum overall efficiency of 33% calculated by Trajkovic et al. (2007). However, the experimental results of Dönitz et al. (2009b) demonstrate regenerative efficiencies of only 13.8%. This is quite low compared to HEVs which can have efficiencies of about 60% (Dönitz et al. 2009b).

Other researchers have shown that compressed gas technology can be competitive when it comes to fuel savings. Early simulations performed by Higelin, Charlet and Chamaillard (2002) suggested fuel savings of around 15% over the NEDC test cycle. However, Dönitz et al. (2009a) concluded that fuel savings of 34% were achievable over the NEDC by using a downsized camless engine with pneumatic hybridization. This can be compared with the 18% demonstrated by Flybrid Automotive Limited (2014) for their Flywheel technology over the NEDC test cycle. Furthermore, Volvo Car Group (2014) claim fuel consumption reductions of 25% for their joint tests with Flybrid Automotive. Meanwhile, Toyota Motor Corporation Australia Ltd (n.d.) claim

ambitious fuel savings of up to 50% for their Prius model compared to similar size vehicles. However, it remains unclear how they have calculated and arrived at these impressive results.

The literature reviewed as part of this project suggests that compressed gas technology also has the advantage of reduced weight, which affects vehicle performance and fuel consumption. The additional weight for a pressure vessel, VVT and other hydraulic components is estimated to be just 25 kg (Dönitz et al. 2009a). If the energy is used for supercharging, this will also allow for downsizing of the engine, which can reduce the overall mass by more the 25kg (Dönitz et al. 2009b). This is substantially less than a HEV such as the Prius, which has battery mass of 53.3 kg according to Berman (2008). This is without even considering the extra components such as the electric motor to deliver power back to the drivetrain.

All technologies have a safety factor. Compressed gas requires pressure vessels that must be maintained. HEVs obviously add electricity to the equation which presents new dynamics to safety in crashes. They also have chemical components that can be toxic. Finally, Flywheels store a high amount of kinetic energy in a confined volume. Failure of such a device requires the housing to be manufactured to withstand the energy in the event of failure.

5.2.2 Ability to Use the Engine as a Compressor

The literature reviewed in this study reveals that the ability to use the engine as a compressor is fairly established. It appears that the concept requires very few additional components or modifications.

The ability to implement the concept hinges on the use of variable valve timing. This solution provides the engine with the ability to not just operate in compression mode, but also as a pneumatic engine. Furthermore, it provides benefits when the engine is operating conventionally. Dönitz et al. (2009a) concluded that it could improve fuel consumption by 8% alone without any other improvements.

Modifying the cylinder head was also a prominent feature in the literature. Although many configurations were witnessed, an addition of a single charging valve seemed to be the most widely accepted solution.

Finally, a storage tank would be required to store the compressed gas. The size of the tank is dependent upon trade-off between the cost, optimal energy recoverable and the space constraints. With this component, also comes the need for safety considerations, including the need to ensure that tank temperature and pressure do not exceed design specifications.

5.2.3 Applications of the Compressed Gas

The applications considered in this project while limited, were very applicable to reducing fuel consumption. The two main uses considered were supercharging and pneumatic engines. Researchers have shown that both applications have their benefits. Dönitz et al. (2009a) concluded that supercharging allows for downsizing of the engine resulting in greater fuel savings. Using the compressed gas to supercharge also doesn't suffer from lag associated with turbochargers or losses with superchargers.

The alternate application is to use either the engine in a pneumatic motor mode, or using a dedicated pneumatic motor. Using the engine as a pneumatic motor reduces the need for extra componentry, therefore reducing overall vehicle mass and subsequently fuel consumption. However, dedicated pneumatic motors used in parallel with the engine also provide the ability to recover heat by recycling the exhaust gas, as shown by Huang and Tzeng (2005).

5.3 Conclusion

Overall, the concept of using compressed gas to recover kinetic energy appears to be viable. With additional components and modifications, an engine can be used as a compressor. The technology has many benefits and potential to improve with time.

However, current performance in experimental results appear inferior (to some degree) than the performance of the other two prominent technologies.

Whether or not it could compete with HEVs in the market, is still currently unclear. The research suggests that more effort needs to be invested in producing experimental results and subsequently optimising the system to improve overall performance.

5.4 Further Work

Due to the timeframe constraints associated with the development of this study, many factors have been identified as needing to be either considered, or considered in more depth. In continuance of this project, the simulation produced needs to fully consider the effects of heat transfer, leakage, and flow losses through the intake system and across the valves. While these factors have already been considered to some extent, the considerations in the model are relatively limited and should be investigated in more depth in order to provide more meaningful comparisons with any eventual experimental setup. Furthermore, the application of the compressed gas needs to be considered in the simulation and the associated fuel savings and regenerative efficiency over the whole cycle.

6 References

Asmus, TW 1982, 'Valve Events and Engine Operation', SAE Paper 820749.

Berman, B 2008, *The Hybrid Car Battery: A Definitive Guide*, Hybrid Cars, viewed 27 October 2014, <http://www.hybridcars.com/hybrid-car-battery/>.

Boretti, A 2010, 'Comparison of fuel economies of high efficiency diesel and hydrogen engines powering a compact car with a flywheel based kinetic energy recovery systems', *International Journal of Hydrogen Energy*, vol. 35, no. 16, pp. 8417-24.

Buttsworth, D 2002, *Spark Ignition Internal Combustion Engine Modelling using Matlab*, Faculty of Engineering & Surveying, University of Southern Queensland.

Ceviz, M 2007, 'Intake plenum volume and its influence on the engine performance, cyclic variability and emissions', *Energy Conversion and Management*, vol. 48, no. 3, pp. 961-6.

Ceviz, M & Akin, M 2010, 'Design of a new SI engine intake manifold with variable length plenum', *Energy Conversion and Management*, vol. 51, no. 11, pp. 2239-44.

DieselNet 2013, *Emission Test Cycles: ECE15 + EUDC/NEDC*, United Nations Environment Program, viewed 11 October 2014, <https://www.dieselnet.com/standards/cycles/ece_eudc.php>.

Dönitz, C, Vasile, I, Onder, C & Guzzella, L 2009a, 'Dynamic programming for hybrid pneumatic vehicles', in American Control Conference 2009, Hyatt Regency Riverfront, St. Louis, MO, USA, pp. 3956-63.

Dönitz, C, Vasile, I, Onder, C & Guzzella, L 2009b, 'Realizing a Concept for High Efficiency and Excellent Driveability: The Downsized and Supercharged Hybrid Pneumatic Engine', SAE Paper 2009-01-1326.

Elkady, M, Elmarakbi, A, Knapton, D, Saleh, M, Abdelhameed, M & Bawady, A 2013, 'Theoretical and Experimental Analysis of Electromagnetic Variable Valve Timing Control Systems for Improvement of Spark Ignition Engine Performance', *Advances in Automobile Engineering*, viewed 27 October 2014, <http://omicsgroup.org/>.

Ferguson, CR 1986, *Internal Combustion Engines, Applied Thermosciences*, John Wiley and Sons, New York.

Flybrid Automotive Limited 2014, *Road Car Systems*, Flybrid Automotive Limited, viewed 18 October 2014, <http://www.flybridsystems.com/Roadcar.html>.

Fontana, G & Galloni, E 2009, 'Variable valve timing for fuel economy improvement in a small spark-ignition engine', *Applied Energy*, vol. 86, no. 1, pp. 96-105.

Fuhs, A 2009, *Hybrid vehicles and the future of personal transportation*, CRC Press, Boca Raton.

Gordon, S & McBride, BJ 1971, *Computer Program for Calculation of Complex Chemical Equilibrium Composition, Rocket Performance, Incident and Reflected Shocks, and Chapman-Jouguet Detonations*, NASA publication SP-273.

Hanlon, P 2001, *Compressor handbook*, McGraw-Hill, New York.

Heywood, J 1988, *Internal combustion engine fundamentals*, McGraw-Hill, New York.

Higelin, P, Charlet, A & Chamaillard, Y 2002, 'Thermodynamic Simulation of a Hybrid Pneumatic-Combustion Engine Concept', *International journal of applied thermodynamics*, vol. 5, no. 1, pp. 1-11.

Huang, KD & Tzeng, S-C 2005, 'Development of a hybrid pneumatic-power vehicle', *Applied Energy*, vol. 80, no. 1, pp. 47-59.

Huang, KD, Tzeng, S-C, Ma, W-P & Chang, W-C 2005, 'Hybrid pneumatic-power system which recycles exhaust gas of an internal-combustion engine', *Applied Energy*, 10//, pp. 117-32.

International Organization of Motor Vehicle Manufacturers n.d.-a, *International Energy Statistics* International Organization of Motor Vehicle Manufacturers, viewed 2 June 2014, <http://www.eia.gov/cfapps/ipdbproject/IEDIndex3.cfm?tid=5&pid=57&aid=6>.

International Organization of Motor Vehicle Manufacturers n.d.-b, *2013 Production Statistics*, International Organization of Motor Vehicle Manufacturers, viewed June 2, <http://www.oica.net/category/production-statistics/>.

Kang, H, Tai, C, Smith, E, Wang, X, Tsao, T-C, Stewart, J & Blumberg, P 2008, 'Demonstration of Air-Power-Assist (APA) Engine Technology for Clean Combustion and Direct Energy Recovery in Heavy Duty Application', SAE Paper 2008-01-1197.

Motor Trend Magazine 2014a, *Flywheel KERS: Flywheel Module*, Motor Trend Magazine, viewed 18 October 2014, <http://wot.motortrend.com/volvo-experimenting-flywheel-hybrid-claims-reduce-fuel-consumption-20-percent-82025.html/volvo-flywheel-kers-diagram-1/>.

Motor Trend Magazine 2014b, *Flywheel KERS: System Layout*, Motor Trend Magazine, viewed 18 October 2014, <http://wot.motortrend.com/volvo-experimenting-flywheel-hybrid-claims-reduce-fuel-consumption-20-percent-82025.html/volvo-flywheel-kers-diagram-2/>.

Organization of the Petroleum Exporting Countries 2013, *2013 World Oil Outlook*, Organization of the Petroleum Exporting Countries, <http://www.opec.org/opec_web/static_files_project/media/downloads/publications/WOO_2013.pdf>.

Pritchard, P 2011, *Fox and McDonald's Introduction to Fluid Mechanics*, 8th edn, John Wiley & Sons, Inc., Hoboken, N.J.

Pulkrabek, W 1997, *Engineering fundamentals of the internal combustion engine*, Prentice Hall, Upper Saddle River, N.J.

Schechter, M 1999, *New Cycles for Automobile Engines*, SAE Paper 1999-01-0623.

Tai, C, Tsao, T-C, Levin, M, Barta, G & Schechter, M 2003, 'Using Camless Valvetrain for Air Hybrid Optimization', SAE Paper 2003-01-0038.

Toyota Motor Corporation Australia Ltd n.d., *Hybrid Performance*, viewed 20 October 2014, <http://www.toyota.com.au/prius/features/hybrid-performance>.

Trajkovic, S, Tunestål, P, Johansson, B, Carlson, U & Höglund, A 2007, 'Introductory Study of Variable Valve Actuation for Pneumatic Hybridization', SAE Paper 2007-01-0288.

U.S. Energy Information Administration n.d.-a, *International Energy Statistics*, U.S. Energy Information Administration, viewed 31 May 2014, <http://www.eia.gov/>.

U.S. Energy Information Administration n.d.-b, *Frequently Asked Questions*, U.S. Energy Information Administration, viewed 20 October 2014, <http://www.eia.gov/tools/faqs/faq.cfm?id=24&t=10>.

U.S. Government n.d.-a, *Where the Energy Goes: Gasoline Vehicles*, U.S. Government, viewed 2 June 2014, <http://www.fueleconomy.gov/feg/atv.shtml>.

U.S. Government n.d.-b, *How Hybrids Work*, U.S. Government, viewed 20 October 2014, <http://www.fueleconomy.gov/feg/hybridtech.shtml>.

Volvo Car Group 2014, *Volvo Car Group and Flybrid Conduct UK Testing of Flywheel KERS Technology*, Volvo Car Group, viewed 18 October 2014, <https://www.media.volvocars.com/uk/en-gb/media/pressreleases/141626/volvo-car-group-and-flybrid-conduct-uk-testing-of-flywheel-kers-technology>.

Woschni, G 1967, 'A Universally Applicable Equation for the Instantaneous Heat Transfer Coefficient in the Internal Combustion Engine', SAE Paper 670931.

Appendix A – Project Specification

University of Southern Queensland
FACULTY OF HEALTH, ENGINEERING AND SCIENCES

ENG4111/ENG41112
PROJECT SPECIFICATION

FOR:	Rick Kruger
TOPIC:	KINETIC ENERGY RECOVERY SYSTEM USING COMPRESSED GAS
SUPERVISOR:	Dr Ray Malpress
ENROLMENT:	ENG4111 – S1 2014
	ENG4112 – S2 2014
PROJECT AIM:	This project seeks to investigate the potential recovery of kinetic energy using compressed gas of a moving motor vehicle under braking, considering the amount of energy recoverable and the potential uses of that energy.
PROGRAMME:	Version 1, 17 March 2014

1. Research the background information relating to automotive Kinetic Energy Recovery Systems and compression systems.
2. Critically evaluate current Kinetic Energy Recovery Systems and their use.
3. Investigate, analyse and evaluate alternate uses of compressed gas in automotive systems.
4. Design a model of a Kinetic Energy Recovery System using compressed gas (Matlab).
5. Calculate expected energy recovery and compare with current systems.
6. Analyse and conclude on practicality, efficiency/fuel savings, cost and limitations.
7. Submit an academic dissertation on the research.

As time permits:

8. Design and build a small working model of the system.
9. Collect output data, analyse and compare data to the theoretical model calculations.
10. Investigate potential improvements.

AGREED:

_____ (Student) _____ (Supervisor) _____ (Examiner)

__/__/____ __/__/____ __/__/____

Appendix B1 – Results: Optimised Braking Speed

Deceleration Event	Braking force required (N)	Average BMEP required (kPa)	Optimised Engine Speed (RPM)	Average BMEP produced (kPa)
1	931.43	101.79	509	99.68
2	890.76	130.11	820	129.44
3	596.62	137.77	1331	137.68
4	799.17	129.05	742	128.43
5	630.28	147.52	1922	147.50
6	1,019.17	129.30	3554	129.26

Table 16 – Engine speed optimised to meet the braking requirements for the NEDC deceleration events.

Deceleration Event	Braking force required (N)	Average BMEP required (kPa)	Optimised Engine Speed (RPM)	Average BMEP produced (kPa)
1	931.43	101.79	509	100.18
2	890.76	136.43	782	135.50
3	596.62	144.26	1,271	144.22
4	799.17	135.41	707	134.36
5	630.28	154.75	1,827	154.74
6	1,019.17	131.19	3,503	131.19

Table 17 – Optimised engine speed for intake conditions at atmospheric pressure and temperature.

Appendix B2 – Results: Required BMEP vs Actual BMEP

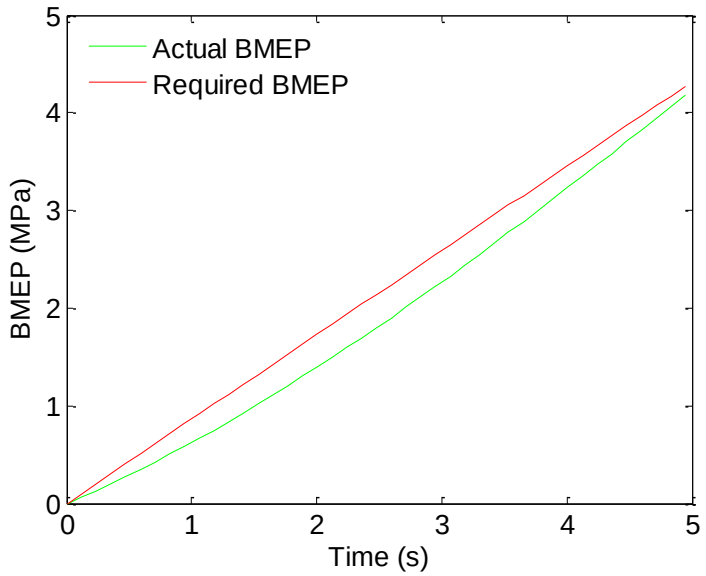

Figure 35 – Cumulative BMEP produced over time during deceleration Event 1 compared to the average BMEP required.

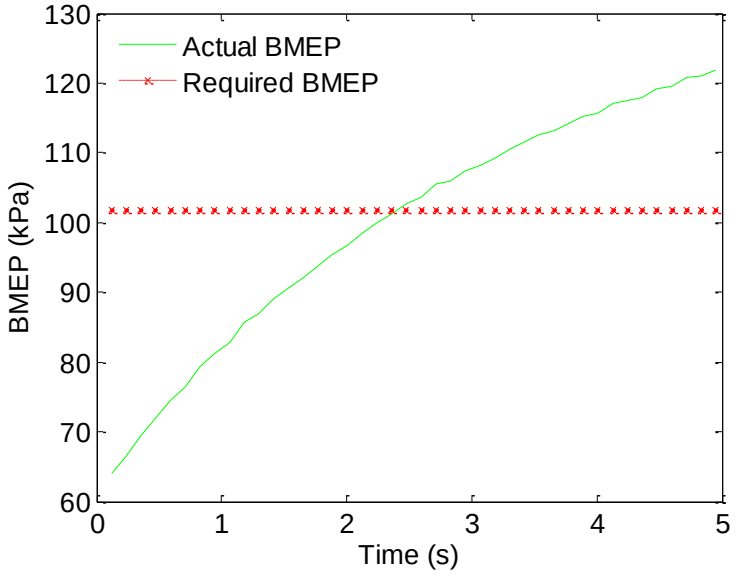

Figure 36 – BMEP produced during deceleration Event 1 compared to the average BMEP required.

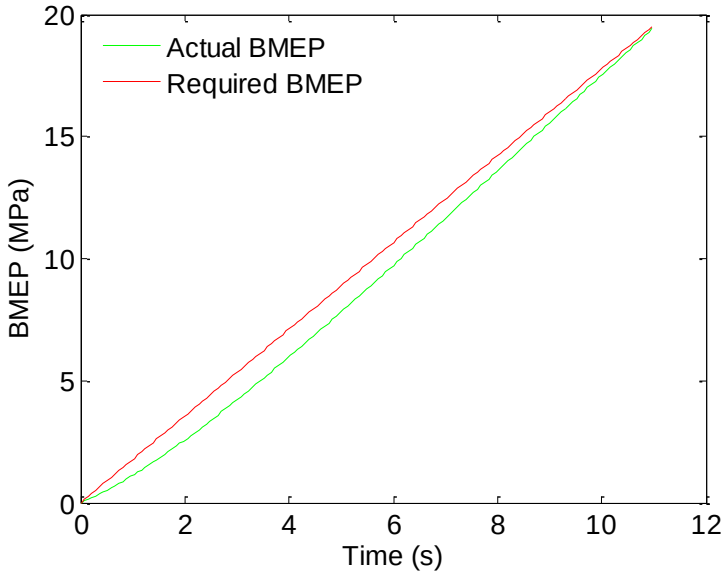

Figure 37 – Cumulative BMEP produced over time during deceleration Event 2 compared to the average BMEP required.

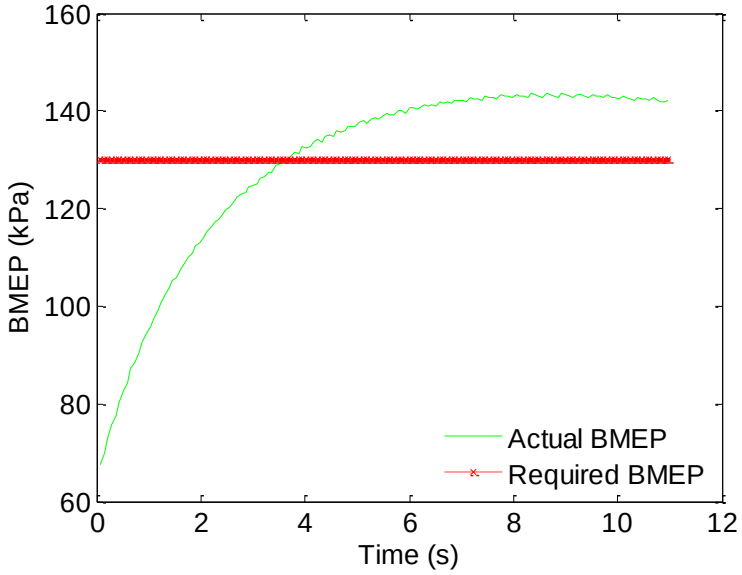

Figure 38 – BMEP produced during deceleration Event 2 compared to the required average BMEP required.

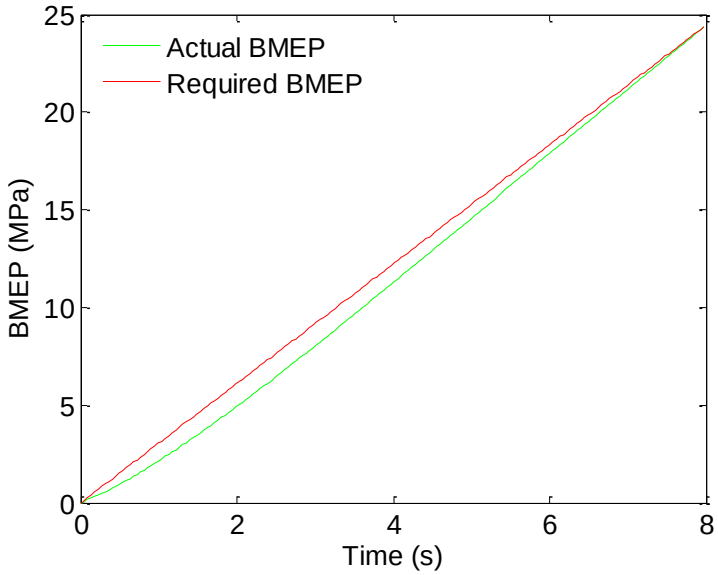

Figure 39 – Cumulative BMEP produced over time during deceleration Event 3 compared to the average BMEP required.

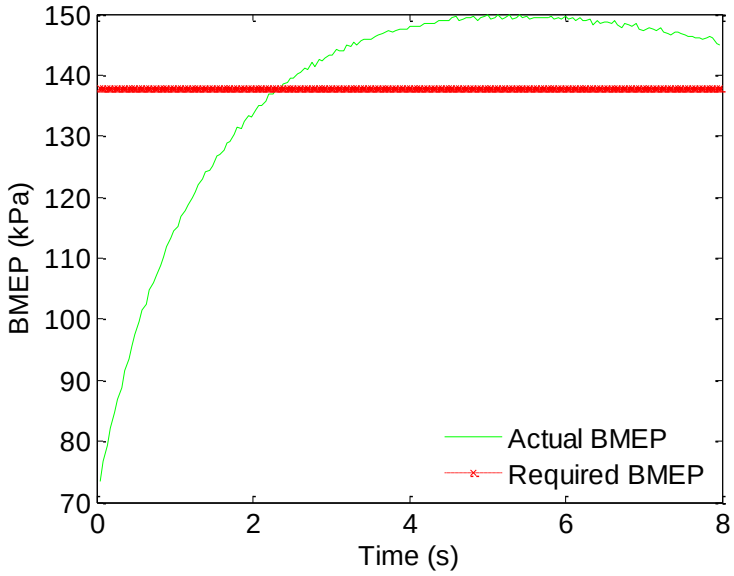

Figure 40 – BMEP produced during deceleration Event 3 compared to the required average BMEP required.

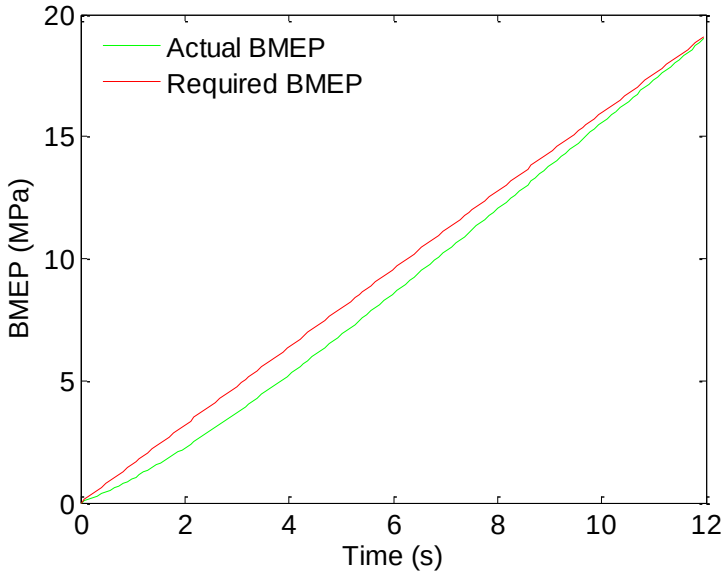

Figure 41 – Cumulative BMEP produced over time during deceleration Event 4 compared to the average BMEP required.

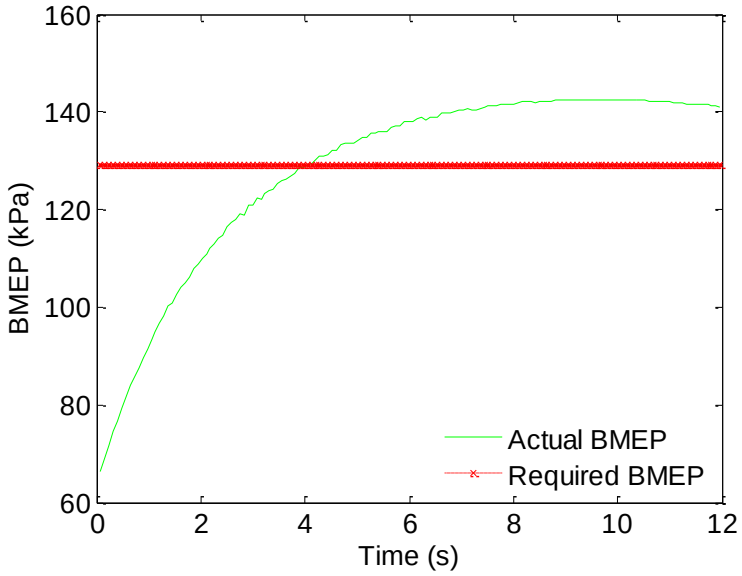

Figure 42 – BMEP produced during deceleration Event 4 compared to the required average BMEP required.

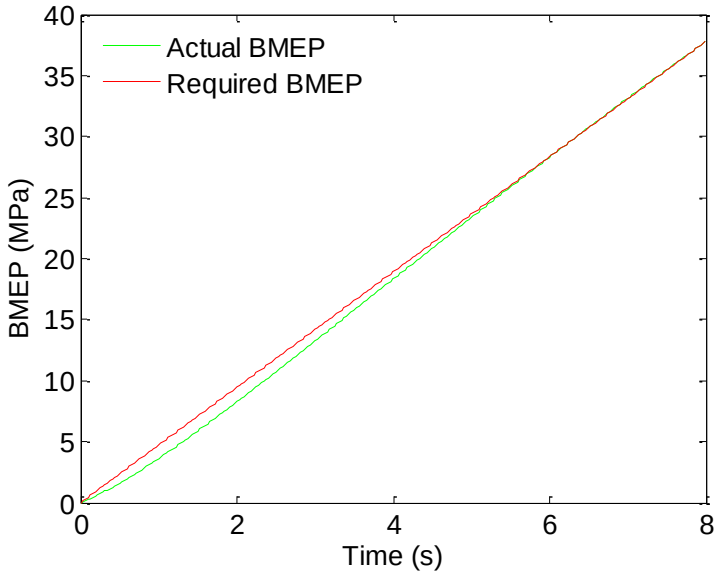

Figure 43 – Cumulative BMEP produced over time during deceleration Event 5 compared to the average BMEP required.

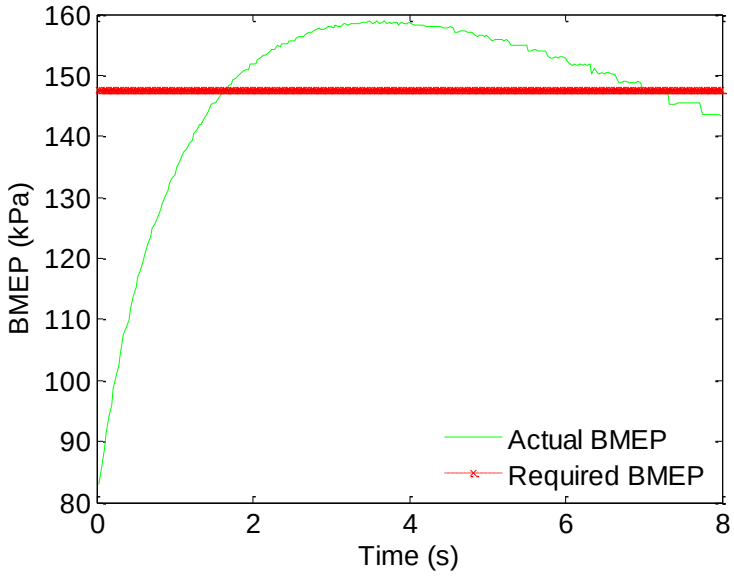

Figure 44 – BMEP produced during deceleration Event 5 compared to the required average BMEP required

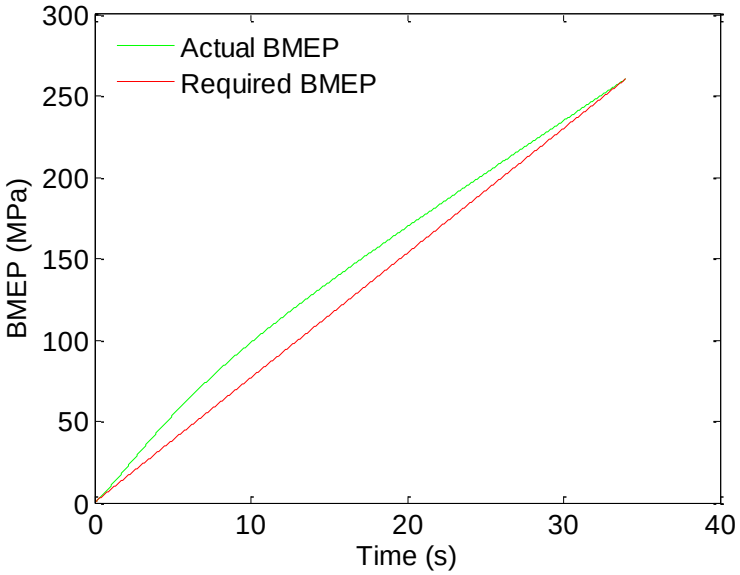

Figure 45 – Cumulative BMEP produced over time during deceleration Event 6 compared to the average BMEP required.

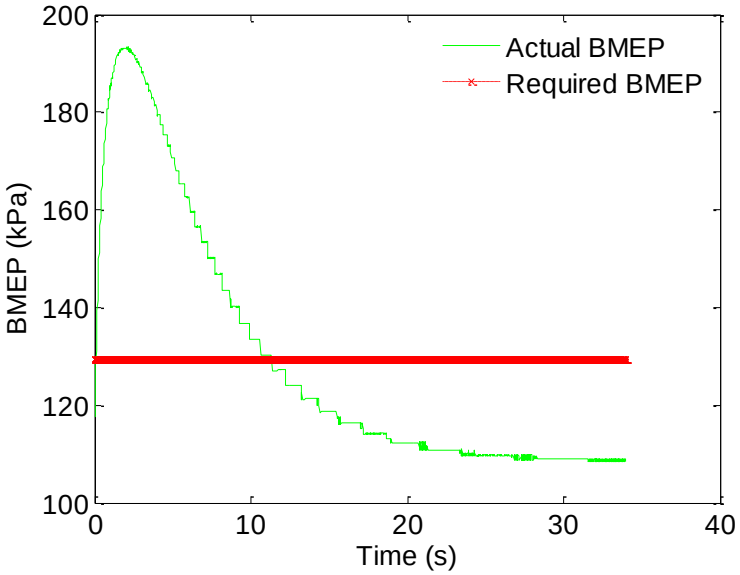

Figure 46 – BMEP produced during deceleration Event 6 compared to the required average BMEP required.

Appendix B3 – Results: Energy Recovered

Deceleration Event	Energy Recovered (kJ)	Frequency	Total Energy Recovered (kJ)
1	5.069	4	20.276
2	28.699	4	114.796
3	35.457	4	141.828
4	28.165	4	112.662
5	53.439	1	53.439
6	131.019	1	131.019
TOTAL			574.020

Table 18 – Energy recovered with optimised engine speed for the NEDC cycle deceleration events.

Deceleration Event	Energy Recovered (kJ)	Frequency	Total Energy Recovered (kJ)
1	5.059	4	20.236
2	28.621	4	114.483
3	35.371	4	141.482
4	28.089	4	112.354
5	53.332	1	53.332
6	131.229	1	131.229
TOTAL			573.116

Table 19 – Energy recovered for each deceleration event without heat transfer.

Deceleration Event	Energy Recovered (kJ)	Frequency	Total Energy Recovered (kJ)
1	5.262	4	21.047
2	29.700	4	118.802
3	36.237	4	144.949
4	29.212	4	116.848
5	54.305	1	54.305
6	134.335	1	134.335
TOTAL			590.286

Table 20 – Energy recovered for each deceleration event without blowby.

Deceleration Event	Energy Recovered (kJ)	Frequency	Total Energy Recovered (kJ)
1	3.532	4	14.129
2	24.740	4	98.958
3	31.389	4	125.554
4	24.159	4	96.636
5	49.352	1	49.352
6	135.061	1	135.061
TOTAL			519.690

Table 21 – Energy recovered for each deceleration event without intake flow losses.

Appendix C1 – Airdata.m

```
function A=airdata(scheme);
%
% A=airdata(scheme)
%
% Routine to specify the thermodynamic properties of air and
% combustion products.
% Data taken from:
% 1. Gordon, S., and McBride, B. J., 1971, "Computer Program for
% Calculation of Complex Chemical Equilibrium Composition, Rocket
% Performance, Incident and Reflected Shocks, and Chapman-Jouguet
% Detonations," NASA SP-273.  As reported in Ferguson, C. R., 1986,
% "Internal Combustion Engines", Wiley.
% 2. Kee, R. J., et al., 1991, "The Chemkin Thermodynamic Data Base",
% Sandia Report, SAND87-8215B. As reported in
% Turns, S. R., 1996, "An Introduction to Combustion:
% Concepts and Applications", McGraw-Hill.
% ********************************************************************
% input:
% scheme switch:
% 'GMcB_low' - Gordon and McBride 300 < T < 1000 K
% 'GMcB_hi' - Gordon and McBride 1000 < T < 5000 K
% 'Chemkin_low' - Chemkin 300 < T < 1000 K
% 'Chemkin_hi' - Chemkin 1000 < T < 5000 K
% output:
% A - matrix of polynomial coefficients for cp/R, h/RT, and s/R
% of the form h/RT=a1+a2*T/2+a3*T^2/3+a4*T^3/4+a5*T^4/5*a6/T (for
% example) where T is expressed in K
% columns 1 to 7 are coefficients a1 to a7, and
% rows 1 to 10 are species CO2 H2O N2 O2 CO H2 H O OH and NO
% ********************************************************************

switch scheme
case 'GMcB_low'
   A=[ 0.24007797E+01  0.87350957E-02 -0.66070878E-05  0.20021861E-08
...
       0.63274039E-15 -0.48377527E+05  0.96951457E+01
       0.40701275E+01 -0.11084499E-02  0.41521180E-05 -0.29637404E-08
...
       0.80702103E-12 -0.30279722E+05 -0.32270046E+00
```

```
       0.36748261E+01 -0.12081500E-02  0.23240102E-05 -0.63217559E-09
...
      -0.22577253E-12 -0.10611588E+04  0.23580424E+01
       0.36255985E+01 -0.18782184E-02  0.70554544E-05 -0.67635137E-08
...
       0.21555993E-11 -0.10475226E+04  0.43052778E+01
       0.37100928E+01 -0.16190964E-02  0.36923594E-05 -0.20319674E-08
...
       0.23953344E-12 -0.14356310E+05  0.29555350E+01
       0.30574451E+01  0.26765200E-02 -0.58099162E-05  0.55210391E-08
...
      -0.18122739E-11 -0.98890474E+03 -0.22997056E+01
       0.25000000E+01  0.00000000E+00  0.00000000E+00  0.00000000E+00
...
       0.00000000E+00  0.25471627E+05 -0.46011762E+00
       0.29464287E+01 -0.16381665E-02  0.24210316E-05 -0.16028432E-08
...
       0.38906964E-12  0.29147644E+05  0.29639949E+01
       0.38375943E+01 -0.10778858E-02  0.96830378E-06  0.18713972E-09
...
      -0.22571094E-12  0.36412823E+04  0.49370009E+00
       0.40459521E+01 -0.34181783E-02  0.79819190E-05 -0.61139316E-08
...
       0.15919076E-11  0.97453934E+04  0.29974988E+01];
case 'GMcB_hi'
   A=[ 0.44608041E+01  0.30981719E-02 -0.12392571E-05  0.22741325E-09
...
      -0.15525954E-13 -0.48961442E+05 -0.98635982E+00
       0.27167633E+01  0.29451374E-02 -0.80224374E-06  0.10226682E-09
...
      -0.48472145E-14 -0.29905826E+05  0.66305671E+01
       0.28963194E+01  0.15154866E-02 -0.57235277E-06  0.99807393E-10
...
      -0.65223555E-14 -0.90586184E+03  0.61615148E+01
       0.36219535E+01  0.73618264E-03 -0.19652228E-06  0.36201558E-10
...
      -0.28945627E-14 -0.12019825E+04  0.36150960E+01
       0.29840696E+01  0.14891390E-02 -0.57899684E-06  0.10364577E-09
...
      -0.69353550E-14 -0.14245228E+05  0.63479156E+01
```

```
       0.31001901E+01  0.51119464E-03  0.52644210E-07 -0.34909973E-10
...
       0.36945345E-14 -0.87738042E+03 -0.19629421E+01
       0.25000000E+01  0.00000000E+00  0.00000000E+00  0.00000000E+00
...
       0.00000000E+00  0.25471627E+05 -0.46011763E+00
       0.25420596E+01 -0.27550619E-04 -0.31028033E-08  0.45510674E-11
...
      -0.43680515E-15  0.29230803E+05  0.49203080E+01
       0.29106427E+01  0.95931650E-03 -0.19441702E-06  0.13756646E-10
...
       0.14224542E-15  0.39353815E+04  0.54423445E+01
       0.31890000E+01  0.13382281E-02 -0.52899318E-06  0.95919332E-10
...
      -0.64847932E-14  0.98283290E+04  0.67458126E+01];
case 'Chemkin_low'
   A=[ 0.02275724E+02  0.09922072E-01 -0.10409113E-04  0.06866686E-07
...
      -0.02117280E-10 -0.04837314E+06  0.10188488E+02
       0.03386842E+02  0.03474982E-01 -0.06354696E-04  0.06968581E-07
...
      -0.02506588E-10 -0.03020811E+06  0.02590232E+02
       0.03298677E+02  0.14082404E-02 -0.03963222E-04  0.05641515E-07
...
      -0.02444854E-10 -0.10208999E+04  0.03950372E+02
       0.03212936E+02  0.11274864E-02 -0.05756150E-05  0.13138773E-08
...
      -0.08768554E-11 -0.10052490E+04  0.06034737E+02
       0.03262451E+02  0.15119409E-02 -0.03881755E-04  0.05581944E-07
...
      -0.02474951E-10 -0.14310539E+05  0.04848897E+02
       0.03298124E+02  0.08249441E-02 -0.08143015E-05 -0.09475434E-09
...
       0.04134872E-11 -0.10125209E+04 -0.03294094E+02
       0.02500000E+02  0.00000000E+00  0.00000000E+00  0.00000000E+00
...
       0.00000000E+00  0.02547162E+06 -0.04601176E+01
       0.02946428E+02 -0.16381665E-02  0.02421031E-04 -0.16028431E-08
...
       0.03890696E-11  0.02914764E+06  0.02963995E+02
```

```
       0.03637266E+02  0.01850910E-02 -0.16761646E-05  0.02387202E-07
...
      -0.08431442E-11  0.03606781E+05  0.13588605E+01
       0.03376541E+02  0.12530634E-02 -0.03302750E-04  0.05217810E-07
...
      -0.02446262E-10  0.09817961E+05  0.05829590E+02];
case 'Chemkin_hi'
   A=[ 0.04453623E+02  0.03140168E-01 -0.12784105E-05  0.02393996E-08
...
      -0.16690333E-13 -0.04896696E+06 -0.09553959E+01
       0.02672145E+02  0.03056293E-01 -0.08730260E-05  0.12009964E-09
...
      -0.06391618E-13 -0.02989921E+06  0.06862817E+02
       0.02926640E+02  0.14879768E-02 -0.05684760E-05  0.10097038E-09
...
      -0.06753351E-13 -0.09227977E+04  0.05980528E+02
       0.03697578E+02  0.06135197E-02 -0.12588420E-06  0.01775281E-09
...
      -0.11364354E-14 -0.12339301E+04  0.03189165E+02
       0.03025078E+02  0.14426885E-02 -0.05630827E-05  0.10185813E-09
...
      -0.06910951E-13 -0.14268350E+05  0.06108217E+02
       0.02991423E+02  0.07000644E-02 -0.05633828E-06 -0.09231578E-10
...
       0.15827519E-14 -0.08350340E+04 -0.13551101E+01
       0.02500000E+02  0.00000000E+00  0.00000000E+00  0.00000000E+00
...
       0.00000000E+00  0.02547162E+06 -0.04601176E+01
       0.02542059E+02 -0.02755061E-03 -0.03102803E-07  0.04551067E-10
...
      -0.04368051E-14  0.02923080E+06  0.04920308E+02
       0.02882730E+02  0.10139743E-02 -0.02276877E-05  0.02174683E-09
...
      -0.05126305E-14  0.03886888E+05  0.05595712E+02
       0.03245435E+02  0.12691383E-02 -0.05015890E-05  0.09169283E-09
...
      -0.06275419E-13  0.09800840E+05  0.06417293E+02];
end
```

Appendix C2 – Compressor_mode.m

```
% compressor_mode.m
%
% Script file to determine the performance of a fuel inducted engine
% operating as a compressor.
% ********************************************************************
% Originally based on a file to determine the performance of a fuel
% inducted engine (user-specified) arbitrary heat release profile as a
% function of crank angle.
% ********************************************************************
% input:
% enginedata.m - this is another script file that defines all of the
% relevant engine parameters and operating conditions.
% output:
% output.mat - this file contains all of the variables.
% ********************************************************************

clear
timestart=cputime;

global b stroke eps r Cblowby f fueltype airscheme phi ...
   thetas thetab omega ...
   heattransferlaw hcu hcb ...
   Tw theta1 Vtdc Vbdc mass1 ...
   p1 T1 V1 RPM thetac cylinders ...
   Vd Cv Rair Tref Pa Ta k g rho r ...
   stoptime speedkm endspeedkm

% load the engine parameters and initial conditions
enginedata

% Set vehicle parameters
stoptime=8;         % time to complete stop
speedkm(1)=70;      % initial speed of the MV in km/h
endspeedkm=50;       % ending speed
MVmass=1360;        % mass of the MV in kg
%*********************************************************************
speedm(1)=speedkm*1000/3600;        % initial speed of the MV in m/s
endspeedm=endspeedkm*1000/3600;     % ending speed
Vmean=(speedm(1)+endspeedm)/2;      % mean velocity
MVKE(1)=0.5*MVmass*speedm(1)^2;     % initial KE of the vehicle
decel=(speedm(1)-endspeedm)/stoptime; % deceleration
distance=speedm(1)*stoptime-0.5*decel*stoptime^2; % braking distance
revolutions=round(RPM/60*stoptime)+1; % total engine revolutions

% Calculate braking requirements
f=0.015;    % rolling friction coefficient
Cd=0.3;     % coefficient of drag
A=2.3;      % total surface area in contact with the air (m^2)
rt=0.3;     % tire radius
nt=0.9;     % mechanical efficiency of the transmission and driveline
rg=revolutions/(distance/(pi*rt*2)); % average gear ratio (RPM:tire)
Fi=MVmass*decel;    % inertial force
Frf=MVmass*g*f;     % rolling friction force
Fd=Cd*0.5*rho*(Vmean^2)*A;  % drag force
Fb=Fi-Frf-Fd;       % braking force required
BMEPR=Fb*2*pi*rt*nt/(rg*Vd);     % Average required BMEP per rev
```

```
% Set intake pressure and temperature
Tintake=T1;
Pintake=p1;

% Set initial tank parameters
Ptank(1)=Pa;
Ttank(1)=Ta;
Tref=Ttank(1);
Vtank=0.05;
Mtank(1)=Ptank(1)*Vtank/(Ttank(1)*Rair);
UTank(1)=Mtank(1)*Cv*(Ttank(1)-Tref);
Ptankmax=Pintake*r^k;

% Set initial values
time(1)=0;
p23=p1;
T23=T1;
p14=p1;
T14=T1;
Ucharge14(1)=0;
Ucharge23(1)=0;
UCHARGE(1)=0;
UCHARGEC(1)=0;
Work(1)=0;
Workcumulative(1)=0;
imep(1)=0;
imepc(1)=0;
bmepc(1)=0;
BMEP(1)=0;
TBDC(1)=T1;
PBDC(1)=p1;
TeBDC(1)=T1;
PeBDC(1)=p1;

for i=2:revolutions

time(i)=time(i-1)+60/RPM;

% integration parameters
dtheta=1*pi/180;
options=odeset('RelTol',1e-3);

% Cylinders 2 & 3

% reset initial conditions

[h1,u1,v1,s1,Y1,cp1,dlvlT1,dlvlp1]=farg(p23,T23,phi,f,fueltype,airsche
me);
mass1=Vbdc/v1;
U1=u1*mass1;

% integration during compression phase
[thetacomp,pTuWQlHl]=ode45('RatesComp', ...
   [-pi:dtheta:thetac],[p23 T23 0 0 0],options);

% tank charging (when pressure equals tank pressure)
% process assuming tank volume is large compared to cylinder volume
[Cdif Cindex]=min(abs(pTuWQlHl(:,1)-Ptank(i-1)));
thetacv=thetacomp(Cindex,1);
Pcylinder=pTuWQlHl(Cindex,1);
```

```
Tcylinder=pTuWQlHl(Cindex,2);
Vcylinder=Vtdc*(1+(r-1)/2*(1-cos(thetacv)+1/eps...
    *(1-(1-eps^2*sin(thetacv).^2).^0.5)))*cylinders/2;
Mcylinder=Pcylinder*Vcylinder/(Rair*Tcylinder);
Mtdc=Pcylinder*(Vtdc*cylinders/2)/(Rair*Tcylinder);
Mcharge=Mcylinder-Mtdc;
Mtank(i)=Mcharge+Mtank(i-1);
Ucharge23(i)=Mcharge*Cv*(Tcylinder-Tref);
Utank=Mtank(i-1)*Cv*(Ttank(i-1)-Tref);
Utotal=Ucharge23(i)+Utank;
Ttank(i)=Utotal/(Cv*Mtank(i))+Tref;
Ptank(i)=Mtank(i)/Vtank*Rair*Ttank(i);

thetacheckc(i)=Cindex;
PCVO(i)=pTuWQlHl(Cindex,1);
TCVO(i)=pTuWQlHl(Cindex,2);

% charging process outputs
PCharge(1)=pTuWQlHl(Cindex,1);
TCharge(1)=pTuWQlHl(Cindex,2);
WCharge(1)=pTuWQlHl(Cindex,3);
thetacharge(1)=thetacv;
for x=2:1:(pi/dtheta+2-Cindex)
    thetacharge(x)=thetacharge(x-1)+dtheta;
    thetacharge(x+1)=thetacharge(x-1)+dtheta*2;
    dVdthetacharge=(Vtdc*(1+(r-1)/2*(1-cos(thetacharge(x+1))...
        +1/eps*(1-(1-eps^2*sin(thetacharge(x+1)).^2).^0.5)))...
        -Vtdc*(1+(r-1)/2*(1-cos(thetacharge(x-1))+1/eps...
        *(1-(1-eps^2*sin(thetacharge(x-1)).^2).^0.5))))/2;
    WCharge(x)=WCharge(x-1)+Pcylinder*dVdthetacharge;
    PCharge(x)=Pcylinder;
    TCharge(x)=Tcylinder;
end

% test imep calculated with another method (per Schechter 2000)
R=(Ptank(i-1)/p23)^(1/k);
rhoair=p23/(Rair*T23);
imeptest23(i)=(rhoair*Cv*T23+p23)*(R^(k-1)-1)*(r-R)/(r-1)/2;

% specification of initial conditions at start of expansion phase
pe=interp1(thetacomp,pTuWQlHl(:,1),thetacv);
Tbe=interp1(thetacomp,pTuWQlHl(:,2),thetacv);
We=WCharge(1,pi/dtheta+2-Cindex);
Qle=interp1(thetacomp,pTuWQlHl(:,4),thetacv);
Hle=interp1(thetacomp,pTuWQlHl(:,5),thetacv);

% integration during expansion phase
[thetaexp,pTbWQlHl]=ode45('RatesExp', ...
   [thetac:dtheta:pi],[pe Tbe We Qle Hle],options);

% set new initial variables (when pressure equals intake pressure)
[Idif Iindex]=min(abs(pTbWQlHl(:,1)-Pintake));
thetai=thetaexp(Iindex,1);
Pcylinder=pTbWQlHl(Iindex,1);
Tcylinder=pTbWQlHl(Iindex,2);
Vcylinder=Vtdc*(1+(r-1)/2*(1-cos(thetai)+1/eps*(1-(1-eps^2 ...
    *sin(thetai).^2).^0.5)))*cylinders/2;
Mcylinder=Pcylinder*Vcylinder/(Rair*Tcylinder);
VI23(i)=Vbdc*cylinders/2-Vcylinder;
MI23(i)=Pintake*VI23(i)/(Tintake*Rair);
```

```
Mcylinderbdc=MI23(i)+Mcylinder;
p23=Pintake*MI23(i)/(Mcylinderbdc)+Pcylinder*Mcylinder/(Mcylinderbdc);
T23=p23*(Vbdc*cylinders/2)/(Mcylinderbdc*Rair);

TBDC(i)=T23;
PBDC(i)=p23;
PeBDC(i)=pTbWQlHl(Iindex,1);
TeBDC(i)=pTbWQlHl(Iindex,2);
thetacheck(i)=Iindex;

% intake process outputs
PIntake(1)=pTbWQlHl(Iindex,1);
TIntake(1)=pTbWQlHl(Iindex,2);
WIntake(1)=pTbWQlHl(Iindex,3);
thetaintake(1)=thetai;
for x=2:1:(pi/dtheta+2-Iindex)
    thetaintake(x)=thetaintake(x-1)+dtheta;
    thetaintake(x+1)=thetaintake(x-1)+dtheta*2;
    dVdthetaintake=(Vtdc*(1+(r-1)/2*(1-cos(thetaintake(x+1))...
        +1/eps*(1-(1-eps^2*sin(thetaintake(x+1)).^2).^0.5)))...
        -Vtdc*(1+(r-1)/2*(1-cos(thetaintake(x-1))+1/eps...
        *(1-(1-eps^2*sin(thetaintake(x-1)).^2).^0.5))))/2;
    WIntake(x)=WIntake(x-1)+Pcylinder*dVdthetaintake;
    PIntake(x)=Pcylinder;
    TIntake(x)=Tcylinder;
end

% mean effective pressure
W23(i)=WIntake(1,(pi/dtheta+2-Iindex))*2;

% ****************************************************************

% Cylinders 1 & 4

% reset initial conditions
[h1,u1,v1,s1,Y1,cp1,dlvlT1,dlvlp1]=farg(p14,T14,phi,f,fueltype,airsche
me);
mass1=Vbdc/v1;
1=u1*mass1;

% integration during compression phase
[thetacomp,pTuWQlHl]=ode45('RatesComp', ...
    [-pi:dtheta:thetac],[p14 T14 0 0 0],options);

% tank charging (when pressure equals tank pressure)
% process assuming tank volume is large compared to cylinder volume)
[Cdif Cindex]=min(abs(pTuWQlHl(:,1)-Ptank(i)));
thetacv=thetacomp(Cindex,1);
Pcylinder=pTuWQlHl(Cindex,1);
Tcylinder=pTuWQlHl(Cindex,2);
Vcylinder=Vtdc*(1+(r-1)/2*(1-cos(thetacv)+1/eps...
    *(1-(1-eps^2*sin(thetacv).^2).^0.5)))*cylinders/2;
Mcylinder=Pcylinder*Vcylinder/(Rair*Tcylinder);
Mtdc=Pcylinder*(Vtdc*cylinders/2)/(Rair*Tcylinder);
Mcharge=Mcylinder-Mtdc;
Utank=Mtank(i)*Cv*(Ttank(i)-Tref);
Mtank(i)=Mcharge+Mtank(i);
Ucharge14(i)=Mcharge*Cv*(Tcylinder-Tref);
Utotal=Ucharge14(i)+Utank;
```

```
Ttank(i)=Utotal/(Cv*Mtank(i))+Tref;
Ptank(i)=Mtank(i)/Vtank*Rair*Ttank(i);

% charging process outputs
PCharge(1)=pTuWQlHl(Cindex,1);
TCharge(1)=pTuWQlHl(Cindex,2);
WCharge(1)=pTuWQlHl(Cindex,3);
thetacharge(1)=thetacv;
for x=2:1:(pi/dtheta+2-Cindex)
    thetacharge(x)=thetacharge(x-1)+dtheta;
    thetacharge(x+1)=thetacharge(x-1)+dtheta*2;
    dVdthetacharge=(Vtdc*(1+(r-1)/2*(1-cos(thetacharge(x+1))...
        +1/eps*(1-(1-eps^2*sin(thetacharge(x+1)).^2).^0.5)))...
        -Vtdc*(1+(r-1)/2*(1-cos(thetacharge(x-1))+1/eps...
        *(1-(1-eps^2*sin(thetacharge(x-1)).^2).^0.5))))/2;
    WCharge(x)=WCharge(x-1)+Pcylinder*dVdthetacharge;
    PCharge(x)=Pcylinder;
    TCharge(x)=Tcylinder;
end

% test imep calculated with another method (per Schechter 2000)
R=(Ptank(i-1)/p23)^(1/k);
rhoair=p14/(Rair*T14);
imeptest14(i)=(rhoair*Cv*T14+p14)*(R^(k-1)-1)*(r-R)/(r-1)/2;

% specification of initial conditions at start of expansion phase
pe=interp1(thetacomp,pTuWQlHl(:,1),thetacv);
Tbe=interp1(thetacomp,pTuWQlHl(:,2),thetacv);
We=WCharge(1,pi/dtheta+2-Cindex);
Qle=interp1(thetacomp,pTuWQlHl(:,4),thetacv);
Hle=interp1(thetacomp,pTuWQlHl(:,5),thetacv);

% integration during expansion phase
[thetaexp,pTbWQlHl]=ode45('RatesExp', ...
   [thetac:dtheta:pi],[pe Tbe We Qle Hle],options);

% set new initial variables (when pressure equals intake pressure)
[Idif Iindex]=min(abs(pTbWQlHl(:,1)-Pintake));
thetai=thetaexp(Iindex,1);
Pcylinder=pTbWQlHl(Iindex,1);
Tcylinder=pTbWQlHl(Iindex,2);
Vcylinder=Vtdc*(1+(r-1)/2*(1-cos(thetai)+1/eps...
    *(1-(1-eps^2*sin(thetai).^2).^0.5)))*cylinders/2;
Mcylinder=Pcylinder*Vcylinder/(Rair*Tcylinder);
VI14(i)=Vbdc*cylinders/2-Vcylinder;
MI14(i)=Pintake*VI14(i)/(Tintake*Rair);
Mcylinderbdc=MI14(i)+Mcylinder;

p14=Pintake*MI14(i)/(Mcylinderbdc)+Pcylinder*Mcylinder/(Mcylinderbdc);
T14=p14*(Vbdc*cylinders/2)/(Mcylinderbdc*Rair);

% intake process outputs
PIntake(1)=pTbWQlHl(Iindex,1);
TIntake(1)=pTbWQlHl(Iindex,2);
WIntake(1)=pTbWQlHl(Iindex,3);
thetaintake(1)=thetai;
for x=2:1:(pi/dtheta+2-Iindex)
    thetaintake(x)=thetaintake(x-1)+dtheta;
    thetaintake(x+1)=thetaintake(x-1)+dtheta*2;
    dVdthetaintake=(Vtdc*(1+(r-1)/2*(1-cos(thetaintake(x+1))...
```

```
        +1/eps*(1-(1-eps^2*sin(thetaintake(x+1)).^2).^0.5)))...
        -Vtdc*(1+(r-1)/2*(1-cos(thetaintake(x-1))+1/eps...
        *(1-(1-eps^2*sin(thetaintake(x-1)).^2).^0.5))))/2;
    WIntake(x)=WIntake(x-1)+Pcylinder*dVdthetaintake;
    PIntake(x)=Pcylinder;
    TIntake(x)=Tcylinder;
end

% mean effective pressure
W14(i)=WIntake(1,(pi/dtheta+2-Iindex))*2;

% ********************************************************************

% work, mep and power
    FMEP=(0.97+0.15*(RPM/1000)+0.05*(RPM/1000)^2)*100000/2;
    Work(i)=-W14(i)-W23(i);
    Workcumulative(i)=Work(i)+Work(i-1);
    imep(i)=Work(i)/Vd;
    bmep(i)=imep(i)+FMEP;
    imepc(i)=imep(i)+imepc(i-1);
    bmepc(i)=bmep(i)+bmepc(i-1);
    BMEP(i)=BMEPR+BMEP(i-1);
    imeptest(1)=0;
    imeptest(i)=imeptest23(i)+imeptest14(i);
    imeptestc(1)=0;
    imeptestc(i)=imeptestc(i-1)+imeptest(i);
    BMEPS=mean(bmep(2:i));
    BMEPF=max(bmepc);
    BMEPE=max(BMEP);

% energy
    speedm(i)=speedm(1)-decel*time(i);
    MVKE(i)=0.5*MVmass*(speedm(i))^2;
    UTank(i)=Mtank(i)*Cv*(Ttank(i)-Tref);
    UCHARGE(i)=Ucharge23(i)+Ucharge14(i);
    UCHARGEC(i)=UCHARGE(i)+UCHARGEC(i-1);

% efficiency
    efficiency(i)=(UCHARGE(i))/(imep(i)*Vd);
    efficiencym(i)=mean(efficiency(2:i));

end

% set for plots
PCVO(1)=PCVO(2);
TCVO(1)=TCVO(2);
Revs=1:revolutions;

timefinish=cputime;
timetaken=timefinish-timestart;

% save all data
save output.mat

clear
```

Appendix C3 – Enginedata.m

```
% enginedata.m
%
% Script file used by the function compressor_mode.m to
% define the engine properties and initial conditions

% ***** Variable ****************************************************
RPM=2000;

% ***** engine geometry *********************************************
b=0.088; % engine bore (m)
stroke=0.082; % engine stroke (m)
eps=0.25; % half stroke to rod ratio, s/2l
r=10; % compression ratio
Vtdc=pi/4*b^2*stroke/(r-1); % volume at TDC
Vbdc=pi/4*b^2*stroke+Vtdc; % volume at BDC
cylinders=4; % sets the number of cylinders
Vd=(Vbdc-Vtdc)*cylinders; % engine size

% ***** engine thermofluids parameters ******************************
Cblowby=0.0; % piston blowby constant (s^-1)
f=0.0; % residual fraction
fueltype='gasoline';
airscheme='GMcB';
phi=0.0; % equivalence ratio
thetas=-35*pi/180; % start of burning
thetab=60*pi/180; % burn duration angle
thetac=0; % tank charging valve close
omega=RPM*pi/30; % engine speed in rad/s
heattransferlaw='constant'; % 'constant', or 'Woschni'
hcu=0; % unburned zone heat transfer coefficient/weighting
hcb=0; % burned zone heat transfer coefficient/weighting
Tw=273+185; % engine surface temperature
Rair=286.9; % gas constant
Cv=1005-Rair; % specific heat
Pa=101*10^3;    % atmospheric pressure
Ta=300; % atmospheric temperature
k=1.4; % specific heat ratio
g=9.81; % gravity
rho=1.19; % density of air


% ***** initial conditions ******************************************
p1=90e3;
T1=330;
theta1=-pi;
V1=Vbdc;
[h1,u1,v1,s1,Y1,cp1,dlvlT1,dlvlp1]=farg(p1,T1,phi,f,fueltype,airscheme
);
mass1=Vbdc/v1;
U1=u1*mass1;
```

Appendix C4 – Farg.m

```
function
[h,u,v,s,Y,cp,dlvlT,dlvlp]=farg(p,T,phi,f,fueltype,airscheme);
%
% [h,u,v,s,Y,cp,dlvlT,dlvlp]=farg(p,T,phi,f,fueltype,airscheme)
%
% Routine to determine the state of mixtures of fuel, air
% and residual combustion products at low temperatures.
% Method closely follows that of:
% 1. Ferguson, C.R., 1986, "Internal Combustion Engines", Wiley, p108;
% who uses the results of:
% 2. Hires, S.D.,  Ekchian, A., Heywood, J.B., Tabaczynski, R.J., and
% Wall, J.C., 1976, "Performance and NOx Emissions Modeling of a Jet
% Ignition Pre-Chamber Stratified Charge Engine", SAE Trans., Vol 85,
% Paper 760161.
% ******************************************************************
% input:
% p,T,phi - pressure (Pa), temperature (K), and equivalence ratio
% f - residual mass fraction; set f=0 if no combustion products
% are present and f=1 if only combustion products are present
% fueltype - 'gasoline', 'diesel', etc - see fueldata.m for full list
% airscheme - 'GMcB' (Gordon and McBride) or 'Chemkin'
% output:
% h - enthalpy (J/kg), u - internal energy (J/kg),
% v - specific volume (m^3/kg), s - entropy (J/kgK),
% Y - mole fractions of 6 species: CO2, H2O, N2, O2, CO, and H2,
% cp - specific heat (J/kgK),
% dlvlT - partial derivative of log(v) wrt log(T)
% dlvlp - partial derivative of log(v) wrt log(p)
% ******************************************************************

[alpha,beta,gamma,delta,Afuel]=fueldata(fueltype);
switch airscheme
case 'GMcB'
   A=airdata('GMcB_low');
case 'Chemkin'
   A=airdata('Chemkin_low');
end
```

```
Ru=8314.34; % J/kmolK
table=[-1 1 0 0 1 -1]';
M=[44.01 18.02 28.008 32.000 28.01 2.018]'; % kg/kmol

MinMol=1e-25;

dlvlT=1; dlvlp=-1;
eps=0.210/(alpha+0.25*beta-0.5*gamma);

if phi <= 1.0 % stoichiometric or lean
   nu=[alpha*phi*eps beta*phi*eps/2 0.79+delta*phi*eps/2 ...
         0.21*(1-phi) 0 0]';
   dcdT=0;
else % rich
   z=1000/T;
   K=exp(2.743+z*(-1.761+z*(-1.611+z*0.2803)));
   dKdT=-K*(-1.761+z*(-3.222+z*0.8409))/1000;
   a=1-K;
   b=0.42-phi*eps*(2*alpha-gamma)+K*(0.42*(phi-1)+alpha*phi*eps);
   c=-0.42*alpha*phi*eps*(phi-1)*K;
   nu5=(-b+sqrt(b^2-4*a*c))/2/a;
   dcdT=dKdT*(nu5^2-nu5*(0.42*(phi-1)+alpha*phi*eps)+ ...
      0.42*alpha*phi*eps*(phi-1))/(2*nu5*a+b);
   nu=[alpha*phi*eps-nu5 0.42-phi*eps*(2*alpha-gamma)+nu5 ...
         0.79+delta*phi*eps/2 0 nu5 0.42*(phi-1)-nu5]';
end

% mole fractions and molecular weight of residual
tmoles=sum(nu);
Y=nu/tmoles;
Mres=sum(Y.*M);

% mole fractions and molecular weight of fuel-air
fuel=eps*phi/(1+eps*phi);
o2=0.21/(1+eps*phi);
n2=0.79/(1+eps*phi);
Mfa=fuel*(12.01*alpha+1.008*beta+16*gamma+14.01*delta)+ ...
   32*o2+28.02*n2;

% mole fractions of fuel-air-residual gas
```

```
Yres=f/(f+Mres/Mfa*(1-f));
Y=Y*Yres;
Yfuel=fuel*(1-Yres);
Y(3)=Y(3)+n2*(1-Yres);
Y(4)=Y(4)+o2*(1-Yres);

% component properties
Tcp0=[1 T T^2 T^3 T^4]';
Th0=[1 T/2 T^2/3 T^3/4 T^4/5 1/T]';
Ts0=[log(T) T T^2/2 T^3/3 T^4/4 1]';
cp0=A(1:6,1:5)*Tcp0;
h0=A(1:6,1:6)*Th0;
s0=A(1:6,[1:5 7])*Ts0;
Mfuel=12.01*alpha+1.008*beta+16.000*gamma+14.01*delta;
a0=Afuel(1); b0=Afuel(2); c0=Afuel(3); d0=Afuel(6); e0=Afuel(7);
cpfuel=Afuel(1:5)*[1 T T^2 T^3 1/T^2]';
hfuel=Afuel(1:6)*[1 T/2 T^2/3 T^3/4 -1/T^2 1/T]';
s0fuel=Afuel([1:5 7])*[log(T) T T^2/2 T^3/3 -1/T^2/2 1]';

% set min value of composition so log calculations work
if Yfuel<MinMol
   Yfuel=MinMol;
end
i=find(Y<MinMol);
Y(i)=ones(length(i),1)*MinMol;

% properties of mixture
h=hfuel*Yfuel+sum(h0.*Y);
s=(s0fuel-log(Yfuel))*Yfuel+sum((s0-log(Y)).*Y);
cp=cpfuel*Yfuel+sum(cp0.*Y)+sum(h0.*table*T*dcdT*Yres/tmoles);
MW=Mfuel*Yfuel+sum(Y.*M);

R=Ru/MW;
h=R*T*h;
u=h-R*T;
v=R*T/p;
s=R*(-log(p/101.325e3)+s);
cp=R*cp;
```

Appendix C5 – Fueldata.m

```
function [alpha,beta,gamma,delta,Afuel]=fueldata(fuel);
%
% [alpha,beta,gamma,delta,Afuel]=fueldata(fuel)
%
% Routine to specify the thermodynamic properties of a fuel.
% Data taken from:
% 1. Ferguson, C.R., 1986, "Internal Combustion Engines", Wiley;
% 2. Heywood, J.B., 1988, "Internal Combustion Engine Fundamentals",
%    McGraw-Hill; and
% 3. Raine, R. R., 2000, "ISIS_319 User Manual", Oxford Engine Group.
% ********************************************************************
% input:
% fuel switch
% from Ferguson: 'gasoline', 'diesel', 'methane', 'methanol',
% 'nitromethane', 'benzene';
% from Heywood: 'methane_h', 'propane', 'hexane', 'isooctane_h',
% 'methanol_h', 'ethanol', 'gasoline_h1', gasoline_h2', 'diesel_h';
% from Raine: 'toluene', 'isooctane'.
% output:
% alpha, beta, gamma, delta - number of C, H, 0, and N atoms
% Afuel - vector of polynomial coefficients for cp/R, h/RT, and s/R
% of the form h/RT=a1+a2*T/2+a3*T^2/3+a4*T^3/4-a5/T^2+a6/T (for
% example) where T is expressed in K.
% ********************************************************************

% Set values for conversion of Heywood data to nondimensional format
% with T expressed in K
SVal=4.184e3/8.31434;
SVec=SVal*[1e-3 1e-6 1e-9 1e-12 1e3 1 1];

switch fuel
case 'gasoline' % Ferguson
   alpha=7; beta=17; gamma=0; delta=0;
   Afuel=[4.0652 6.0977E-02 -1.8801E-05 0 0 -3.5880E+04 15.45];
case 'diesel' % Ferguson
   alpha=14.4; beta=24.9; gamma=0; delta=0;
   Afuel=[7.9710 1.1954E-01 -3.6858E-05 0 0 -1.9385E+04 -1.7879];
case 'methane' % Ferguson
```

```
   alpha=1; beta=4; gamma=0; delta=0;
   Afuel=[1.971324 7.871586E-03 -1.048592E-06 0 0 -9.930422E+03
8.873728];
case 'methanol' % Ferguson
   alpha=1; beta=4; gamma=1; delta=0;
   Afuel=[1.779819 1.262503E-02 -3.624890E-06 0 0 -2.525420E+04
1.50884E+01];
case 'nitromethane' % Ferguson
   alpha=1; beta=3; gamma=2; delta=1;
   Afuel=[1.412633 2.087101E-02 -8.142134E-06 0 0 -1.026351E+04
1.917126E+01];
case 'benzene' % Ferguson
   alpha=6; beta=6; gamma=0; delta=0;
   Afuel=[-2.545087 4.79554E-02 -2.030765E-05 0 0 8.782234E+03
3.348825E+01];
case 'toluene' % Raine
   alpha=7; beta=8; gamma=0; delta=0;
   Afuel=[-2.09053 5.654331e-2 -2.350992e-5 0 0 4331.441411
34.55418257];
case 'isooctane' % Raine
   alpha=8; beta=18; gamma=0; delta=0;
   Afuel=[6.678E-1 8.398E-2 -3.334E-5 0 0 -3.058E+4 2.351E+1];
case 'methane_h' % Heywood
   alpha=1; beta=4; gamma=0; delta=0;
   Afuel=[-0.29149 26.327 -10.610 1.5656 0.16573 -18.331
19.9887/SVal].*SVec;
case 'propane' % Heywood
   alpha=3; beta=8; gamma=0; delta=0;
   Afuel=[-1.4867 74.339 -39.065 8.0543 0.01219 -27.313
26.4796/SVal].*SVec;
case 'hexane' % Heywood
   alpha=6; beta=14; gamma=0; delta=0;
   Afuel=[-20.777 210.48 -164.125 52.832 0.56635 -39.836
79.5542/SVal].*SVec;
case 'isooctane_h' % Heywood
   alpha=8; beta=18; gamma=0; delta=0;
   Afuel=[-0.55313 181.62 -97.787 20.402 -0.03095 -60.751
27.2162/SVal].*SVec;
case 'methanol_h' % Heywood
   alpha=1; beta=4; gamma=1; delta=0;
```

```
   Afuel=[-2.7059 44.168 -27.501 7.2193 0.20299 -48.288
31.1406/SVal].*SVec;
case 'ethanol' % Heywood
   alpha=2; beta=6; gamma=1; delta=0;
   Afuel=[6.990 39.741 -11.926 0 0 -60.214 8.01623/SVal].*SVec;
case 'gasoline_h1' % Heywood
   alpha=8.26; beta=15.5; gamma=0; delta=0;
   Afuel=[-24.078 256.63 -201.68 64.750 0.5808 -27.562 NaN].*SVec;
case 'gasoline_h2' % Heywood
   alpha=7.76; beta=13.1; gamma=0; delta=0;
   Afuel=[-22.501 227.99 -177.26 56.048 0.4845 -17.578 NaN].*SVec;
case 'diesel_h' % Heywood
   alpha=10.8; beta=18.7; gamma=0; delta=0;
   Afuel=[-9.1063 246.97 -143.74 32.329 0.0518 -50.128 NaN].*SVec;
end
```

Appendix C6 – Ratescomp.m

```
function yprime=RatesComp(theta,y,flag);
%
% yprime=RatesComp(theta,y,flag)
%
% Function that returns the drivatives of the following 5 variables
% w.r.t. crank angle (theta) for the compression phase:
% 1) pressure; 2) unburned temperature;
% 3) work; 4) heat transfer; and 5) heat leakage.
% See Ferguson, C.R., 1986, "Internal Combustion Engines", Wiley,
% p174.

global b stroke eps r Cblowby f fueltype airscheme phi ...
   thetas thetab omega ...
   heattransferlaw hcu ...
   Tw theta1 Vtdc mass1 ...

p=y(1);
Tu=y(2);
yprime=zeros(5,1);

% mass in cylinder accounting for blowby:
mass=mass1*exp(-Cblowby*(theta-theta1)/omega);
% volume of cylinder:
V=Vtdc*(1+(r-1)/2*(1-cos(theta)+ ...
   1/eps*(1-(1-eps^2*sin(theta).^2).^0.5)));
% derivate of volume:
dVdtheta=Vtdc*(r-1)/2*(sin(theta)+ ...
   eps/2*sin(2*theta)./sqrt(1-eps^2*sin(theta).^2));

switch heattransferlaw
case 'constant'
   hcoeff=hcu;
case 'Woschni'
   upmean=omega*stroke/pi; % mean piston velocity
   C1=2.28;
   hcoeff=3.26*b^(-0.2)*Tu^(-0.55)*(p/100e3)^(0.8)*(upmean*C1)^0.8;
end

A=1/mass*(dVdtheta+V*Cblowby/omega);
Qconv=hcoeff*(pi*b^2/2+4*V/b)*(Tu-Tw);
Const1=1/omega/mass;

[h,u,v,s,Y,cp,dlvlT,dlvlp]=farg(p,Tu,phi,f,fueltype,airscheme);
B=Const1*v/cp*dlvlT*Qconv/Tu; % note typo on p174, eq. 4.76
C=0;
D=0;
E=v^2/cp/Tu*dlvlT^2+v/p*dlvlp;

yprime(1)=(A+B+C)/(D+E);
yprime(2)=-Const1/cp*Qconv+v/cp*dlvlT*yprime(1);
yprime(3)=p*dVdtheta;
yprime(4)=Qconv/omega;
yprime(5)=Cblowby*mass/omega*h;
```

Appendix C7 – Ratesexp.m

```
function yprime=RatesExp(theta,y,flag);
%
% yprime=RatesExp(theta,y,flag)
%
% Function that returns the drivatives of the following 5 variables
% w.r.t. crank angle (theta) for the expansion phase:
% 1) pressure; 2) unburned temperature;
% 3) work; 4) heat transfer; and 5) heat leakage.
% See Ferguson, C.R., 1986, "Internal Combustion Engines", Wiley,
% p174.

global b stroke eps r Cblowby f fueltype airscheme phi ...
   thetas thetab RPM omega ...
   heattransferlaw hcb ...
   p1 T1 V1 Tw theta1 Vtdc Vbdc mass1

p=y(1);
Tb=y(2);
yprime=zeros(5,1);

% mass in cylinder accounting for blowby:
mass=mass1*exp(-Cblowby*(theta-theta1)/omega);
% volume of cylinder:
V=Vtdc*(1+(r-1)/2*(1-cos(theta)+ ...
   1/eps*(1-(1-eps^2*sin(theta).^2).^0.5)));
% derivate of volume:
dVdtheta=Vtdc*(r-1)/2*(sin(theta)+ ...
   eps/2*sin(2*theta)./sqrt(1-eps^2*sin(theta).^2));

switch heattransferlaw
case 'constant'
   hcoeff=hcb;
case 'Woschni'
   upmean=omega*stroke/pi; % mean piston velocity
   C1=2.28;
   hcoeff=3.26*b^(-0.2)*Tb^(-0.55)*(p/100e3)^(0.8)*(upmean*C1)^0.8;
end

A=1/mass*(dVdtheta+V*Cblowby/omega);
Qconv=hcoeff*(pi*b^2/2+4*V/b)*(Tb-Tw);
Const1=1/omega/mass;

[h,u,v,s,Y,cp,dlvlT,dlvlp]=farg(p,Tb,phi,1,fueltype,airscheme);
B=Const1*v/cp*dlvlT*Qconv/Tb;
C=0;
D=v^2/cp/Tb*dlvlT^2+v/p*dlvlp;
E=0;

yprime(1)=(A+B+C)/(D+E);
yprime(2)=-Const1/cp*Qconv+v/cp*dlvlT*yprime(1);
yprime(3)=p*dVdtheta;
yprime(4)=Qconv/omega;
yprime(5)=Cblowby*mass/omega*h;
```